PROGRESS REPORT TO THE NATIONAL AERONAUTICS AND SPACE ADMINISTRATION

Research Grant No. NsG 239-62

February, 1965

Prepared by the
Texas Engineering Experiment Station
Space Technology Division

Texas A&M University
College Station, Texas

PROGRESS REPORT TO THE NATIONAL AERONAUTICS AND SPACE ADMINISTRATION

Research Grant No. NsG 239-62

February 1965

Report submitted by

ORIGINAL SIGNED BY
H. E. WHITMORE

Harry E. Whitmore
Head, Space Technology Division

Prepared by the

Texas Engineering Experiment Station
Space Technology Division

Texas A&M University
College Station, Texas

INDEX

SUMMARY

Research at Texas A&M under NASA Grant NsG 239-62 now consists of ten major projects which are covered in this report. Of the ten projects, eight were being pursued at the time of the last semi-annual report i.e., Projects 2, 3, 5, 7, 8, 9, 10 and 11. Projects 12 and 13 have been originated since the last report. It should be pointed out that due to lack of funds, projects 2 and 5 have been continued at a low level of effort without support from this grant.

The following separate proposals resulting from work under this grant have been submitted to NASA for consideration during this reporting period.

Project 8 - A proposal for the Analysis of Structurally Orthotropic Shells by Means of the Compliance Method.

Project 11- Material Science - Studies on Properties in Radiation Damaged Solids at Low Temperatures.

A proposal was submitted on 1 November 1964 for renewal of NASA Grant NsG 239-62 at a level of $150,000 per year. Firm planning for a research program, at that level, has been accomplished. It is hoped that an indication of approval of the proposal at least verbally can be received early in February. It is desirable to reorient personnel from teaching to research at the beginning of the spring semester.

Plans for the NASA supported Space Research Center at Texas A&M

have reached the working drawing stage. At no urging from NASA, Texas A&M has essentially matched NASA funding on this complex in order to almost double the facility. This Grant is proving to be indispensible in establishing new research programs in keeping with expanding space-oriented personnel and facilities.

SPACE TECHNOLOGY PROJECT NO. 2

CONCENTRATED WASTE STABILIZATION BY MINIMUM VOLUME BIOLOGICAL UNITS

CONCENTRATED WASTE STABILIZATION BY MINIMUM VOLUME BIOLOGICAL UNITS

Project Investigator

W. W. Meinke, Professor of Chemical Engineering and Head of the Chemurgic Research Laboratory

I. Introduction

Laboratory investigations on this phase of the research program funded by NASA Research Grant No. NsG 239-62 were terminated as of 31 August, 1964. However, additional funding to support further research in this area has been requested in the proposal for the renewal of Research Grant NsG 239-62. This renewal proposal entitled "A Proposal for Renewal of Research Grant NsG 239-62 for Interdisciplinary Space Oriented Research in the Physical, Life, and Engineering Sciences" was submitted to NASA on 1 November, 1964.

One of the suggested approaches in the renewal proposal is to employ a "minimum volume" photosynthetic algae system as an auxiliary treatment for the effluent provided by a "minimum volume - modified activated sludge system." In addition to this proposed photosynthetic study, an independent research proposal on "Industrial Photosynthesis" is being prepared in cooperation with North American Aviation, Inc. North American currently has a research program in progress on Industrial Photosynthesis with funds provided by NASA. Details of the proposed contribution of Texas A&M University to the Industrial Photosynthesis program is provided in Section IV of this report.

II. Investigations on Minimum Volume Biological Waste Stabilization Systems - A Summary

Experimental approaches and research data obtained by these approaches have been provided in earlier progress reports.* In general, body wastes - feces and urine - were blended and then diluted to desired concentration for subsequent stabilization action by different microbiological systems. Conventional laboratory glass ware - flasks and bottles - were employed to contain the body waste blend and the stabilizing microflora. Light, and aeration (by shaking), no aeration or aeration (by pulling air through the media) were physical factors imposed on specific biological stabilization systems. Furthermore, all studies were by "batch" procedures rather than by "continuous flow" methods. Finally, the conventional Biological Oxygen Demand (BOD) technique was employed to evaluate the efficiency of a particular system under investigation.

Research results obtained have shown an activated sludge - or rather a modified activated sludge - biological stabilization unit is capable of oxidizing large amounts of organic matter provided by body wastes. For example, an activated sludge system developed from settled sewage influent to a municipal plant was capable - after a proper acclimation period - of destroying essentially 90% of the BOD of a feces-urine blend at concentrates of blend in the range of 1.43% to 26.68% of the total volume contained in the biological stabilization system. The blend of feces-urine (100 grams of feces reduced

---

* Research Grant No. NsG 239-62 Progress Reports of September 1963, February 1964 and August 1964.

to a slurry in a Blender with 1000 ml of urine) at the 1.43% level provided a stabilization mixture with a BOD value of 353 ppm. After 24 hours the BOD of the effluent had been reduced to 90 ppm. This value of 90 ppm is an average figure for 3 successive days of feces-urine blend addition at the 1.43 volume % level. Average residual values of 90 and 144 ppm were obtained with blend concentrations of 2.86 and 6.67%, respectively. At a level of 13.34% of blend in the system there was evidence of a slight build up of BOD; that is, residual BOD values - 24 hours after the addition of this level of blend - increased from 144 to 175, 175 to 204 and 204 to 293 ppm, respectively, with the addition of 3 samples of blend at 24 hour intervals. With the daily addition of 26.68% blend, the residual BOD rose to a level of 456 ppm after the first addition followed by 24 hours of action by the sludge, to a level of 566 ppm after the second addition and to a final value of 716 ppm after the third addition of the highest test level of blend - namely, 26.68 volume %.

The 1.43% blend concentration approaches the normal or average dilution provided the wastes of a man before it arrives as an influent to a municipal waste treatment plant. Based on this dilution ratio, the average daily body wastes voided by man - essentially 100 grams of feces and one liter of urine - would require a processing volume of approximately 77 liters or 24 gallons. In contrast the 2.86, 6.67 and 13.34% blend additions produced a final supernatant essentially equivalent to that supplied by the original 1.43% blend but was accomplished in process volumes of approximately

12.0, 5.1 and 2.6 gallons, respectively. Expressed in another way these data indicate the feasibility of treating the daily body wastes of approximately 10 men in a 24 gallon unit and provide essentially 90% reduction in the BOD of the body wastes. Such a 24 gallon, 10 man unit coupled with a second 24 gallon unit could provide for stabilization of much of the remaining BOD.

The above data - despite the relatively short test period of 3 days - have significance in the design of waste management systems for extended space explorations - for example, for orbiting space stations. On such installations, it may be desirable to process the concentrated body waste and solid or liquid food waste with a "minimum volume" activated sludge system as a primary treatment. The effluent from the activated sludge system would be combined with the wash water and converted to potable water by distillation or other physical means which have proven of merit for space explorations. Further work is required to provide the true merit of this system for space ventures.

Perhaps the greatest value or most significant feature of the concentrate waste study is related to terrestial - rather than space-waste control and management. Specifically, the data which have been obtained demonstrate the ability of a modified activated sludge unit to stabilize large quantities of organic matter if the organic matter - feces and urine - are supplied to the unit in high concentration. These data suggest the use of terrestial waste

stabilization units which employ smaller quantities of dilution water to provide transit of domestic and industrial wastes from the point of origin to the municipal or industrial treatment plant. Smaller conduits for transfer of the waste could be employed and smaller units could be constructed at the treatment plants.

It is also envisioned that the anaerobic digesters of municipal plants could possible be eliminated and replaced by an aerobic process - such as the modified activated sludge system. This could be considered desirable because the liquid withdrawn from anaerobic digesters must be subjected to further aerobic treatment. Furthermore, the residual solids which collect in the anaerobic digester must be removed at periodic intervals and dewatered - usually on sand filter beds. During rainy weather the dewatering operation can present a problem. It is possible that the modified activated sludge process could also stabilize the solids provided by the influent to a sewage treatment plant.

The "modified activated sludge" also has potential merit for industrial wastes. In general the industrial approach is to dilute their concentrated wastes prior to treatment or release to waterways The concepts of concentrate waste treatment with a "modified activated sludge" method indicate the possibility of treating concentrated wastes and thus permit smaller industrial waste management plants and also provide a better control of waterway pollution by industrial effluents.

Concentrated waste treatment systems should provide continuous efficient operation once equilibrium has been reached and as long as the system receives a waste of uniform composition. However, the functioning of the concentrated waste units could be altered by change in concentration or composition of the waste being supplied to the unit. Micro constituents - such as antibiotics excreted in body wastes during antibiotic therapy - have an adverse effect on th efficiency of a biosystem. Normal constituents of body wastes also could adversely influence the efficient operation of a biological stabilization system if a proper balance of these constituents is not maintained. The biological oxidation process is realized throug enzyme systems of microbial origin. Many of these enzyme systems require the presence of specific metal cations - Ca^{++}, Mg^{++}, Mn^{++}, Zn^{++}, etc. Furthermore, the presence of the excess of a given cation - say Ca^{++} - could obviate the desired effect of an essential cation - i.e. Mn^{++} - and thereby biological activity would be impaire or cease. Thus, it is evident that the proper balance of inorganic constituents must be maintained in the biological waste stabilization unit.

The role of an essential metal cation may be further influenced by organic matter of chelation potential. It has been suggested tha the metal ion need for a given enzymatic transformation forms a chelate with the enzyme. This chelate complex - metal ion and enzyme - then brings about the desired biological trnasformation. However,

in the presence of excess organic matter, which is also capable of forming a chelate with the essential metal ion, a competitive type of situation arises. That is, the metal ion is not available for saturation of the enzyme because it also has been tied up in a chelate bonding with the other organic matter. As a result the rate of enzyme activity is decreased and biological activity is decreased and in some instances essentially stopped.

III. Further Planned Research Approaches On Concentrated Waste Stabilization by Biosystems

Details of further work planned in the area of concentrated waste treatment by biosystems are provided in the proposal of 1 November 1964 which is a request for the renewal of Research Grant NsG 239-62. The planned research approaches submitted in this renewal request are as follows:

A. A Study of the Efficiency and Performance of Activated Sludge Systems With Concentrated Body Wastes Over Extended Periods of Time,

B. Study on Biological Systems as Auxilaries to the Activated Sludge-Concentrated Waste Systems,

C. Basic Investigations On The Interrelationships of Antibiotics and Metal Cations In BOD Evaluations of Domestic Sewage Influents of Variable BOD Content, and

D. Continuous Flow Biological Units.

IV. Research On A New Approach To Industrial Photosynthesis

Currently a research proposal is being prepared in cooperation

with North American Aviation, Inc. on a new approach to Industrial Photosynthesis. Industrial Photosynthesis - as defined by Dr. R. H. T. Mattoni of North American Aviation - is a term to describe the controlled growth of complex populations of microrganisms, principally unicellular green algae. Furthermore, Industrial Photosynthesis combined into systems for waste water management is capable of:

A. Purifying waste water,

B. Providing reclaimed water, and

C. Producing high protein feed - algae.

This new approach stems from observations made during an investigation on Evaporation Retardation In Small Reservoirs through the application of evaporation retardant films of hexa- and octadecanol.* In this study it was observed that the continued applicatio of a 50-50 mixture of hexa- and octadecanol had a pronounced effect upon the clarity of the water contained both in small test containers (Figure 1) and in a dug earthen pond of approximately 1/5 acre water surface. In contrast the water in containers or an earthen pond that received no film treatment remained turbid and supported abundant growth of unicellular forms of algae which tended to remain in suspension in the water. The film treated waters soon became clear and in the case of the earthen pond the clear water supported the growth

---

* Meinke, W. W. and Waldrip, W. J., Research On Evaporation Retardation In Small Reservoirs, 1958-63, Texas Water Commission Bulletin 6401, (March 1964).

Figure 1

Evaporation Control Investigations In Small Containers

of bottom fixed macro forms of photosynthetic plants. The plants grew and flourished in water depths as great as six feet. These differences in water clarity and biota in the two earthen ponds cannot b attributed to differences in the ponds or water supply because they were constructed at the same time at the same location - in fact separated only by a center dike - and were filled with water from the same large earthen reservoir. Thus, the changes observed must have been due to the film chemical which was applied.

There are possibly three explanations for the results which were observed; namely,

A. The long straight chain fatty alcohols - hexa- and octadecanol - were oxidized to carboxylic acids by the microflora of the water. These fatty acids then combined with calcium and/or magnesium ions of the water to produce a water insoluble soap. The insoluble soap then combined with colloidal particles of the water and ultimately sank to the bottom of the pond.

B. The fatty acids, arising from the oxidation of the fatty alcohols, also could have been toxic for specific microbial forms in the water - perhaps the algae.

C. The fatty acids arising from the oxidation of the fatty alcohols likewise could have removed nutrients - phosphate or essential metal cations - from the water and thereby prevented or reduced the growth of the unicellular algae.

In the proposed research program, which is being developed in cooperation with North American, the water evaporation retardant film chemicals (hexa- and octadecanol) will be added to the surface of the settled waste effluents in order to evaluate the quantity of water which can be saved due to evaporation abatement, to evaluate the economics of such an evaporation control program, and to see if film chemicals can control or change the biota of settled sewage effluent. Films of the higher molecular weight straight chain fatty alcohols, as depicted by Figure 2, are readily degradable by microorganisms, permit free gas exchange, are non-toxic to fish life, and reduce the rate at which water molecules can escape from the water surface to the air above the body of water. In the final analysis it is hoped that the film chemicals - when applied to oxidation ponds - will not only serve to reduce water losses by evaporation but will serve to establish - with proper seeding - and maintain a macro form of bottom fixed or rooted photosynthetic plants. It is envisioned that this form of photosynthetic plants can be harvested by a mowing operation which will cut the plants at a given level below the water. As these plants are cut below the water surface they will be collected, taken to shore based processing units, and finally utilized as animal feed.

V. Conclusions

Spplication of the research findings on the Minimum Volume Biological Waste Stabilization Units to immediate or near future space ventures cannot be visualized. However, the data obtained could

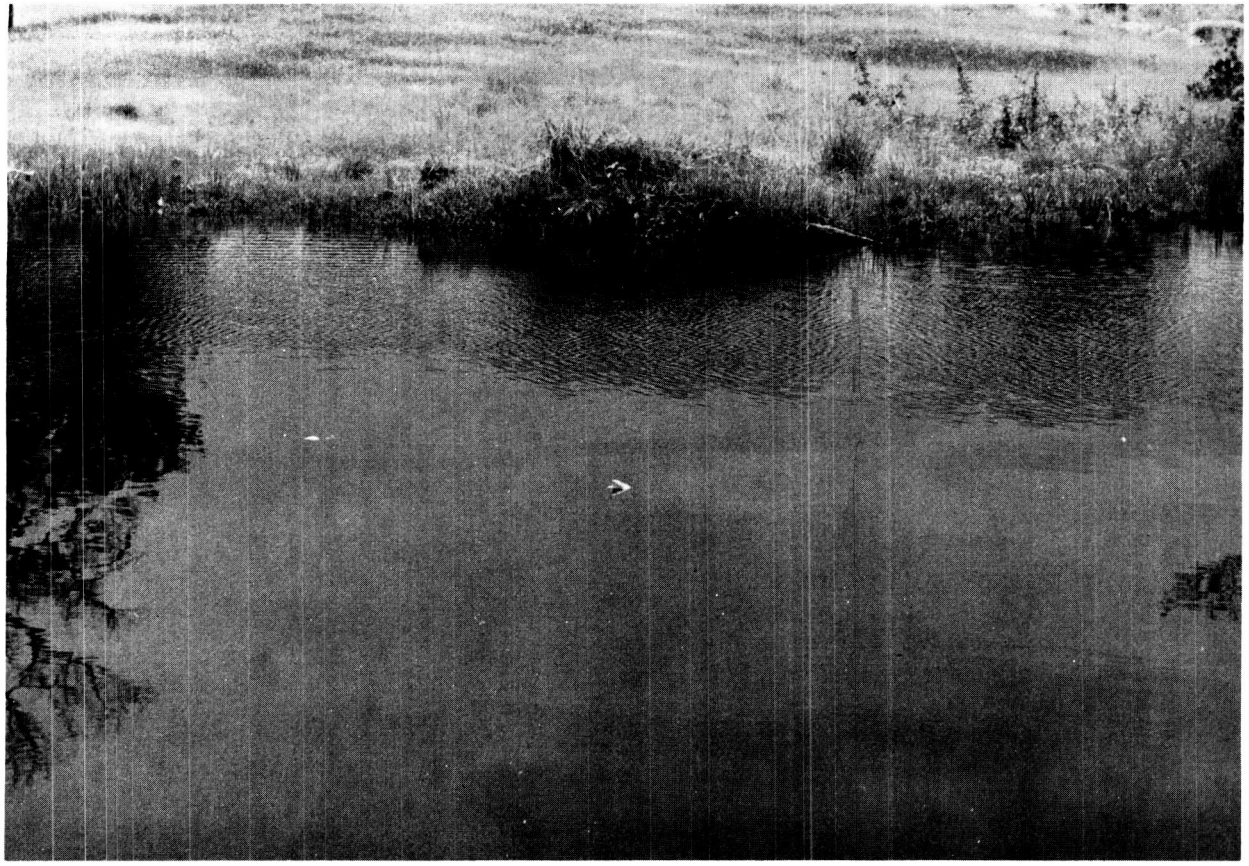

Figure 2 - Advancing Chemical Film On The Surface Of A Farm Pond

have merit in considering space oriented waste management problems of the future - for example, for space stations or for extended lunar explorations.

The data obtained to date have their greatest implication or spin-off value for terrestial waste management problems. Treatment of concentrated wastes - both domestic and industrial - possibly could be realized with greater efficiency in smaller biosystems and thereby decrease the pollution of the nation's rivers and streams. This concept is essentially opposite to current waste management approaches which in essence employ dilution prior to treatment or prior to release into rivers and streams.

The new approach to Industrial Photosynthesis - Section IV - requires further basic research and it is hoped that funding can be obtained for the investigation. If the concepts of the proposed research could be realized it would be possible to recover larger volumes of reclaimed water because losses due to evaporation would have been reduced, and it would be easier to recover the macro photosynthetic plants and reclaimed water - that is, phase separation would be easier than with unicellular algae.

In his State of the Union address, President Johnson pointed to the need for increasing the beauty of the nation and ending the poisoning of rivers and the atmosphere. In the opinion of this investigator, the research concepts presented above - with proper research and development - could aid in keeping our waterways free of pollution and thus enhance the beauty of our nation.

SPACE TECHNOLOGY PROJECT NO. 3

HEAT TRANSFER FROM PLASMA JETS

HEAT TRANSFER FROM PLASMA JETS

Project Investigators:

Dr. P. T. Eubank, Department of Chemical Engineering

Mr. J. R. Johnson, Graduate Assistant

I. Experimental

Considerable difficulty has occured in attempting to obtain experimental heat transfer data from the plasma jet apparatus. Thes difficulties have been traced to the generator system which determines the operating characteristics of the arc.

The arc is always started at a low power input from the generato The power is then gradually increased by increasing the output generator voltage. In this case, the generator voltage cannot be increased continuously but takes discrete jumps which can cause the arc to be broken. This phenomena was occuring in our system particularly with nitrogen gas as the carrier. By placing a large transformer in the circuit, this difficulty has been considerably reduced. Also, it is helpful to begin operation on argon and gradually blend nitrogen into the system after a high energy arc has been stabilized.

Not so easily corrected is the failure of the generator system to supply energy to the arc at or near the rated output energy of the generator. It has not been possible to place more than 4 kilowatts into the arc from a 10-12 kw generator. While this low-energy data was desired, it would appear that only through the purchase of a considerably larger generator can high-energy arcs be obtained.

Numerous experimental runs have been made using argon as the carrier gas. This heat transfer data will not be correlated until the nitrogen and helium data is complete. The argon data appears normal except the maximum heat flux to the cooling chamber walls occurs not in the first chamber but rather the second indicating that the plasma arc moves out of the orifice and nears the cooling wall at the second chamber. Plasma temperature decreases as it journeys down the cooling section. Thus, the maximum heat flux would be expected immediately after the orifice in the first chamber. The distance from the outer boundary of the plasma core to the cooling walls decreases as the plasma moves downstream. Decreasing this distance should increase the heat flux. Together, these factors provide a logical explanation for the occurance of the maximum heat flux at the second chamber.

II. Theoretical

Calculations indicate that flow in the apparatus should be laminar. Several empirical equations have been found in the literature for the heat transfer coefficient to an entrance section of a pipe where flow is laminar and the walls are maintained at a constant temperature.

Work is also proceeding on a differential equation to describe the temperature variation in a tube apparatus with respect to the radial and longitudinal direction. The coefficients in such an equation are composed of physical constants which vary greatly with

the extreme temperature differences of this problem. Using physical property data from the literature, it is hoped that a complete solution to the problem may be obtained by numerical integration of the differential equation on the digital computer.

SPACE TECHNOLOGY PROJECT NO. 5

A MATHEMATICAL INVESTIGATION OF THE STRUCTURE OF LIGHT METALS

A MATHEMATICAL INVESTIGATION OF THE STRUCTURE OF LIGHT METALS

Project Investigators

Dr. E. R. Keown, Principal Investigator, Professor of Mathematics

Mr. W. F. Curry, Graduate Student

Mr. D. L. Hardcastle, Graduate Student

Mr. T. R. Ramsey, Graduate Student

Capt. G. E. Smart, Graduate Student

Mr. D. R. Wiff, Graduate Student

This is a report of continued research on a project formerly supported by the National Aeronautics and Space Administration as Project 5, NsG 239-62 on which a final report was issued in August 1964.[1] Work has proceeded at a reduced pace due to lack of funding, but worthwhile results have been achieved. Capt. G. E. Smart has rewritten the code of the plane wave symmetrizer which Dr. E. R. Keown developed with the Solid State and Molecular Theory Group, Massachusetts Institute of Technology[2] during the past year. The symmetrizer now not only determines which representations occur in a given plane wave but also sorts out any duplications and punches an input card to John Wood's APW program.[3] It is believed that by February 1, 1965 the program will calculate and punch a complete specification deck for the Augmented Plane Wave program.

Mr. Ramsey has the Herman-Skillman code converted from Fortran II to Fortran IV and operating locally on the computer of the Data

Processing Center. In addition to this, he has written a program to take the punched output of the Herman-Skillman program[4] and convert it to a form acceptable to the APW System. Mr. Curry has not completed the conversion of the main APW System from Fortran II to Fortran IV; however, the Data Processing Center has granted limited permission to use the existing Fortran II program on the IBM 7094. It is anticipated that the complete conversion will be carried out by Mr. Curry and Mr. Wiff.

Mr. Wiff has now passed his examination for admission to candidacy for the degree of doctor of philosophy in the department of physics. He plans to do his doctoral research in computational solid state physics. He will calculate the energy bands of various crystals of the zincblende structure, starting with boron nitride. This calculation requires a serious modification of the APW program, including a possible conversion to complex arithmetic since the zincblende crystal does not possess a center of inversion symmetry. He will begin his work with some calculations on the band structure of germanium with the existing program in order to familiarize himself with the details of the APW method.

Mr. D. L. Hardcastle has joined the program and plans to revive our calculation of the hyperfine structure of lithium.[5] He will program the calculation by a procedure recently suggested by Prof. John Gammel of the Department of Physics, Texas A&M University. This proposed new method has the potential advantage of providing

a solution of the proper symmetry in contrast to some other competing calculations.[6,7]

This report contains some "final" bands for the diamond crystal which have been completed since the last report as Figures 1 and 2.

ENERGY BANDS FOR DIAMOND

LATTICE CONSTANT	=	6.7406	ATOMIC UNITS
APW SPHERE RADIUS	=	1.4594	ATOMIC UNITS
POTENTIAL AT SPHERE RADIUS	=	-2.7356	RYDBERGS
AVERAGE POTENTIAL BETWEEN SPHERES	=	-1.3928	RYDBERGS

CRYSTAL POTENTIAL DERIVED FROM ATOMIC CONFIGURATION

$(1s)^2\ (2s)^1\ (2p)^3$

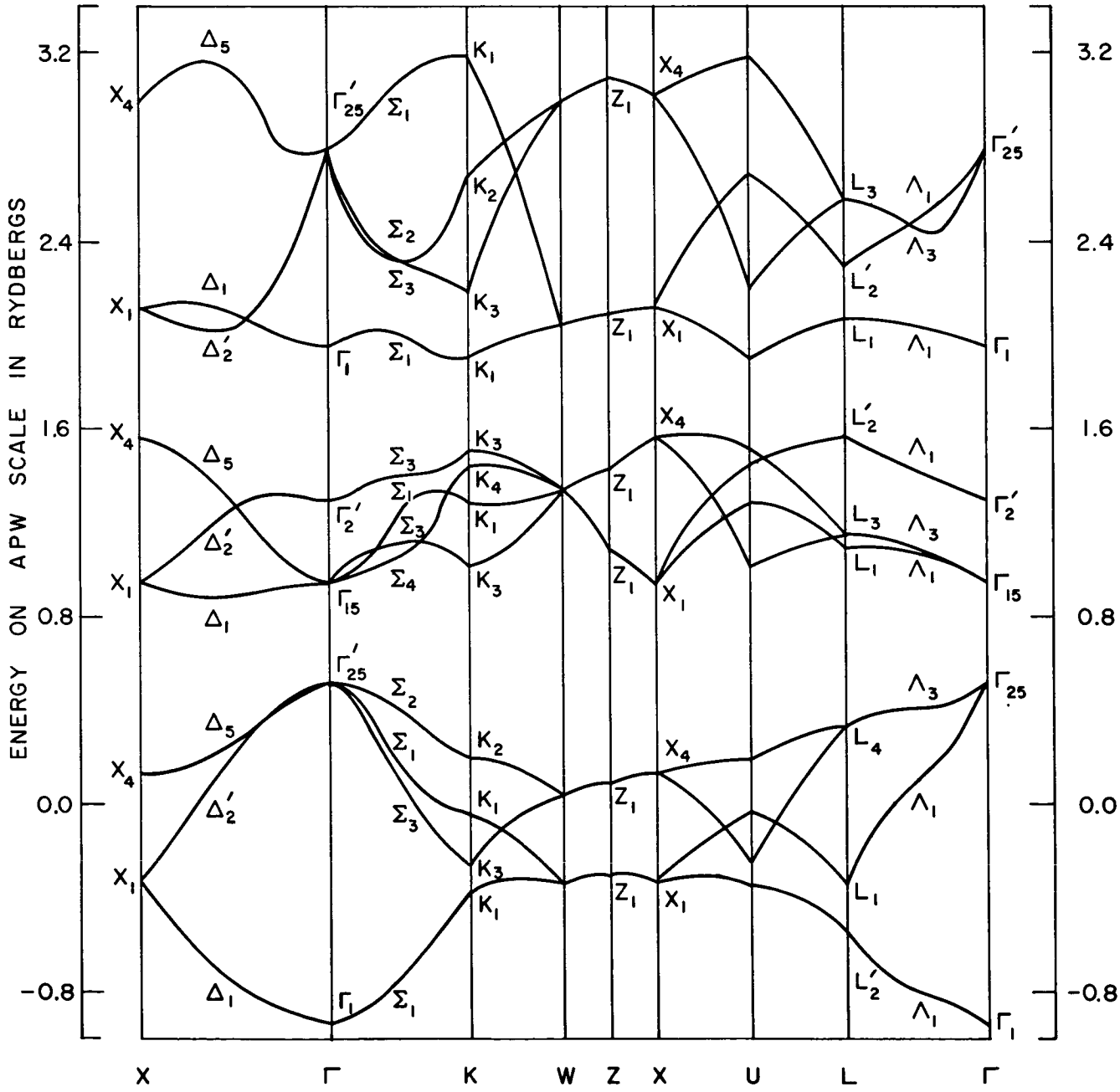

FIGURE 1

ENERGY BANDS FOR DIAMOND

LATTICE CONSTANT	=	6.7406	ATOMIC UNITS
APW SPHERE RADIUS	=	1.4594	ATOMIC UNITS
POTENTIAL AT SPHERE RADIUS	=	−2.7356	RYDBERGS
AVERAGE POTENTIAL BETWEEN SPHERES	=	−1.3928	RYDBERGS

CRYSTAL POTENTIAL DERIVED FROM ATOMIC CONFIGURATION

$(1s)^2(2s)^1(2p)^3$

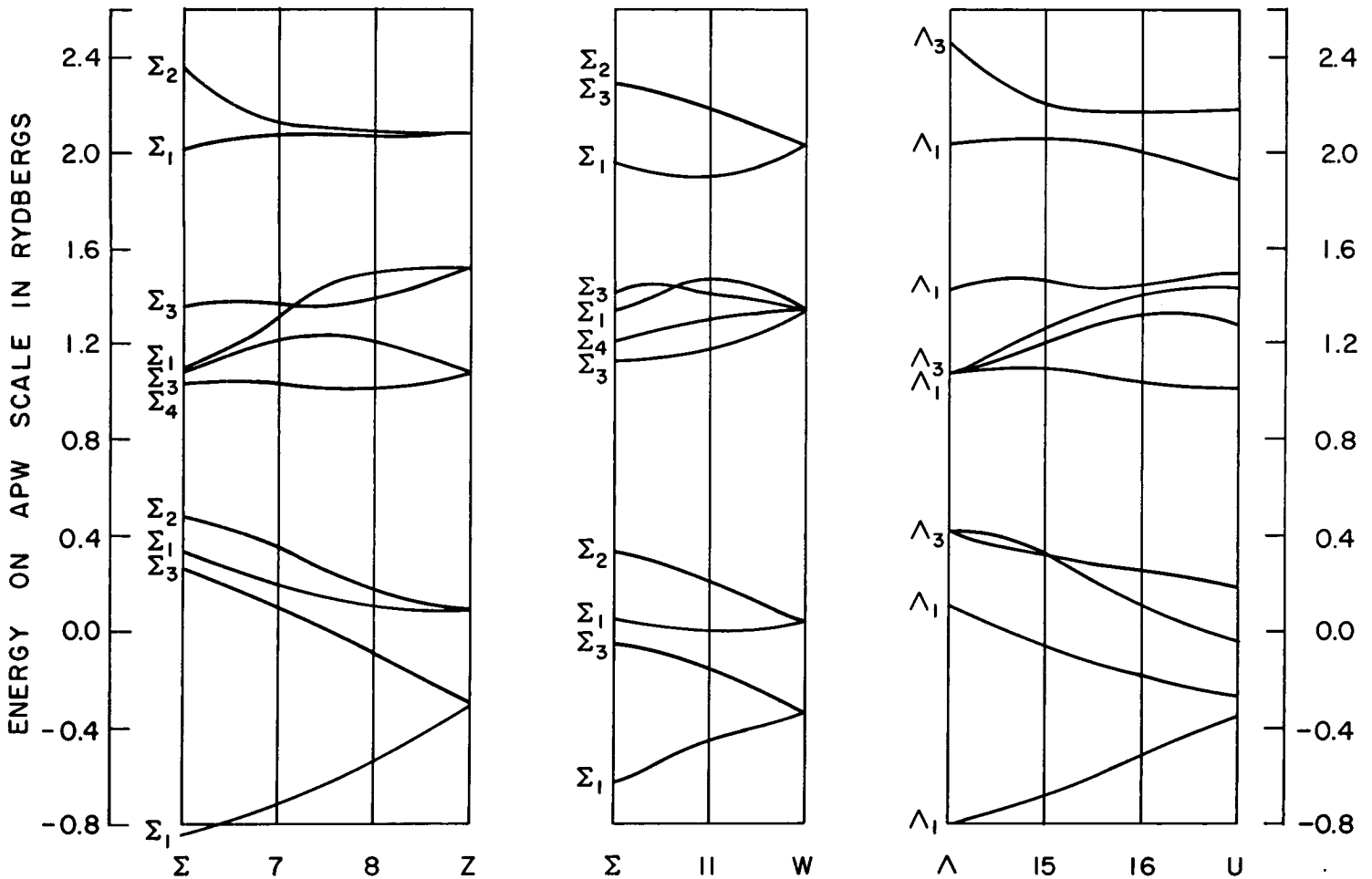

FIGURE 2

BIBLIOGRAPHY

1. Progress Report to the National Aeronautics and Space Administration, Texas A&M University, August, 1964.

2. E. R. Keown, Quarterly Progress Report No. 51, Solid-State and Molecular Theory Group, M.I.T., January, 1964.

3. J. H. Wood, Augmented Plane Wave Manual, Solid-State and Molecular Theory Group, M.I.T., Unpublished.

4. F. Herman and S. Skillman, Atomic Structure Calculations, Prentice-Hall, 1963.

5. Progress Report to the National Aeronautics and Space Administration (Supplement on Project No. 5), Texas A&M University, August, 1963.

6. L. M. Sachs, Phys. Rev. 117, 1505(1960).

7. K. F. Berggren and R. F. Wood, Phys. Rev. 130, 198(1963).

SPACE TECHNOLOGY PROJECT # 7

COSMIC RAY MUONS

COSMIC RAY MUONS

Project Investigators

Dr. N. M. Duller, Principal Investigator, Associate Professor of Physics

Mr. W. G. Cantrell, Graduate Research Assistant

Mr. D. L. Edens, Graduate Research Assistant

Mr. A. V. Jelinek, Graduate Research Assistant

Mr. J. R. Sharber, Graduate Research Assistant

Mr. E. L. Walker, Graduate Research Assistant

Mr. J. D. Winningham, Graduate Research Assistant

I. Review of the Work of the Past Period

Progress has been made on all the major muon detector components discussed in the last report: (1) The large spark chamber has moved slowly but the large aluminum plates are now being machined at the edges for vertical mounting within the next month. (2) The wire chamber system described in the report on the preceding period has been temporarily abandoned for a new module-type rod spark chamber which has the same advantages of the wire spark chamber but will be easier to fabricate with accurate spacing between the electrodes. The module consists simply of a Plexiglas box with the rods extending through the walls of the box for electrical contact and to eliminate the edge sparking, which is a common trouble with plates and rods which terminate within the gas enclosure. Further details of this type of chamber will be given in the next report since it is still

in a formative stage. (3) The work on Geiger and proportional counters of large dimensions has proceeded. Of particular interest are counters made of Pyrex glass tubes with tin-oxide conducting coatings deposited on the interior to act as cathodes. These are still being developed but appear to hold considerable promise not only for large counters but also as spark tubes completely analogous to rectangular spark chambers, since the tin-oxide layer permits clea vision through the tube walls. (4) The transistorized hodoscope is now being assembled and tested.

A new and important activity in this project is the development of electromagnets to be used in the spectrometer-telescopes which will form the heart of the high-energy muon experiments. These magnets are to be solid-iron magnetic circuit devices (no air gaps). The configurations of the iron being worked with are displayed in Figures 1 and 2. Figure 1 shows a single iron loop formed by slabs of Armco magnetic ingot iron. In this configuration the copper windings are laid on the two long legs of the iron loop, and it is through these two legs that the high-energy muons will pass and within which they will be deflected by the saturated magnetic field of about 20 kilogauss. Figure 2 shows a mock-up of another arrangement of laminations which form a conventional H-frame with two return flux paths on the outside but without air gap in the middle leg where the flux is concentrated. In this configuration inexpensive mild structural steel can probably be used in the outer loops where

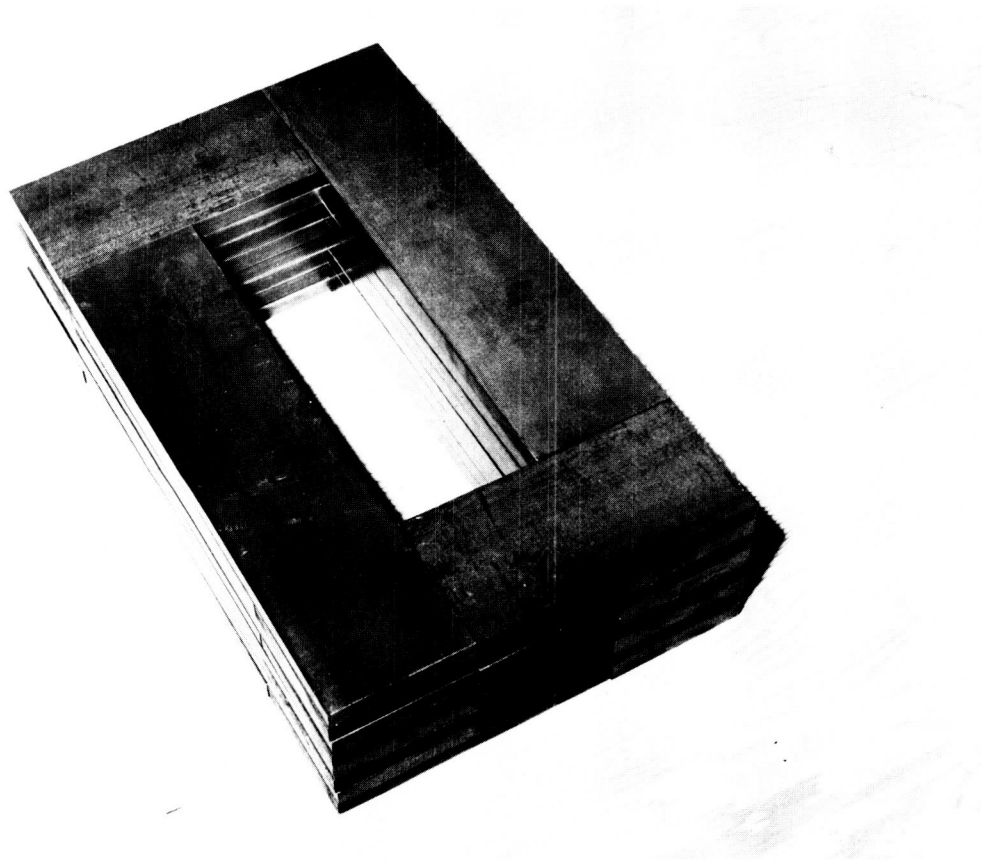

Figure 7-1.

The simpler of two configurations of the iron laminations in the solid-iron electromagnets.

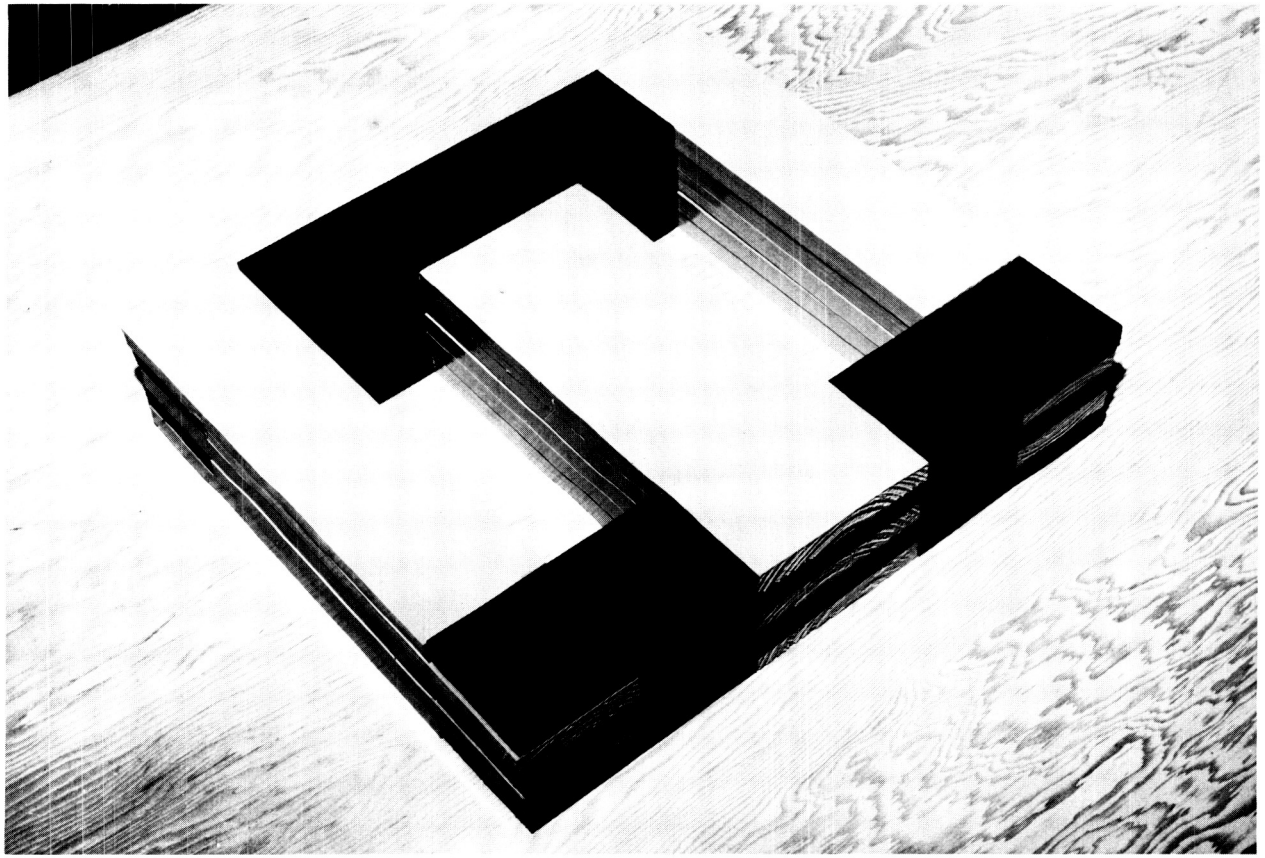

Figure 7-2.

A wood-slab mock-up of the H-frame configuration of iron laminations to be used in solid-iron electromagnets.

the copper will be wound, especially if the cross sectional area of the outer loops exceeds that of the middle leg. As now planned the middle leg will be of magnetic ingot iron laminations and free of copper windings, and it will be through this element of the magnet that the particles will pass to be deflected. At least two such magnets will be required for each spectrometer. Spark chambers will be situated in the particle trajectory regions outside the magnets and between them for recording initial and final directions of each penetrating non-nuclear particle (presumably always an energetic cosmic ray muon). Analysis of the tracks in the outside chambers will give the momentum and the charge of each particle detected. The chamber between the magnets will give near-redundant information which will help to evaluate the multiple Coulomb scattering of the muons within the iron.

II. Work Planned for the Next Period

The magnets will be the principal item of development during the next few months. It is hoped that with the operation of the spark chambers and triggering systems (including the hodoscope) very soon, two magnets will complete one spectrometer-telescope with which we may begin actual intensity measurements with spectral details and charge determinations.

SPACE TECHNOLOGY PROJECT NO. 8

SPACE STRUCTURES

SPACE STRUCTURES

Project Investigators:

Dr. Charles H. Samson, Jr., Professor and Head
Department of Civil Engineering

Dr. Thomas J. Kozik, Associate Professor
Department of Mechanical Engineering

Mr. Harry J. Sweet, Assistant Professor
Departments of Aerospace and Civil Engineering

Mr. A. J. Chaput
NASA Doctoral Trainee

Mr. R. E. Harvey
Graduate Research Assistant

I. Introduction

This project is concerned with two areas of research:

1. Behavior of Isotropic and Anisotropic Shells
2. Impact Attenuation Devices

The objectives of the shell research are specified in four phases as follows:

a. Development of a general set of thin shell equations for an orthotropic material.

b. Development of a general set of equations for a material exhibiting plane anisotropy.

c. Development of a general set of shell equations exhibiting plane anisotropy whereby the elastic constants do not exhibit diagonal symmetry.

d. Limited testing of the various structurally anisotropic materials when applied to different shell configurations to determine the degree of compliance between theory and test.

The impact attenuation research has involved the development and evaluation of various energy absorption devices which rely on the failure of a structural device as the energy absorption medium.

This report covers the work accomplished from July, 1964, through December, 1964.

II. Progress on Shell Research

Part (a) was completed in the previous reporting period and was included in the August, 1964 progress report. Work has progressed on part (b) and it is expected that a final report on this portion will be included in the August, 1965 progress report. Work on Part (c) has continued.

Further research is being planned to investigate the discrepancy between the displacement shell equations and the stress resultant shell equations. Toward this end, a paper has been submitted for publication which deals with the development of the displacement equations starting with the Navier equations of elasticity (see Enclosure 1). The stress resultant equations can and have been directly derived from the Beltrami-Michell equations.

The basis for the discrepancy lies in the Kirchoff hypothesis. Since this is an approximation, there is no reason to expect that its effect on the displacement equations is the same as on the stress resultant equations. However, since the Kirchoff condition does lead to only approximate equations, the question does arise as to which set of equations leads to a more accurate solution. One of the hopes of the present research is to take the residue terms from either the displacement or stress resultant equations, that is, terms from one

system which do not have a counterpart in the other system, and relate them to some physical entity such as middle surface strains. Inspection of these terms may indicate the magnitude of the error and possibly which system of equations is a better approximation.

III. Progress on Impact Attenuation Research

The investigation of the energy absorption characteristics of frangible tubes has continued. A final report of the work done by Mr. A. J. Chaput is given in Enclosure 2. Mr. R. E. Harvey is in the process of conducting additional tests in order to better establish the relationship between the theoretical forces and those actually encountered in a franging tube.

THE EFFECTS OF THE SECOND OF THE KIRCHOFF HYPOTHESES ON THE DISPLACEMENT FORMULATION OF THE THIN ELASTIC SHELL EQUATIONS*

by

T. J. KOZIK

DEPARTMENT OF MECHANICAL ENGINEERING

TEXAS A&M UNIVERSITY

*The paper presented here has been submitted for publication to Journal of Applied Mechanics.

ENCLOSURE 1

THE EFFECTS OF THE SECOND OF THE KIRCHOFF HYPOTHESES ON THE DISPLACEMENT FORMULATION OF THE THIN ELASTIC SHELL EQUATIONS[1]

T. J. Kozik[2]

ABSTRACT

The purpose of this paper is two fold. First, to develop in a systematic manner the thin elastic shell displacement equations starting from a modified form of the Navier equations of elasticity stated in curvalinear coordinates. Second, to illustrate that the displacement formulation of the shell problem is sensitive to the discrepancy that arises in simultanously assuming a plane stress and plane strain condition as is normally done when the stress resultant approach is used in shell analysis. The ensuing development demonstrates that it is necessary to discard the second of the Kirchoff hypotheses if a plane stress solution for the displacement formulation is desired.

INTRODUCTION

The classical assumptions of elastic thin shell theory are the Kirchoff hypotheses, namely:

a) Straight lines initially normal to the shell middle surface remain so after deformation.

b) A line segment normal to the shell middle surface does not suffer any extensions or contractions.

---

[1]The work here reported was done under NASA research grant NsG 239-62.

[2]Associate Professor of Mechanical Engineering, Texas A&M University, College Station, Texas.

The first assumption neglects the effects of the transverse shearing stress while the second limits the solution to that of plane strain. An additional assumption is also included in thin shell analysis, namely, that the normal stresses normal to the shell middle surface are small in comparison with the remaining stresses and hence may be neglected. The use of this assumption is equivalent to stating that the shell problem is approximately one of plane stress.

The fact that the second of the Kirchoff hypotheses and the normal stress assumption form an inconsistent argument has been noted by Reissner (1)[3] among others. However Reissner points out that the ensuing error in the stress resultant formulation of the shell equations is negligible.

Though shell equations are most frequently developed in stress resultant form, an alternate method of derivation exists whereby the equilibrium conditions for an element are stated in displacement form. In this manner, a set of shell equations may be obtained which are in terms of the middle surface displacement components and whose development obviates the need of stress resultants or compatibility equations. Vlasov, (2), (3), has used this approach in his development of shell theory and a good deal of what follows is based on his work.

The purpose of this paper is to show that a displacement formulation of the shell problem is sensitive to the discrepancy in simultaneously assuming a plane strain and plane stress condition. In order that the shell equations degenerate to those of the plate, it is

[3]Numbers in brackets refer to the references given at the end of this paper.

necessary to assume only the plane stress condition. Thus the second of the Kirchoff hypotheses must be relaxed and as will be shown in the ensuing development, the explicit form of displacement normal to shell middle surface must be determined.

LIST OF SYMBOLS

α, β	Principal curvalinear coordinates for the shell middle surface.
γ	Distance measured normal to the shell middle surface.
A, B	Lamé surface parameters for the middle surface.
h_1, h_2	Lamé surface parameters for a surface parallel to the shell middle surface.
δ	Shell thickness.
$u_\alpha, u_\beta, u_\gamma$	Components of the displacement of a point of the middle surface in the α, β and γ directions.
k_1, k_2	Principal curvatures of the surface in the α and β directions.
K	Gaussian curvature, $k_1 k_2$
H	Mean curvature, $(k_1 + k_2)/2$
E	Young's Modulus and Poisson's Ratio
λ, μ	Lame elastic constants.
Δ	Volume dilatation
ω_γ	Rotation of an element about the axis.

THEORY

The displacement equilibrium equations for a thin elastic shell are directly derivable from a modified form of the Navier equations of elasticity. These latter equations are stated below and their proof may be found in Vlasov (2), Part II.

$$(\lambda+2\mu)\frac{H_2H_3}{H_1}\frac{\partial\Delta}{\partial\alpha}-2\mu\left[\frac{\partial}{\partial\beta}(H_3\omega_\gamma)-\frac{\partial}{\partial\gamma}(H_2\omega_\beta)\right]+H_2H_3P_\alpha=0 \tag{1}$$

$$(\lambda+2\mu)\frac{H_3H_1}{H_2}\frac{\partial\Delta}{\partial\beta}-2\mu\left[\frac{\partial}{\partial\gamma}(H_1\omega_\alpha)-\frac{\partial}{\partial\alpha}(H_3\omega_\gamma)\right]+H_3H_1P_\beta=0 \tag{2}$$

$$(\lambda+2\mu)\frac{H_1H_2}{H_3}\frac{\partial\Delta}{\partial\gamma}-2\mu\left[\frac{\partial}{\partial\alpha}(H_2\omega_\beta)-\frac{\partial}{\partial\beta}(H_1\omega_\alpha)\right]+H_1H_2P_\gamma=0 \tag{3}$$

The quantities H_1, H_2, H_3 are the Lamé coefficients of the quadratic differential form for a line segment ds expressed in terms of an orthogonal system of curvalinear coordinates,

$$ds^2=H_1^2d\alpha^2+H_2^2d\beta^2+H_3^2d\gamma^2$$

The volume dilatation Δ is defined as the sum of the three normal strains and in terms of the displacement components $u_\alpha, u_\beta, u_\gamma$ is expressible as

$$\Delta=\frac{1}{H_1H_2H_3}\left[\frac{\partial}{\partial\alpha}(H_2H_3u_\alpha)+\frac{\partial}{\partial\beta}(H_3H_1u_\beta)+\frac{\partial}{\partial\gamma}(H_1H_2u_\gamma)\right] \tag{4}$$

The components of the rotation of an element, ω_α, ω_β and ω_γ taken about axis tangent to the α, β and γ coordinate lines respectively are given as

$$2\omega_\alpha=\frac{1}{H_2H_3}\left[\frac{\partial}{\partial\beta}(H_3u_\gamma)-\frac{\partial}{\partial\gamma}(H_2u_\beta)\right] \tag{5}$$

$$2\omega_\beta = \frac{1}{H_3 H_1}\left[\frac{\partial}{\partial \gamma}(H_1 u_\alpha) - \frac{\partial}{\partial \alpha}(H_3 u_\gamma)\right] \tag{6}$$

$$2\omega_\gamma = \frac{1}{H_1 H_2}\left[\frac{\partial}{\partial \alpha}(H_2 u_\beta) - \frac{\partial}{\partial \beta}(H_1 u_\alpha)\right] \tag{7}$$

Finally, the quantities P_α , P_β and P_γ represent components of the volume loading.

In dealing with thin elastic shells, the curvalinear coordinate lines, α and β , are chosen so as to be parallel to the lines of principal curvature of the shell middle surface and the coordinate γ is taken to be normal to and zero at that surface. Positive γ is directed toward the convex side of the shell or toward the centers of negative curvature if the signs of the radii of curvature are not the same.

For an element of length, dS , lying on the middle surface, the quadratic differential form becomes

$$ds^2 = A^2 d\alpha^2 + B^2 d\beta^2$$

and for an element ds lying in the interior of the shell,

$$ds^2 = h_1^2 d\alpha^2 + h_2^2 d\beta^2 + d\gamma^2$$

where

$$h_1 = A(1 + k_1\gamma) \quad ; \quad h_2 = B(1 + k_2\gamma)$$

Thus for a shell;

$$H_1 = h_1 \quad ; \quad H_2 = h_2 \quad ; \quad H_3 = 1$$

The equations of equilibrium for an elastic shell may then be written as;

$$(\lambda + 2\mu)\frac{h_2}{h_1}\frac{\partial \Delta}{\partial \alpha} - 2\mu\left[\frac{\partial \omega_\gamma}{\partial \beta} - \frac{\partial}{\partial \gamma}(h_2 \omega_\beta)\right] + h_2 P_\alpha = 0 \tag{8}$$

$$(\lambda+2\mu)\frac{h_1}{h_2}\frac{\partial\Delta}{\partial\beta}-2\mu\left[\frac{\partial}{\partial\gamma}(h_1\omega_\alpha)-\frac{\partial\omega_\gamma}{\partial\alpha}\right]+h_1P_\beta=0 \tag{9}$$

$$(\lambda+2\mu)h_1h_2\frac{\partial\Delta}{\partial\gamma}-2\mu\left[\frac{\partial}{\partial\alpha}(h_2\omega_\beta)-\frac{\partial}{\partial\beta}(h_1\omega_\alpha)\right]+h_1h_2P_\gamma=0 \tag{10}$$

The volume dilatation and the rotation are given as;

$$\Delta=\frac{1}{h_1h_2}\left[\frac{\partial}{\partial\alpha}(h_2u_\alpha)+\frac{\partial}{\partial\beta}(h_1u_\beta)+\frac{\partial}{\partial\gamma}(h_1h_2u_\gamma)\right] \tag{11}$$

$$2\omega_\alpha=\frac{1}{h_2}\left[\frac{\partial u_\gamma}{\partial\beta}-\frac{\partial}{\partial\gamma}(h_2u_\beta)\right] \tag{12}$$

$$2\omega_\beta=\frac{1}{h_1}\left[\frac{\partial}{\partial\gamma}(h_1u_\alpha)-\frac{\partial u_\gamma}{\partial\alpha}\right] \tag{13}$$

$$2\omega_\gamma=\frac{1}{h_1h_2}\left[\frac{\partial}{\partial\alpha}(h_2u_\beta)-\frac{\partial}{\partial\beta}(h_1u_\alpha)\right] \tag{14}$$

The equations (8), (9), and (10) represent the general displacement shell equations and are applicable to thick as well as thin shells. Any solution which purports to be an exact one must satisfy this system of equations.

In applying the above system of equations to a thin elastic shell, use will be made of the first of the Kirchoff hypotheses. The various parameters which enter into the equations will be expressed as power series in γ. Since the shell is assumed to be thin, the series will be truncated at that point where the further contribution of the omitted terms will be smaller than the inherent error due to the Kirchoff hypothesis, namely $k\delta$.

The consequence of the first of the Kirchoff hypothesis in linear shell theory is to prescribe a linear variation in the γ direction for the tangential displacements u_α and u_β. The corresponding strains, $e_{\alpha\alpha}$, $e_{\beta\beta}$ and $e_{\alpha\beta}$ can then be shown to be linear in the coordinate though to do so it is necessary to truncate a Taylor expansion. Assuming now that the plane stress condition exists, namely $\sigma_{zz} \approx 0$, then at each point in the shell the normal strain $e_{\gamma\gamma}$ will be a linear function of the strains $e_{\alpha\alpha}$, $e_{\beta\beta}$, and hence will be of the same order of magnitude as these strains. Thus $e_{\gamma\gamma}$ will also be a linear function of the coordinate γ. The net result is that the dilatation, which is the sum of the three normal strains, will also be a linear function of the variable γ.

The rotation component ω_γ is involved with the tangential displacements u_α and u_β, both linear in γ. But more importantly, it can be shown that this component of rotation is of the same order of magnitude as the shear strain $e_{\alpha\beta}$ which is linear in γ. Thus the rotation component ω_γ may be considered a linear function of γ.

The rotation components ω_α and ω_β can be shown to be of the same order of magnitude as the shear strains $e_{\alpha\gamma}$ and $e_{\beta\gamma}$. However nothing can be said of the order of magnitude of these strains and therefore a definite truncated expansion in powers of γ cannot be made for these rotation components. Even if an expansion could be made for these components, a certain contradiction would occur since the Kirchoff hypothesis negates the warpage of the normal and hence the existence of the transverse shear stress.

Rather than deal with rotation components ω_α and ω_β, these terms will be expanded in their displacement form as given by (12) and (13). Since the rotation components are of the same order of magnitude as the transverse shear strains, then in recombining the displacement expressions for the rotations it might well be expected that groups of terms can be readily rearranged to form transverse shear strain and hence shear stress expressions. As is normally done in shell analysis based on the Kirchoff hypothesis, these quantities are then carried along in the equations without any statement regarding their explicit form and ultimately eliminated from the shell equations by substitution.

Based on the above arguments, the equations of equilibrium, (8), (9), and (10), may be rewritten as the following.

$$(\lambda+2\mu)h_2\frac{\partial\Delta}{\partial\alpha}-2\mu h_1\frac{\partial\omega_\gamma}{\partial\beta}+2\mu ABK u_\alpha-2\mu\frac{\partial}{\partial\gamma}\left(h_2\frac{\partial u_\gamma}{\partial\alpha}\right) \tag{15}$$
$$+\frac{1}{h_1}\frac{\partial}{\partial\gamma}\left(h_1^2 h_2\sigma_{\alpha\gamma}\right)+h_1h_2P_\alpha=0$$

$$(\lambda+2\mu)h_1\frac{\partial\Delta}{\partial\beta}+2\mu h_2\frac{\partial\omega_\gamma}{\partial\alpha}+2\mu ABK u_\beta-2\mu\frac{\partial}{\partial\gamma}\left(h_1\frac{\partial u_\gamma}{\partial\beta}\right) \tag{16}$$
$$+\frac{1}{h_2}\frac{\partial}{\partial\gamma}\left(h_2^2 h_1\sigma_{\beta\gamma}\right)+h_1h_2P_\beta=0$$

$$-2(\lambda+2\mu)(H+K\gamma)AB\Delta+2\mu\left[\frac{\partial}{\partial\alpha}(Bk_2u_\alpha)+\frac{\partial}{\partial\beta}(Ak_1u_\beta)+2ABKu_\gamma\right] \tag{17}$$
$$+4\mu AB(H+K\gamma)\frac{\partial u_\gamma}{\partial\gamma}+\frac{\partial}{\partial\alpha}(h_2\sigma_{\alpha\gamma})+\frac{\partial}{\partial\beta}(h_1\sigma_{\beta\gamma})+\frac{\partial}{\partial\gamma}(h_1h_2\sigma_{\gamma\gamma})+h_1h_2P_\gamma=0$$

In deriving the above form, use was made of the conditions of Codazzi and Gauss, namely,

$$\frac{1}{h_2}\frac{\partial h_2}{\partial\gamma}\frac{\partial h_1}{\partial\beta}=\frac{\partial^2 h_1}{\partial\beta\partial\gamma}$$

$$\frac{1}{h_1}\frac{\partial h_1}{\partial \gamma}\frac{\partial h_2}{\partial \alpha} = \frac{\partial^2 h_2}{\partial \alpha \partial \gamma}$$

$$\frac{\partial}{\partial \alpha}\left(\frac{1}{h_1}\frac{\partial h_2}{\partial \alpha}\right) + \frac{\partial}{\partial \beta}\left(\frac{1}{h_2}\frac{\partial h_1}{\partial \beta}\right) = -ABK$$

and the stress strain relations for the transverse shear stresses as well as the displacement definitions for the transverse shear strains.

$$\sigma_{\alpha\gamma} = 2\mu\left[h_1\frac{\partial}{\partial \gamma}\left(\frac{u_\alpha}{h_1}\right) + \frac{1}{h_1}\frac{\partial u_\gamma}{\partial \alpha}\right]$$

$$\sigma_{\beta\gamma} = 2\mu\left[h_2\frac{\partial}{\partial \gamma}\left(\frac{u_\beta}{h_2}\right) + \frac{1}{h_2}\frac{\partial u_\gamma}{\partial \beta}\right]$$

$$\sigma_{\gamma\gamma} = (\lambda+2\mu)\Delta - 2\mu\left[\frac{1}{h_1}\frac{\partial u_\alpha}{\partial \alpha} + \frac{1}{h_1 h_2}\frac{\partial h_1}{\partial \beta}u_\beta + \frac{1}{h_1}\frac{\partial h_1}{\partial \gamma}u_\gamma + \frac{1}{h_2}\frac{\partial u_\beta}{\partial \beta} + \frac{1}{h_1 h_2}\frac{\partial h_2}{\partial \alpha}u_\alpha + \frac{1}{h_2}\frac{\partial h_2}{\partial \gamma}u_\gamma\right]$$

Note that equations (15), (16) and (17) are still the general shell equations in which no simplifications have been introduced. In the third equation, which is equivalent to force summation in the γ direction, it is necessary to explicity state $\sigma_{\gamma\gamma}$ in order to take into account surface loads. In solving these equations, under a plane stress restriction, a contradiction will result in that the third equation will contain functions directly dependent on this normal stress. However the magnitude of error from this descrepancy should be no more than that encountered from the use of the first of Kirchoff hypothesis.

Letting u, v and w represent the displacement components of the middle surface along the tangents to the α, β and γ coordinate axis respectively, the first of the Kirchoff hypothesis leads to the following relations for the tangential displacements

$$u_\alpha = u + \left(k_1 u - \frac{1}{A}\frac{\partial w}{\partial \alpha}\right)\gamma + \left(k_1 u - \frac{1}{A}\frac{\partial w}{\partial \alpha}\right)\int_0^\gamma e_{\gamma\gamma}\,d\gamma$$

$$u_\beta = v + \left(k_2 v - \frac{1}{B}\frac{\partial w}{\partial \beta}\right)\gamma + \left(k_2 v - \frac{1}{B}\frac{\partial w}{\partial \beta}\right)\int_0^\gamma e_{\gamma\gamma}\,d\gamma$$

Since the expression for $e_{\gamma\gamma}$ must certainly contain displacements or their derivatives, a linear solution for the tangential displacements will be

$$u_\alpha = u + \left(k_1 u - \frac{1}{A}\frac{\partial w}{\partial \alpha}\right)\gamma \tag{18}$$

$$u_\beta = v + \left(k_2 v - \frac{1}{B}\frac{\partial w}{\partial \beta}\right)\gamma \tag{19}$$

Hence the tangential displacements are unchanged from the values that would be found if the first and second of the Kirchoff hypotheses were used.

The dilatation Δ in polynomial form is given as

$$\Delta = \Delta_0 + \Delta_1 \gamma \tag{20}$$

and the rotation ω_γ in polynomial form is

$$\omega_\gamma = \omega_0 + \omega_1 \gamma \tag{21}$$

In order to determine the expression for the normal displacement component u_γ, it is first necessary to determine the expression for the strain $e_{\gamma\gamma}$. From the condition of plane stress

$$e_{\gamma\gamma} = -\frac{\nu}{(1-\nu)}\left(e_{\alpha\alpha} + e_{\beta\beta}\right)$$

The above may be rearranged so that

$$e_{\gamma\gamma} = -\frac{\lambda}{2\mu}\Delta \tag{22}$$

Substituting (20) for the dilatation and using the definition for the strain, namely

$$e_{\gamma\gamma} = \frac{\partial u_\gamma}{\partial \gamma}$$

the above equation may be integrated with respect to to yield

$$u_\gamma = w - \frac{\lambda}{2\mu}\Delta_0 \gamma - \frac{\lambda}{4\mu}\Delta_1 \frac{\gamma^2}{2} \tag{23}$$

Hence unlike the tangential displacement components, the normal displacement component must be chosen as a quadratic in γ.

In order to determine the dilatation components expression (18), (19) and (23) together with the expressions for h_1 and h_2 are substituted into (11) and the resulting polynomial in γ is truncated so as to be linear. Comparing this resulting expression with (20), the following result.

$$\Delta_0 = \frac{2\lambda}{(\lambda+2\mu)}\frac{1}{AB}\left[\frac{\partial}{\partial\alpha}(B\mu)+\frac{\partial}{\partial\beta}(Av)\right]+\frac{4\mu}{(\lambda+2\mu)}H w \tag{24}$$

$$\Delta_1 = \frac{4\mu}{(\lambda+2\mu)}\frac{1}{AB}\left[\frac{\partial}{\partial\alpha}(HB\mu)+\frac{\partial}{\partial\beta}(HAv)\right]-\frac{2\mu}{(\lambda+2\mu)}\frac{1}{AB}\left[\frac{\partial}{\partial\alpha}\left(\frac{B}{A}\frac{\partial w}{\partial\alpha}\right)\right.$$
$$\left.+\frac{\partial}{\partial\beta}\left(\frac{A}{B}\frac{\partial w}{\partial\beta}\right)\right]+\frac{8\mu^2}{(\lambda+2\mu)^2}\frac{H}{AB}\left[\frac{\partial}{\partial\alpha}(B\mu)+\frac{\partial}{\partial\beta}(Av)\right]+\frac{4\mu}{(\lambda+2\mu)}\left[K \tag{25}$$
$$-\frac{4(\lambda+\mu)}{(\lambda+2\mu)}H^2\right]w$$

In a similar manner, the rotation components may be determined as follows

$$\omega_0 = \frac{1}{2AB}\left[\frac{\partial}{\partial\alpha}(Bv)-\frac{\partial}{\partial\beta}(A\mu)\right] \tag{26}$$

$$\omega_1 = -\frac{(k_1-k_2)}{2}\left[\frac{A}{B}\frac{\partial}{\partial\beta}\left(\frac{\mu}{A}\right)+\frac{B}{A}\frac{\partial}{\partial\alpha}\left(\frac{v}{B}\right)\right] \tag{27}$$

Having expressed the dilatation Δ, the rotation ω_γ, the displacements $u_\alpha, u_\beta, u_\gamma$ in polynomials in γ, the three equilibrium equations, (15), (16), and (17) are transformed into polynomials in the variable γ. These equations may first be integrated with respect to $d\gamma$ over the shell thickness δ. The result will be three equations in terms of five unknowns, the three components of the middle surface displacement and the two transverse shear stress resultants. A second integration of the first two of the equilibrium equations, (15) and (16), with respect to

$\gamma d\gamma$ over the shell thickness will result in two additional equations in the same unknowns. Thus five equations in terms of five unknowns result.

Rather than make the substitution for the dilatation and rotation components as given by (24), (25), (26) and (27), or for the displacement component u_γ, it would be simpler to leave the five equations in terms of Δ_0, Δ_1, ω_0, ω_1 and integrals of u_γ. These five equations are as follows

$$(\lambda+2\mu)B\left(\frac{\partial\Delta_0}{\partial\alpha}+k_2\frac{\delta^2}{12}\frac{\partial\Delta_1}{\partial\alpha}\right)-2\mu A\left(\frac{\partial\omega_0}{\partial\beta}+k_1\frac{\delta^2}{12}\frac{\partial\omega_1}{\partial\beta}\right)+2\mu ABK u$$
$$-\frac{2\mu}{\delta}\int_{-\delta/2}^{\delta/2}\frac{\partial}{\partial\gamma}\left(h_2\frac{\partial u_\gamma}{\partial\alpha}\right)d\gamma+\frac{AB}{\delta}k_1 Q_1+\frac{AB}{\delta}X=0 \tag{28}$$

$$(\lambda+2\mu)A\left(\frac{\partial\Delta_0}{\partial\beta}+k_1\frac{\delta^2}{12}\frac{\partial\Delta_1}{\partial\beta}\right)+2\mu B\left(\frac{\partial\omega_0}{\partial\alpha}+k_2\frac{\delta^2}{12}\frac{\partial\omega_1}{\partial\alpha}\right)+2\mu ABK v$$
$$-\frac{2\mu}{\delta}\int_{-\delta/2}^{\delta/2}\frac{\partial}{\partial\gamma}\left(h_1\frac{\partial u_\gamma}{\partial\beta}\right)d\gamma+\frac{AB}{\delta}k_2 Q_2+\frac{AB}{\delta}Y=0 \tag{29}$$

$$-2(\lambda+2\mu)AB\left(H\Delta_0+K\frac{\delta^2}{12}\Delta_1\right)+2\mu\left[\frac{\partial}{\partial\alpha}(Bk_2 u)+\frac{\partial}{\partial\beta}(Ak_1 v)\right]$$
$$+4\mu\frac{ABK}{\delta}\int_{-\delta/2}^{\delta/2}u_\gamma\,d\gamma+4\mu\frac{AB}{\delta}\int_{-\delta/2}^{\delta/2}(H+K\gamma)\frac{\partial u_\gamma}{\partial\gamma}d\gamma+\frac{\partial}{\partial\alpha}\left(\frac{BQ_1}{\delta}\right)$$
$$+\frac{\partial}{\partial\beta}\left(\frac{AQ_2}{\delta}\right)+\frac{AB}{\delta}Z=0 \tag{30}$$

$$(\lambda+2\mu)\frac{B\delta^3}{12}\left(\frac{\partial\Delta_1}{\partial\alpha}+k_2\frac{\partial\Delta_0}{\partial\alpha}\right)-2\mu A\frac{\delta^3}{12}\left(\frac{\partial\omega_1}{\partial\beta}+k_1\frac{\partial\omega_0}{\partial\beta}\right)+2\mu ABK\frac{\delta^3}{12}\left(k_1 u\right.$$
$$\left.-\frac{1}{A}\frac{\partial w}{\partial\alpha}\right)-2\mu\int_{-\delta/2}^{\delta/2}\gamma\frac{\partial}{\partial\gamma}\left(h_2\frac{\partial u_\gamma}{\partial\alpha}\right)d\gamma-ABQ_1=0 \tag{31}$$

$$(\lambda+2\mu)A\frac{\delta^3}{12}\left(\frac{\partial\Delta_1}{\partial\beta}+k_1\frac{\partial\Delta_0}{\partial\beta}\right)+2\mu B\frac{\delta^3}{12}\left(\frac{\partial\omega_1}{\partial\alpha}+k_2\frac{\partial\omega_0}{\partial\alpha}\right)+2\mu ABK\frac{\delta^3}{12}\left(k_2 v\right.$$
$$\left.-\frac{1}{B}\frac{\partial w}{\partial\beta}\right)-2\mu\int_{-\delta/2}^{\delta/2}\gamma\frac{\partial}{\partial\gamma}\left(h_1\frac{\partial u_\gamma}{\partial\beta}\right)d\gamma-ABQ_2=0 \tag{32}$$

In these expressions, the transverse shear stress resultants Q_1 and Q_2 are defined as;

$$Q_1=\frac{1}{B}\int_{-\delta/2}^{\delta/2}h_2\sigma_{\alpha\gamma}d\gamma \qquad Q_2=\frac{1}{A}\int_{-\delta/2}^{\delta/2}h_1\sigma_{\beta\gamma}d\gamma$$

The components of the middle surface loading, X , Y and Z are given as;

$$X = \frac{1}{AB}\left[h_1 h_2 \sigma_{\alpha\gamma}\Big|_{-\delta/2}^{\delta/2} + \int_{-\delta/2}^{\delta/2} h_1 h_2 P_\alpha d\gamma\right]$$

$$Y = \frac{1}{AB}\left[h_1 h_2 \sigma_{\beta\gamma}\Big|_{-\delta/2}^{\delta/2} + \int_{-\delta/2}^{\delta/2} h_1 h_2 P_\beta d\gamma\right]$$

$$Z = \frac{1}{AB}\left[h_1 h_2 \sigma_{\gamma\gamma}\Big|_{-\delta/2}^{\delta/2} + \int_{-\delta/2}^{\delta/2} h_1 h_2 P_\gamma d\gamma\right]$$

Equations (31) and (32) may now be solved for Q_1 and Q_2 and these expressions substituted into (28), (29) and (30). Thus the resulting system of equations will be three in number ultimately containing only three unknowns, namely the components of the middle surface displacement. These resulting equations may be simplified by neglecting terms which give a refinement greater than the error inherent in the analysis from the utilization of the first of the Kirchoff hypothesis. That is, the approximation will be made that $(1+k^2\delta^2)\approx 1$. It will also be assumed that the curvature change and torsion expressions for the middle surface may be simplified so as to include only the normal displacement term w.

Subsituting the expressions for Q_1 and Q_2 and the expressions for the dilatation components, the rotation components and the normal displacement, and simplifying, equations (28), (29), and (30) become the following.

$$\frac{4\lambda(\lambda+\mu)}{(\lambda+2\mu)}\frac{1}{A}\left[\frac{\partial^2(B\mu)}{\partial\alpha^2}+\frac{\partial^2(Av)}{\partial\alpha\partial\beta}\right]+\frac{8\mu(\lambda+\mu)}{(\lambda+2\mu)}B\frac{\partial(Hw)}{\partial\alpha}-\frac{\mu}{B}\left[\frac{\partial^2(Bv)}{\partial\alpha\partial\beta}\right. \qquad (33)$$
$$\left.-\frac{\partial^2(A\mu)}{\partial\beta^2}\right]+2\mu ABK\mu-2\mu Bk_2\frac{\partial w}{\partial\alpha}+\frac{AB}{\delta}X=0$$

$$\frac{4\lambda(\Upsilon+\lambda)}{(\Upsilon+2\lambda)}\frac{1}{B}\left[\frac{\partial^2(A\nu)}{\partial\beta^2}+\frac{\partial^2(B\mu)}{\partial\alpha\partial\beta}\right]+\frac{8\lambda(\Upsilon+\lambda)}{(\Upsilon+2\lambda)}A\frac{\partial(H\omega)}{\partial\beta}-\frac{\lambda}{A}\left[\frac{\partial^2(A\mu)}{\partial\alpha\partial\beta}\right.$$
$$\left.-\frac{\partial^2(B\nu)}{\partial\alpha^2}\right]+2\lambda ABK\nu-2\lambda Ak_1\frac{\partial\omega}{\partial\beta}+\frac{AB}{\delta}Y=0 \qquad (34)$$

$$2\lambda\left[\frac{\partial}{\partial\alpha}(Bk_2\mu)+\frac{\partial}{\partial\beta}(Ak_1\nu)\right]-\frac{8\lambda(\Upsilon+\lambda)}{(\Upsilon+2\lambda)}H\left[\frac{\partial}{\partial\alpha}(B\mu)+\frac{\partial}{\partial\beta}(A\nu)\right]+4\lambda AB\left[K\right.$$
$$\left.-\frac{4(\Upsilon+\lambda)}{(\Upsilon+2\lambda)}H^2\right]\omega-\frac{\lambda(\Upsilon+\lambda)}{3(\Upsilon+2\lambda)}AB\nabla_e^4\omega+\frac{AB}{\delta}Z=0 \qquad (35)$$

The quantity ∇_e^4 is the biharmonic elliptical operator. The harmonic elliptical operator is defined as

$$\nabla_e^2=\frac{1}{AB}\left[\frac{\partial}{\partial\alpha}\left(\frac{B}{A}\frac{\partial}{\partial\alpha}\right)+\frac{\partial}{\partial\beta}\left(\frac{A}{B}\frac{\partial}{\partial\beta}\right)\right]$$

In terms of the elastic constants E and ν, the equations (33), (34) and (35) become

$$\frac{1}{A}\left[\frac{\partial^2(B\mu)}{\partial\alpha^2}+\frac{\partial^2(A\nu)}{\partial\alpha\partial\beta}\right]+2B\frac{\partial(H\omega)}{\partial\alpha}-\frac{(1-\nu)}{2B}\left[\frac{\partial^2(B\nu)}{\partial\alpha\partial\beta}-\frac{\partial^2(A\mu)}{\partial\beta^2}\right]$$
$$+(1-\nu)ABK\mu-(1-\nu)Bk_2\frac{\partial\omega}{\partial\alpha}+(1-\nu^2)\frac{AB}{E\delta}X=0 \qquad (36)$$

$$\frac{1}{B}\left[\frac{\partial^2(A\nu)}{\partial\beta^2}+\frac{\partial^2(B\mu)}{\partial\alpha\partial\beta}\right]+2A\frac{\partial(H\omega)}{\partial\beta}-\frac{(1-\nu)}{2A}\left[\frac{\partial^2(A\mu)}{\partial\alpha\partial\beta}-\frac{\partial^2(B\nu)}{\partial\alpha^2}\right]$$
$$+(1-\nu)ABK\nu-(1-\nu)Ak_1\frac{\partial\omega}{\partial\beta}+(1-\nu^2)\frac{AB}{E\delta}Y=0 \qquad (37)$$

$$(1-\nu)\left[\frac{\partial}{\partial\alpha}(Bk_2\mu)+\frac{\partial}{\partial\beta}(Ak_1\nu)\right]-2H\left[\frac{\partial}{\partial\alpha}(B\mu)+\frac{\partial}{\partial\beta}(A\nu)\right]+2AB\left[(1-\nu)K\right.$$
$$\left.-2H^2\right]\omega-AB\frac{\delta^2}{12}\nabla_e^4\omega+(1-\nu^2)\frac{AB}{E\delta}Z=0 \qquad (38)$$

CONCLUSIONS

The resulting shell equations, (33), (34), (35) or (36), (37), (38), degenerate to the plate equation for $k_1 = k_2 = 0$. If the second of the Kirchoff hypothesis were utilized together with the plane stress assumption,

a displacement development of the shell equations would still be possible. The structure of the equations would be identical to those dreived. However, the elastic coefficients of the resulting equations would differ from those presented. Further, if the solution were degenerated to that of a plate, the resulting plate equation would not be the one that is encountered in plate theory. Though the variable would be the same on the plate equation, the constant dependent on the elastic properties would be the one which would be found if the plate were solved as a plane strain problem. Thus it appears that if the plane stress and plane strain conditions are assumed simultaneously in a displacement formulation of the thin elastic shell equations, the plane strain condition will prevail.

Vlasov develops the thin elastic displacement shell equations in a manner analogous to that described. Unlike the derivation presented, his analysis utilizes the second of the Kirchoff hypotheses and thus assumes that the normal displacement, μ_ν, is constant though the shell thickness. As might be expected, his resulting equations stated in the elastic constants λ and k differ from those presented in this paper. In fact, using the proper definitions of λ and k, his development is that for plane strain rather than plane stress. However, his equations stated in terms of the elastic constants E and ν are the same as (36), (37) and (38). This apparent contradiction comes about from Vlasov's redefinition of λ;

$$\lambda = \frac{E\nu}{(1-\nu^2)}$$

This is the equivalent Lamé elastic constant for the plane stress problem.

REFERENCES

1. Reissner, E., Hildebrand, F. G., Thomas, G. B., "Notes on the Foundations of the Theory of Small Displacements of Orthotropic Shells, NACA Technical Note No. 1833, (March 1949).

2. Vlasov, V. Z., "Basic Differential Equations In the General Theory of Elastic Shells," (translation from Russian), NACA Technical Memorandum 1241, (1951).

3. Vlasov, V. Z., General Theory of Shells and Its Applications to Engineering (translation from Russian), NASA Technical Translation, NASA TT F-99, National Aeronautics and Space Administration, Washington, D. C. (April 1964).

AN ANALYTICAL INVESTIGATION OF THE FRANGIBLE TUBE ENERGY ABSORPTION SYSTEM TO DETERMINE THE AVERAGE STATIC FRAGMENTATION FORCE

by

ARMAND JOSEPH CHAPUT

AEROSPACE ENGINEERING DEPARTMENT AND SPACE TECHNOLOGY DIVISION

TEXAS A&M UNIVERSITY

ENCLOSURE 2

TABLE OF SYMBOLS

Symbol	Description	Units
F	Force	lb.
F_1	Initial force	lb.
$F(\varphi)$	Generalized force	lb.
F_3	Maximum force after initial fragmentation	lb.
F_2	Minimum force	lb.
F_{avg}	Average force	lb.
F_T	Theoretically predicted force	lb.
M	Moment	in-lb/in.
R	Resultant force	lb/in.
P	Resultant force in vertical direction	lb/in.
Q	Resultant force in horizontal direction	lb/in.
T	Frictional force tangent to die surface	lb/in.
N	Force normal to die surface	lb/in.
F_{TY}	Tensile yield stress	psi
F_{TU}	Tensile ultimate stress	psi
f	Coefficient of friction	dimensionless
D	Outside tube diameter	in.
h	Tube thickness	in.
a_t	Initial tube radius	in.
a	Die guide radius	in.
a'	Final radius	in.
r	Forming die radius	in.
C	Tube circumference	in.
ΔC	Change in tube circumference	in.

Symbol	Description	Units
K	Dimensionless coefficient	dimensionless
G	Dimensionless coefficient	dimensionless
φ	Angular position	dimensionless
ψ	Angular position	dimensionless
(X,Y)	Rectangular coordinates	in.
E	Modulus of elasticity	psi
ν	Poisson's ratio	dimensionless
ϵ	Tangential strain at rupture	dimensionless
ϵ_{TY}	Tangential strain at yield	dimensionless

I. Introduction

The critical weight, size, and environmental requirements demanded of spacecraft landing systems have resulted in an extensive research program to formulate, analyze, and experimentally investigate promising energy-absorption systems. Of the many systems investigated, one general method of energy absorption indicates wide application because of its efficiency, simplicity, and reliability. The method is that of mechanically loading a metal structure to produce an impact energy-absorption stroke.

One system employing the above method which appeared to satisfy all the stringent requirements demanded of an effective landing impact dissipation system is the frangible tube energy-absorption system[1]* (see Fig 1).

The frangible tube energy-absorption system dissipates impact energy by a fragmentation process. A tube is pressed over a die shaped such that the end of the tube is caused to break and fragment (see Figs. 2 and 3). This fragmentation is referred to in this report as "franging."

Although a fluctuating force (see Fig. 4) results from the fragmentation process, the mean force furing the fluctuation is approximately constant. It may be noted that a large initial force is required to initiate fragmentation. However, it is recognized that the initial peak force should be reduced as much as possible in efficient impact-attenuation systems.

*Superscripts refer to references listed at the end of this report.

Although the frangible tube energy-absorption system has many desirable qualities, it should not be considered the panacea for energy absorption applications. It was in fact the occurrence of many undesirable phenomena which prompted the analytical investigation in this report. For example, it was noted in loading two geometrically similar tube and die geometries of different scale, that one fragmented in the proper manner while the other suffered local instability with no indication of fragmentation.

It is anticipated that the simplified analysis presented will provide insight into the complicated and complex phenomenon occurring in the frangible tube system. It is recognized by the writer that the simplified approach in the following analysis will not and cannot be expected to faithfully reproduce the complicated loading and stress conditions experienced by a franging tube. However, it is considered that the approach may offer sufficient accuracy for at least preliminary engineering computations.

This report contains not only the final analysis of the system, but also a history of previously attempted analyses performed in conjunction with this research. It is a secondary objective of this report that many of the "blind alleys" encountered during this investigation may be of interest to other investigators.

II. Derivations

The derivations will be presented in the order in which they were developed.

First Analysis - Derivation

The first analysis was attempted under the following simplifying assumptions:

1) Friction is neglected.

2) All deflections are considered small.

3) Failure of the tube occurs as the circumferential strain reaches a maximum value.

4) The tube is considered as a thin cylindrical shell.

Consider the sketch shown in Figure 5. Examining a strip of tubing of unit depth one can see, by calculating forces in the horizontal and vertical directions, Q and P, that

$$Q = R \cos\theta \tag{1a}$$

$$P = R \sin\theta \tag{2a}$$

The applied force is related to P and Q by

$$Q = P\cot\theta = \frac{F}{2\pi a}\cot\theta \tag{3a}$$

From geometric considerations it can also be seen that the deflection w is given by

$$W = r(1 - \cos\theta) \tag{4a}$$

In reference 2 (Eq. 278, p. 469) the and deflection w for a tube subjected to a radial force, Q, is determined to be

$$W = \frac{Q}{2B^3D} \tag{5a}$$

where $B^4 = \frac{3(1-\nu^2)}{a^2h^2}$

and $D = \frac{Eh^3}{12(1-\nu^2)}$

and h and a denote the tube thickness and radius respectively.

Combining Eqs. 3a and 5a produces

$$W = \frac{P\cot\theta}{2B^3D} \tag{6a}$$

From Eq. 4a one finds

$$\cos\theta = 1 - \frac{W}{r} \tag{7a}$$

where r is the radius of the forming die.

From the relationships $\sin^2\theta + \cos^2\theta = 1$ and $\frac{\cos\theta}{\sin\theta} = \cot\theta$.

one finds from Eq. 7a $$\cot\theta = \frac{1-\frac{w}{r}}{\left[2\frac{w}{r} - \left(\frac{w}{r}\right)^2\right]^{1/2}} \tag{8a}$$

The final tube radius a' is given as

$$a' = w_{max} + a$$

and the strain by

$$\epsilon = \frac{\Delta C}{C} = \frac{2\pi(a'-a)}{2\pi a} = \frac{w_{max}}{a}$$

Letting $K = \frac{r}{a}$ results in

$$\frac{w_{max}}{r} = \frac{\epsilon}{K} \tag{9a}$$

The final result is obtained by combining Eqs. 6a, 8a, and 9a when $w = w_{max}$ to give

$$\frac{F_1}{4\pi B^3 D r a} = \frac{\epsilon}{K}\,\frac{\left[2\frac{\epsilon}{K} - \left(\frac{\epsilon}{K}\right)^2\right]^{1/2}}{1-\frac{\epsilon}{K}} \tag{10a}$$

First Analysis - Discussion

Equation 10a was solved for two 2024-T3 aluminum tube and die geometries and compared with actual values given in reference 1. The values for the mechanical properties were obtained from reference 3. On the basis of the comparison, it was determined that for the two geometries studied, highly inaccurate answers resulted. It was assumed that the simplified assumptions made in the analysis were in error. Therefore, a second approach to the problem was attempted using fewer simplifying assumptions.

Second Analysis - Derivation

The second analysis was developed to include the effect of friction. Fragmentation was assumed to be initiated as the bottom

fibers of the tube were stressed to their ultimate value in the tangential direction.

Consider the sketch shown in Fig. 6. Examining a strip of tubing of unit depth it can be seen, by calculating resultant forces in the horizontal and vertical directions, respectively, that

$$P = N\sin\theta + T\cos\theta \tag{1b}$$

$$Q = N\cos\theta - T\sin\theta \tag{2b}$$

where N and T are the normal and frictional forces respectively.

From geometric considerations it can also be seen that

$$W = r(1-\cos\theta) \tag{3b}$$

Since T = fN, equations 1b and 2b can be rewritten

$$P = N(\sin\theta + f\cos\theta) \tag{4b}$$

$$Q = N(\cos\theta - f\sin\theta) \tag{5b}$$

where f denotes the coefficient of friction.

Examining a free body of the tube at rupture as shown in Fig. 7; summing forces horizontally; and assuming $\epsilon \gg \epsilon_{TY}$; one finds the relationship of the radial force Q to the mechanical properties F_{TY} and F_{TU} to be

$$2Q(a+w) = \frac{F_{TU}+F_{TY}}{2}\,2hx_1 \tag{6b}$$

or

$$Q = \frac{F_{TU}+F_{TY}}{2(a+w)}\,hx_1 \tag{7b}$$

Summing forces vertically yields

$$F = 2\pi(a+w)P \tag{8b}$$

Combining 4b, 6b, 7b, and 8b produces

$$F = \pi h x_1 (F_{TU}+F_{TY})\left[\frac{\sin\theta + f\cos\theta}{\sin\theta - f\sin\theta}\right] \tag{9b}$$

From reference 2 (Eq. 478, p. 469) the deflection for a tube subjected to a radial force, Q, is

$$w = -\frac{e^{-Bx}}{2B^3D}\left[Q \cos Bx\right]$$

where

$$B^4 = \frac{3(1-\nu^2)}{a^2h^2}$$

Since w = 0 at $x = x_1$,

$$\cos Bx_1 = 0$$

Then

$$Bx_1 = \frac{\pi}{2}$$

and

$$x_1 = \pi/2B \tag{10b}$$

From Eq. 3b, one finds

$$\cos\theta = 1 - w/r \tag{11b}$$

and from the relationship $\sin^2\theta + \cos^2\theta = 1$, one finds from Eq. 11b

$$\sin\theta = \left[2\frac{w}{r} - \left(\frac{w}{r}\right)^2\right]^{1/2} \tag{12b}$$

Now $a' = w_{max} + a$

and

$$\epsilon = \frac{\Delta C}{C} = \frac{w_{max}}{a}$$

Letting $k = \frac{r}{a}$ results in

$$\frac{w_{max}}{r} = \frac{\epsilon}{k} \tag{13b}$$

The final result is obtained by combining Eqs. 9b, 10b, 11b, 12b, and 13b when $w = w_{max}$ to give

$$F_1 = \frac{\pi^2 h}{2B}\left(F_{Tu} + F_{Ty}\right)\left[\frac{\sqrt{2\frac{\epsilon}{k} - \left(\frac{\epsilon}{k}\right)^2} + f\left(1 - \frac{\epsilon}{k}\right)}{\left(1 - \frac{\epsilon}{k}\right) - f\sqrt{2\frac{\epsilon}{k} - \left(\frac{\epsilon}{k}\right)^2}}\right] \tag{14b}$$

Second Analysis - Discussion

The numerical solution to the expression derived in the previous section for the theoretical peak fragmentation force was solved by

digital computation at the Data Processing Center at Texas A&M University. The results for eleven 2024-T3 aluminum tube and die geometries were compared with actual values obtained from the NASA Langley Research Center[4].

The value of f was initially determined by a trial-and-error solution. Three values of f (f = 0.20, 0.15, and 0.10) were used for each geometry combination and results compared with the actual values. In this manner f = 0.15 was chosen as it gave the best results. The value chosen was then verified by experimental methods.

An experimental method of determining the coefficient of friction was developed (see Fig. 8). An initially curved bar of 2024-T3 aluminum stock was loaded vertically as pictured. One end of the bar was clamped in an Olsen static testing machine while the other end was placed in contact with a machined and polished cold rolled steel plate. The steel plate rested on a roller bearing carriage which was prevented from translating by a strain-gaged thin aluminum sheet. A lubricant similar to that used in the Langley tests was then applied to the steel plate.

As the initially curved bar was loaded, a horizontal frictional force was consequently transferred to the steel plate thus causing the aluminum sheet to strain. By correlating the strain-gage readings with a predetermined calibration curve and comparing the results with the known applied normal force, the coefficient of friction for an edge-loaded aluminum specimen in contact with a lubricated steel plate was determined and found to be 0.149 (see Fig. 9).

The value of ϵ was determined by a "rule-of-thumb" approximation. The values ranged from a maximum of 0.12 to a minimum of 0.10. The value of ϵ used for each tube depended on the tube thickness, such that the maximum value of ϵ was used for the thickest tube and vice versa. For intermediate tube thicknesses, the value of was adjusted proportionately. The "rule-of-thumb" approximation was to choose values of ϵ consistent with values given for 2024-T3 sheet in reference 3.

Comparison of the theoretical and actual results showed an error varying from +27.50% to -9.98%. The average percent error was $\pm$10.50 percent* (see Table 1). It was considered at the time the equation was developed that correlation would be improved when better values of ϵ were determined. Also there was some question as to the validity of using mechanical properties of aluminum sheet to predict the properties of extruded aluminum tubing. In order to satisfy the above, a simple test was devised which would yield in addition to values of ϵ, the strength of aluminum tubing in the tangential direction.

The test consisted of loading various tube geometries such that they were pressed over the conical die shown in Fig. 10. The tubing was loaded axially until failure occurred by a longitudinal splitting of the tube. Recording the load at failure and obtaining pertinent geometry changes yielded the desired results. The validity of the test rested upon the assumption that the stress condition in a tube

*The percent error is given as $\pm$10.5% since the number was obtained so as to represent the absolute magnitude of the errors.

pressed over a forming die could be approximately reproduced by a tube pressed over the conical die just described. A detailed explanation of the test is contained below.

Consider the sketch of a tube pressed over a conical die shown in Fig. 11. Summing forces vertically yields

$$F = 2\pi a_c (N \sin\theta + T \cos\theta) \tag{15b}$$

However,

$$T = fN$$

Thus

$$F = 2\pi a_c N (\sin\theta + f \cos\theta) \tag{16b}$$

Assuming the maximum stress condition shown in Fig. 12 and summing forces vertically gives

$$2N(\cos\theta - f\sin\theta) a_c = 2hL \frac{F_{Tu} + F_{TY}}{2} \tag{17b}$$

or

$$N = \frac{hL}{2a_c} \frac{F_{Tu} + F_{TY}}{\cos\theta - f\sin\theta} \tag{18b}$$

Combining Eqs. 15b and 18b yields the result

$$F = \pi h L (F_{Tu} + F_{TY}) \frac{\sin\theta + f\cos\theta}{\cos\theta - f\sin\theta} \tag{19b}$$

For the die shown in Fig. 10 and lubricated with light oil it is known that

$$\theta = 15^\circ$$

and

$$f = 0.146$$

Combined with the above, Eq. 19b results in the final form

$$F_{TU} + F_{TY} = 0.548 \frac{F}{hL} \tag{20b}$$

Knowing the tube thickness h and measuring F and L experimentally yields the desired mechanical properties. The investigation showed

that the handbook value $(F_{TU} + F_{TY}) = 113$ ksi was valid for extruded aluminum tubing.

The results of the previously described test indicated that handbook strength predictions were sufficiently accurate; however, the values given for percent elongation were found to vary greatly from the experimentally determined values. The error was found to be in the order of 100 percent and greater.

Solving Eq. 14b using the experimental mechanical properties yielded highly unsatisfactory results. Percent errors of 400 percent were not uncommon while for some geometries negative values were calculated. Again it became immediately evident that either the simplifying assumptions or the entire approach to the problem was erroneous.

Final Analysis - Derivation

The period of time spanning from the discovery of the limitations of the second analysis and the derivation of the final analysis was typified in a large degree by attempts to alter Eq. 14b to yield satisfactory results. Various loading conditions were attempted, reference axes were shifted, and new parameters were introduced. The attempts however, were largely unsuccessful. Also during this time an experimental investigation was commenced.

By careful observation of the phenomenon occurring in the experimental investigation it was ascertained that fragmentation was initiated by one of two methods. One was the originally assumed tangential failure of the tube while the other was a flexural failure about the undeflected circumference of the tube (see Fig. 13).

The following analysis is based on the latter mode of failure.

Calculation of Generalized Force F (φ)

Consider the sketch shown in Fig. 14. Resolving normal and tangential forces in the X & Y direction it can be seen that

$$N_x = N \cos\psi \tag{1}$$

$$N_y = N \sin\psi \tag{2}$$

$$T_x = T \sin\psi \tag{3}$$

$$T_y = T \cos\psi \tag{4}$$

Assuming the coefficient of friction remains constant, it is known

$$T = fN \tag{5}$$

From geometric considerations the relationship between ψ and φ is given as

$$\psi = 2\varphi - \pi \tag{6}$$

Therefore, Eqs. 1-4 can be combined with Eqs. 5 and 6 to yield

$$N_x = N \cos 2\varphi \tag{7}$$

$$N_y = N \sin 2\varphi \tag{8}$$

$$T_x = fN \sin 2\varphi \tag{9}$$

$$T_y = fN \cos 2\varphi \tag{10}$$

Referring again to Fig. 14, it is seen that the normal and tangential forces causing the tube to deflect produce resisting moments along the deflected portion of the tube. The moment is assumed to be a maximum at rectangular coordinates (h/2,0) neglecting the effects of circumferential stresses. The moment M at (h/2,0) is given by

$$M = (N_y - T_y)\left(x - \frac{h}{2}\right) - (N_x + T_x)\,y \tag{11}$$

or combined with Eqs. 7-10

$$M = N\left[\cos\varphi(\sin\varphi - f\cos\varphi)(2r-h) - \tfrac{1}{2}fh\right] \quad (12)$$

However, it must be noted that M and N are moment and force per unit length, respectively. It can be seen that N acts along the circumference given by $2\pi(a+x)$ while M acts along the circumference $2\pi(a+h/2)$. Noting the above, Eq. 12 may be solved and the unknown force N determined. N is given by

$$N = \frac{a+h/2}{a+x} M \frac{1}{\cos\varphi(\sin\varphi - f\cos\varphi)(2r-h) - \frac{1}{2}fh} \quad (13)$$

Summing forces vertically, one finds

$$F(\varphi) = 2\pi(a+x)(N_y - T_y) \quad (14)$$

Combining Eq. 14 with Eqs. 8 and 10 yields

$$F(\varphi) = 4N\pi(a+x)\left[\cos\varphi(\sin\varphi - f\cos\varphi) + \frac{f}{2}\right] \quad (15)$$

Equations 13 and 15 may be combined to give

$$F(\varphi) = 4\pi M\left[\frac{1+\frac{f}{2}\frac{\sec\varphi}{\sin\varphi - f\cos\varphi}}{(2r-h) - \frac{1}{2}fh\frac{\sec\varphi}{\sin\varphi - f\cos\varphi}}\right]\left(a+\frac{h}{2}\right) \quad (16)$$

or rearranged in final form

$$F(\varphi) = 2\pi M\frac{\left[\frac{G}{K}+1\right]}{\left[\frac{G}{1+f\eta}-1\right]} \quad (17)$$

where

$$\eta = \frac{\sec\varphi}{\sin\varphi - f\cos\varphi}, \qquad K = \frac{r}{a}$$

and

$$G = \frac{2r}{h}$$

Examination of Eq. 17 reveals that the generalized force $F(\varphi)$ is a function of the moment determined by the stress condition at coordinates (h/2,0) and the angular position of the end of the tube in the forming die. Thus, one need know only the flexural stress condition in the tube at chosen values of φ to determine the applied force. The preceeding approach will be used to determine values of F_3 and F_2, the maximum and minimum fragmentation forces, respectively.

Calculation of the Average Fragmentation Force F_{avg}

It was observed that an initial fragmentation force was required to cause a tube to achieve its initial mode of failure. After initial failure, the fractured end contained numerous cracks and fissures. It is assumed that initial fragmentation was caused by a simultaneous flexural failure about the undeflected tube circumference.

Ideally, at the instant of fragmentation the franging tube will be in an unstressed condition. However, because of the continuously applied loading, the tube will immediately be forced into the die causing the fractured end to split into numerous cantilevered segments.

It can be seen from Eq. 17, that as the tube end is pressed into the die such that

$$\varphi_2 = \frac{1}{2}\,\text{Arc Cot}(-f) \tag{18}$$

the tube will offer the least resistance to the applied loading. Therefore, if the stress condition is assumed to be that shown in Fig. 15, the value of the minimum force F_2 will be given by

$$F_2 = 2\pi \frac{F_{TY} h^2}{4} \frac{\left[\frac{G}{R} + 1\right]}{\left[\frac{G}{1 + f\eta_2} - 1\right]} \tag{19}$$

where

$$\eta_2 = \frac{\text{Sec}\,\varphi_2}{\text{Sin}\,\varphi_2 - f\,\text{Cos}\,\varphi_2} \tag{20}$$

and φ_2 is given by Eq. 18.

As the end of the tube continues past the point defined by φ_2, the ability of the tube to resist the applied loading increases. Thus, as the end of the tube deflects to a point such that

$$\eta_3 = \frac{1}{f}(G - 1) \tag{21}$$

an infinite applied force is required to cause the tube to experience a flexural failure about the undeflected circumference. Eq. 21 indicates that the end of the tube is located such that the resultant of the normal and frictional forces is acting along a line passing through the point $(\frac{h}{2},0)$ the condition imposed by a zero moment at $(\frac{h}{2},0)$ is that no rotation occur about the point. Therefore, the applied force causes the entire deflected portion of the tube to press vertically into the die. Observation of the fragmentation process indicates that the loading on the deflected portion of the tube can be replaced by a single resultant R, acting at a point such that R has no horizontal component or the point defined by the angle φ_2 .

Consider the configuration shown in Fig. 16 summing forces vertically it is seen

$$F_3 = 2\pi(a+x)R \tag{22}$$

It was observed that as a cantilevered segment failed, the segment rotated about a plastic hinge formed at the outside edge of the tube. The moment about the outside edge, or coordinate (h,0), is related to the resultant R by

$$2\pi R(a+x)(x-h) = 2\pi M(a+h) \tag{23}$$

combining Eq. 22 and Eq. 23 yields

$$F_3 = 2\pi M \frac{a+h}{x-h} \tag{24}$$

However, it was assumed that R acted at the point defined by φ_2, therefore

$$x = 2r\cos^2\varphi_2 \tag{25}$$

thus Eq. 24 can be written

$$F_3 = 2\pi M \frac{a+h}{2r\cos^2\varphi - 1} \tag{26}$$

or in another form $$F_3 = \pi M \frac{R1}{G\cos^2\varphi_2 - 1} \tag{27}$$

where G and R1 are defined as

$$G = \frac{2r}{h}$$

and $$R1 = D/h$$

From data obtained in the experimental investigation conducted in conjunction with this report, the value of M was solved by trial and error and found to be $$M = \frac{F_{TU} h^{1.2}}{33.2} \tag{28}$$

thus in the final form, F_3 is given as

$$F_3 = \pi \frac{F_{TU} h^{1.2}}{33.2} \frac{R1}{G\cos^2\varphi_2 - 1} \tag{29}$$

The average fragmentation force F_{avg} is defined as

or $$F_{avg.} = \frac{F_2 + F_3}{2}$$

$$F_{avg.} = \frac{\pi F_{TU}}{2} \left\{ \frac{h^2}{2} \left[\frac{\frac{G}{K} + 1}{\frac{G}{1 + f\eta_2} - 1} \right] + \frac{h^{1.2}}{33.2} \frac{R1}{G\cos^2\varphi_2 - 1} \right\}$$

where

$$G = 2r/h$$

$$R1 = D/h$$

$$k = r/a$$

$$\eta_2 = \frac{\sec\varphi_2}{\sin\varphi_2 - f\cos\varphi_2}$$

and $$\varphi_3 = \frac{1}{2}\,\text{Arc Cot}(-f)$$

III. Experimental Procedures

The equations derived in the proceding section were solved and compared with experimental values for seven tube and die geometries (see Table 2). The tubing used in the experimental investigation was 2024-T3 aluminum. The dies were machined from cold-rolled steel stock and lubricated with light lubricating oil in each test. The static tests were performed on a Baldwin 60,000 pound capacity hydraulic static testing machine.

Because of the rapidly fluctuating forces which were expected in the testing, it was felt that a mechanical load-recording device would be required. Also it was considered desirable to simultaneously record displacement readings. As the testing machine did not have suitable instrumentation to allow mechanical recording, it became necessary to design and construct a suitable system.

The instrumentation system used in the experimental investigation is seen in Fig. 17. A Trans-Sonics type 1090 pressure transducer is located at the top of the Baldwin machine and tapped into a convenient orifice in the hydraulic system. Similarly, a Bourns type 109-89-752 linear displacement transducer is affixed between the stationary and movable heads of the testing machine to simultaneously record displacement readings. The recorder used in conjunction with the transducers was a twelve-channel Honeywell Visicorder recording oscilograph employing Honeywell M-200-120 glavonometers with a flat frequency response of 200 cps.

In both cases the transducers were employed such that they would be the variable resistance in a Wheatstone bridge circuit. The displacement transducer had a self-contained bridge and power supply attached. The pressure transducer had an external power supply

and bridge. The bridge for the pressure transducer was constructed with three variable resistances so that the bridge could be applied to any general instrumentation situation employing such a device. The bridge can be seen located to the left of the Honeywell recorder in Fig. 17.

The instrumentation was then calibrated and gave excellent service throughout the period of the experimental investigation.

The frangible tube specimens were placed on the compression side of the testing machine loading head and fragmented through the dissipation stroke.

The tubing used in the investigation was the standard size and quality. Prior to testing, all specimens were faced in a lathe and polished to remove all surface imperfections. The geometry was then determined and the tube fragmented in the static testing machine (see Fig. 18).

IV. Experimental Verification and Disucssion

The experimental verification consisted of solving the equation predicting the average fragmentation force and comparing the theoretical with actual results. The equation was solved by digital computation and the results presented in tabular formal for a wide range of tube and die geometries. The solutions in a design table format are presented in Tables 4 through 50.

By initially solving the equations for specific geometries and three valves of the coefficient of friction (f = 0.10,0.15 and 0.20), it was found that a variation of f within the described range had little effect on the final result. Therefore, the tabular results were all solved for f = 0.15.

The exponents of the tube thickness in Eq. 30 ($h^{1.2}$ and h^2) prevent the solution from being presented in the form of dimensionless ratios. However, to allow for variation of mechanical properties of 2024-T3 aluminum, the solution is given in the form of F_{avg} / F_{tu}. In order to set the upper limit on the allowable h/r ratios, the computer solution was programed such that if the average stress in the tube exceeded yield, the value of F_{avg} / F_{tu} would be output as 0.0.

Note that in each design table, D/h is held constant while the parameters h/r and h vary. The parameter h/r is defined as R2 and appears down the left hand side of the table. For each value of $\frac{h}{r}$ the corresponding row yields values of F_{avg} / F_{tu} for standard aluminum tube wall thicknesses (h = .022,.028,.035,.049,.058,.065, .083 and .095). Separate tables appear for each value of D/h, from D/h = 3.75 to D/h = 60.0 at intervals of D/h = 1.25. The range of h/r is from h/r = .20 to h/r = .80 at intervals of h/r = .125.

Although an upper limit is given for h/r, note that no such lower limit exists. As a rule, values of h/r less than 0.30 generally produce a rolling type failure rather than the more desirable fragmentation failure.

The resulting design tables were used to calculate the theoretical average fragmentation force for the seven tube and die geometries described in the experimental portion of this investigation. Linear interpolation was used to obtain the solutions. The results are presented in Table 2 of the Appendix. In addition, 25 tube and die geometries investigated in Ref. 4 were solved for the specific geometries involved correlated and appear in Table 3 of the Appendix.

In order to determine the ultimate strength of the seven tube geometries investigated experimentally, static tensile tests were performed. The tests yielded the value $F_{tu} = 73$ KSI. The experimentally determined value is considered quite high compared to values given in Ref. 3. Therefore, the handbook value $F_{tu} = 65$KSI was used in the solution of the 25 geometries in Table 3.

Note in Table 2 that two of the seven geometries investigated were not considered. It was found by examination of the two dies that the forming die cross sections were not circular but elliptic or parabolic in shape. The unacceptable geometries were assumed to be the result of machining errors. The two geometries do however, indicate the great influence of machining errors on resulting forces. Thus, considerable care must be exercised in the fabrication of dies used in the frangible tube system.

Examination of Tables 2 and 3 theorizes that a 66% confidence level exists for predicting the average fragmentation force within $\pm$20% accuracy. The correlation between theoretical and actual results is considered to be acceptable for preliminary engineering purposes.

V. Conclusions and Recommendations

A series of expressions has been developed in an attempt to analytically explain the phenomenon occurring in the frangible tube energy absorption process. The expressions provide not only a quantitative knowledge of the problem, but in addition a simplified explanation of the complicated mechanism which occurs during the fragmentation stroke.

The inability of the early analyses to accurately predict the actual behavior of the frangible tube system indicates the assumed

circumfrential tensile failure to be in error. The assumed mode of plastic flexural failure of the cantilevered end segments is substantialed by correlation with experimental data.

Comparison of the theoretically predicted and the actual average fragmentation force for seven tube and die geometries investigated in conjunction with this report yielded correlation well within the limits of engineering accuracy.

Correlation with twenty five geometries investigated in Ref. 1 is considered quite good. It is felt that accuracy could be improved by a knowledge of the specific mechanical properties of the tubing tested and a detailed study of the experimental methods employed. However, operating under the above handicap still indicates the theoretical values respond quite accurately to changes in geometric parameters.

The theoretically predicted upper limits on h/r ratios agree well with actual values. However, additional research is needed to develop a similar set of lower limits.

Since the theoretical equations are only valid for static applications and substantiated for only one material, additional research is required before the analytical approach contained in this report can be considered anything more than promising.

REFERENCES

1) John R. McGehee, A Preliminary Experimental Investigation of an Energy-Absorption Process Employing Frangible Metal Tubing, NASA TN D-1477, October, 1962.

2) S. Timoshenko and S. Woinowsky-Krieger, Theory of Plates and Shells, McGraw-Hill Book Company Inc., 1959.

3) Department of Defense, Military Handbook V, March, 1955.

4) NASA Langley Research Center, Unpublished Axial Force-Displacement Plots for the 2024-T3 Aluminum Frangible Tube Energy Absorption Process, November, 1963.

5) G. H. Irwin, Fracturing and Fracture Mechanics, T&AM Rpt. 202, Department of Theoretical and Applied Mechanics, University of Illinois, October, 1961.

APPENDIX

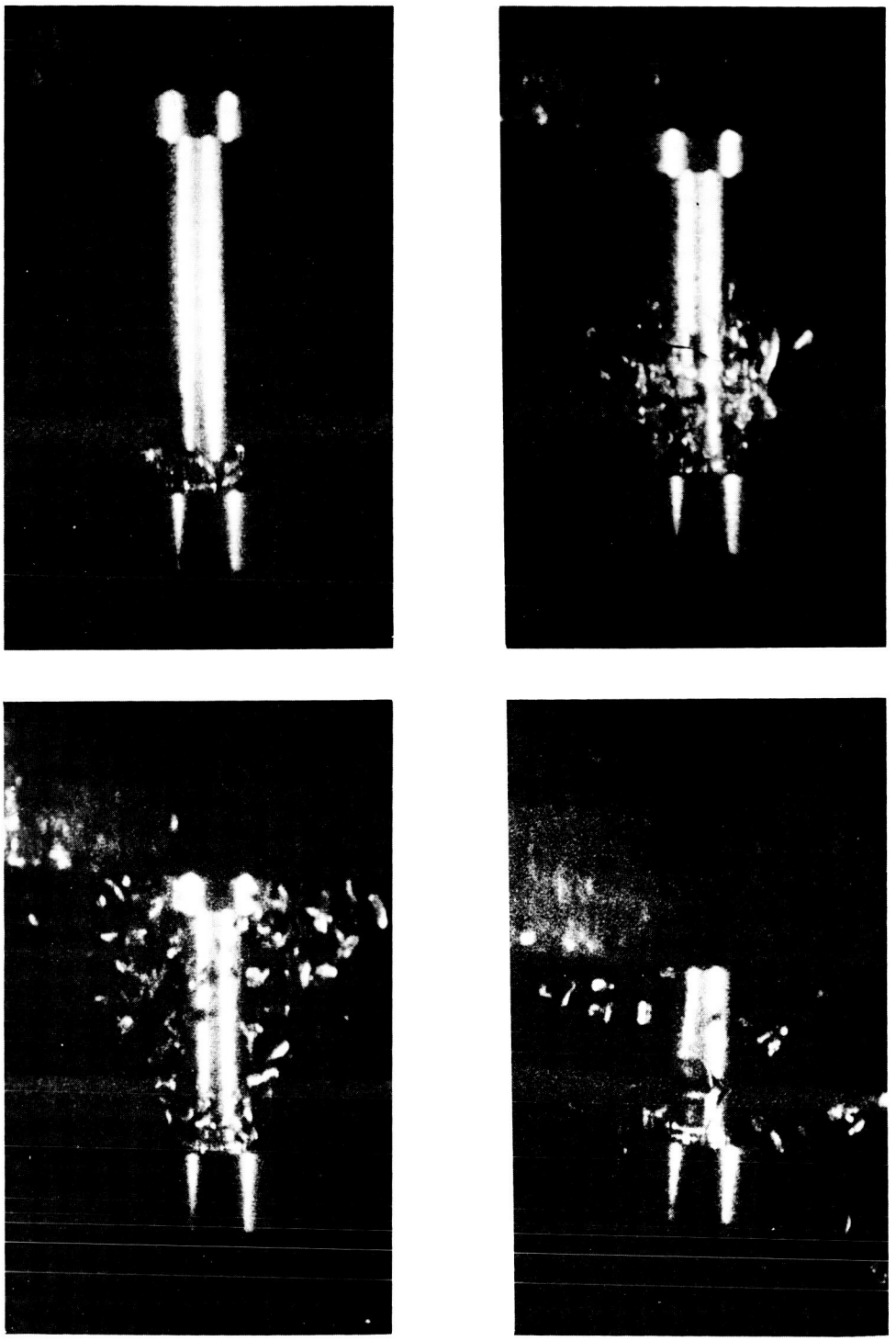

Figure 1.

Sequence Of High Speed Photographs Showing A Typical Dynamic Fragmentation Process.

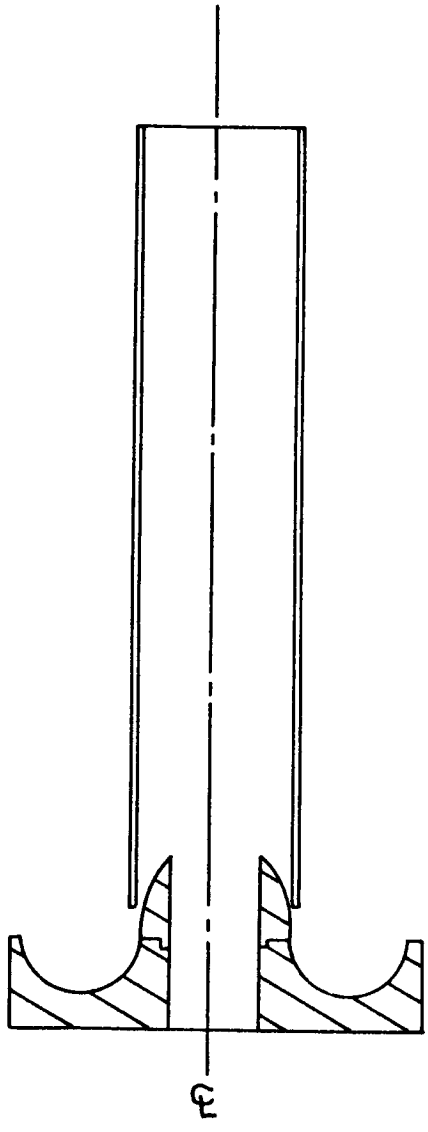

a)

Cross Section of Tube and
Die Prior to Loading

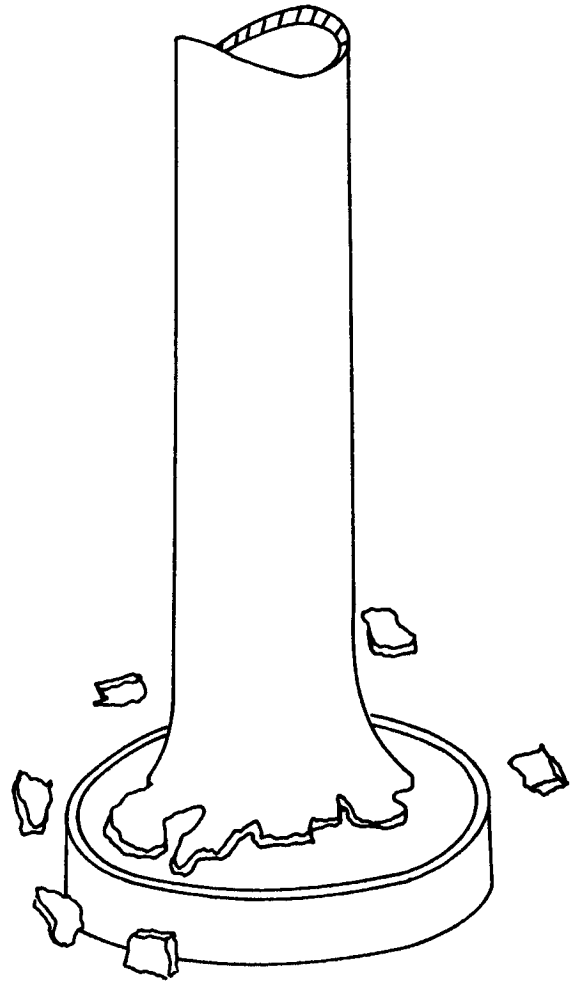

b)

Pictorial Sketch of
Fragmentation Process

Fig 2

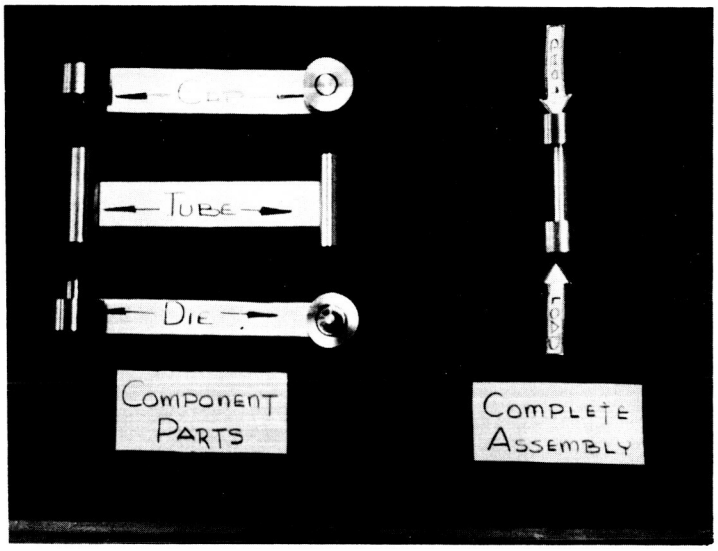

Figure 3.

Photograph of Typical Frangible Tube System With Breakdown Into Component Parts.

Typical Force vs. Displacement
Diagram for the 2024-T3 Aluminum
Frangible Tube Energy Absorption Process

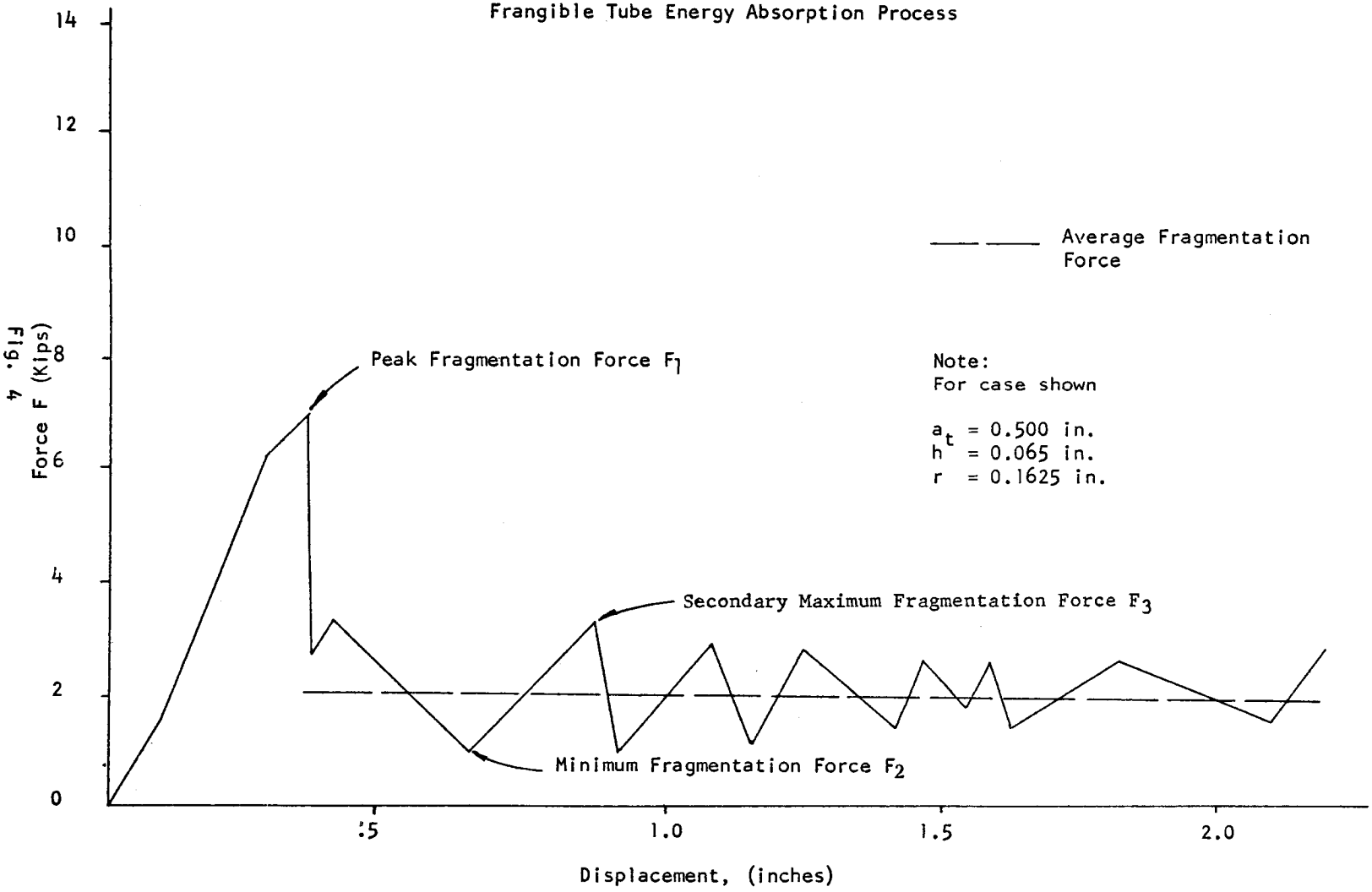

Fig. 4

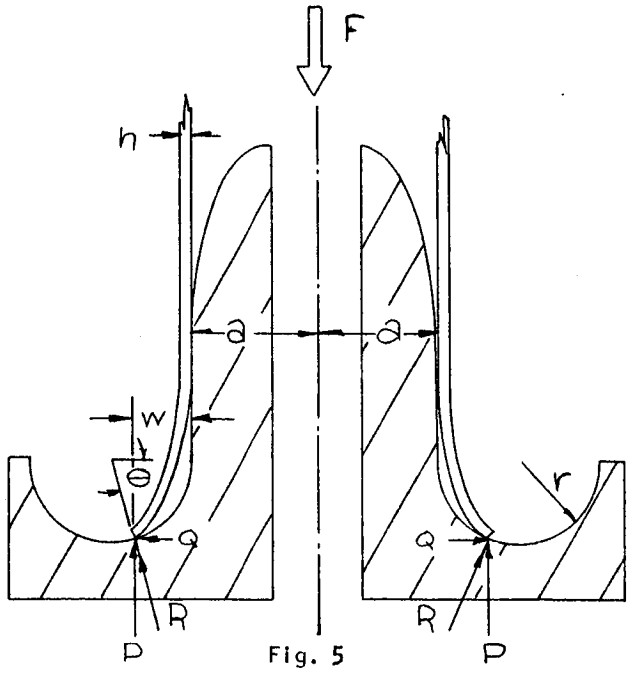

Fig. 5

Cross-Sectional View of
Tube and Die Prior to $F=F_1$
(First Analysis)

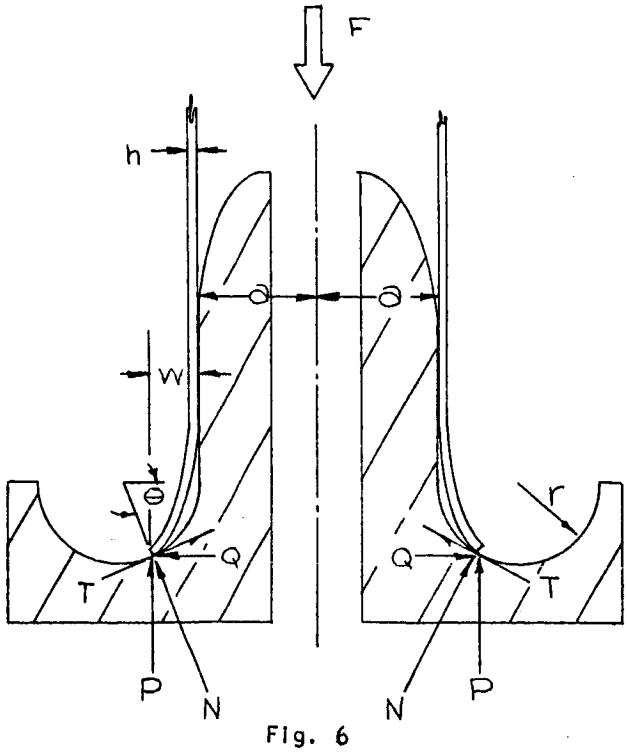

Fig. 6

Cross-Sectional View of
Tube and Die Prior to $F=F_1$
(Second Analysis)

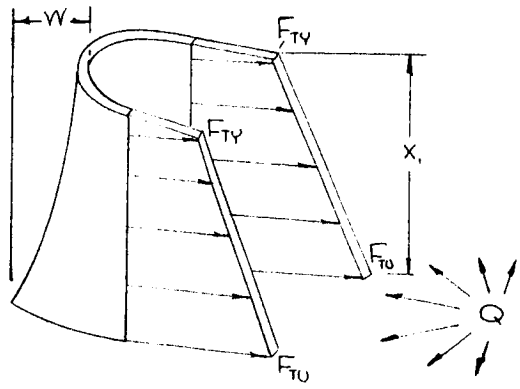

Fig. 7

Pictorial Cross Section of
Tube at $F=F_1$ Showing
Circumfrential Stresses

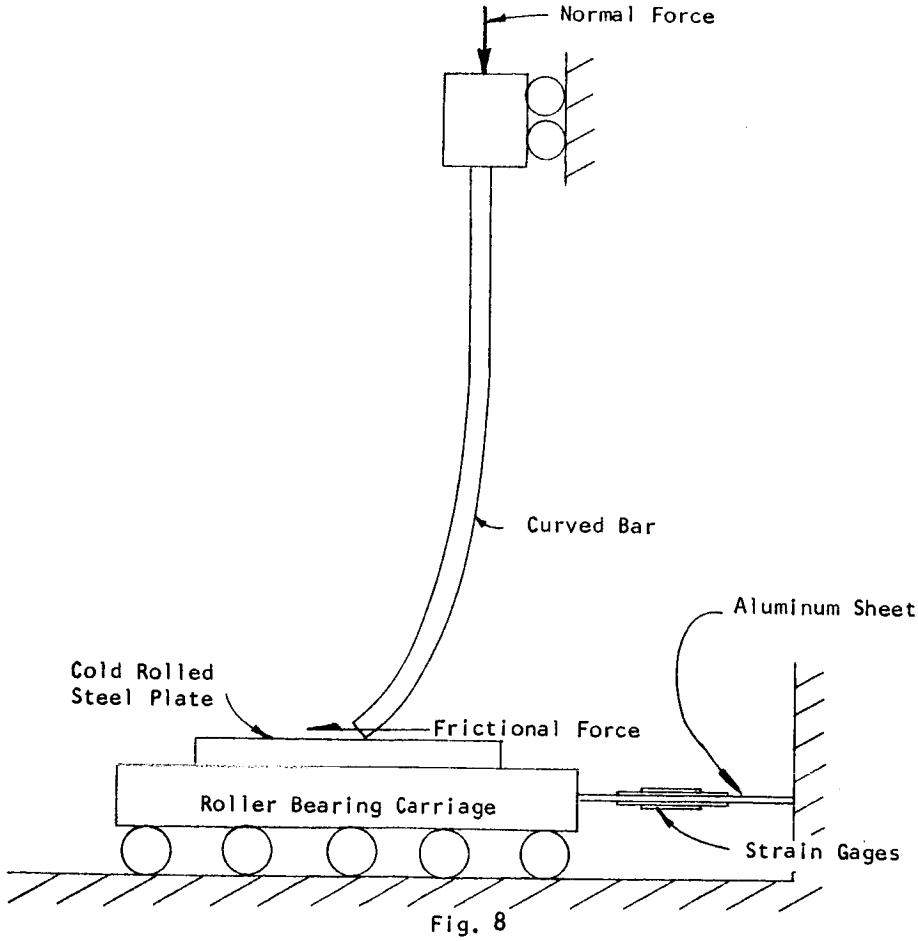

Fig. 8

Schematic of Apparatus
Used to Determine
Coefficient of Friction

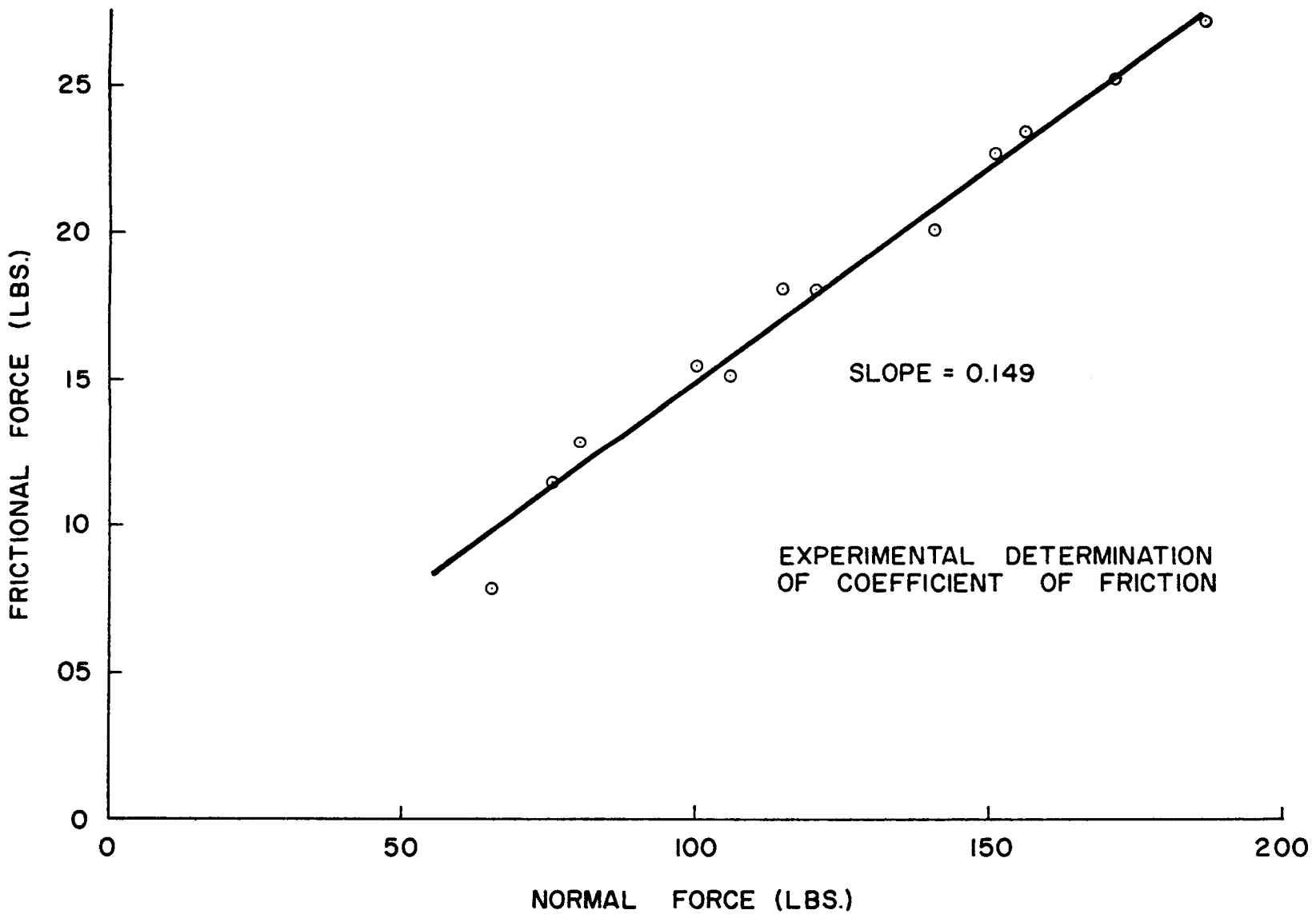
25
20
15
10
05
0
0
50
100
150
200
FRICTIONAL FORCE (LBS.)
NORMAL FORCE (LBS.)
SLOPE = 0.149
EXPERIMENTAL DETERMINATION
OF COEFFICIENT OF FRICTION

FIGURE 9

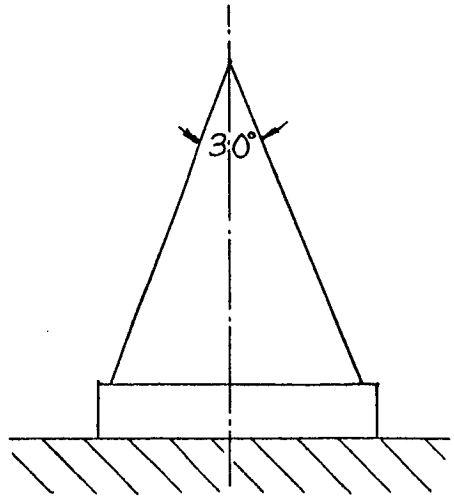

Fig. 10

Conical Die Used to Determine
Mechanical Properties

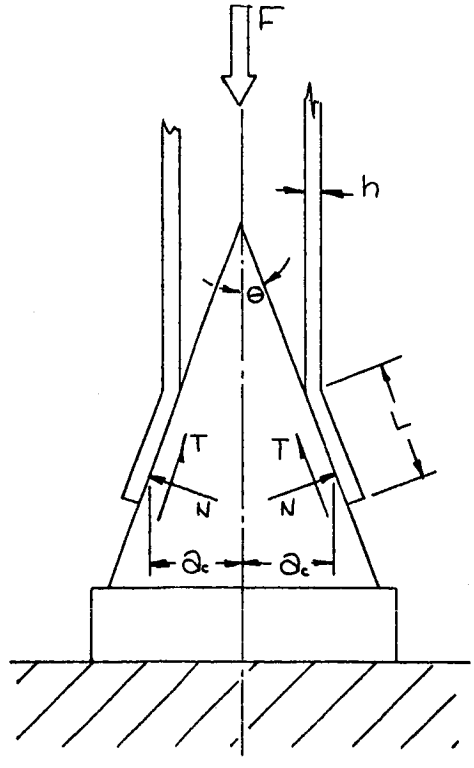

Fig. 11

Cross-Section of Tube and
Conical Die Showing Forces

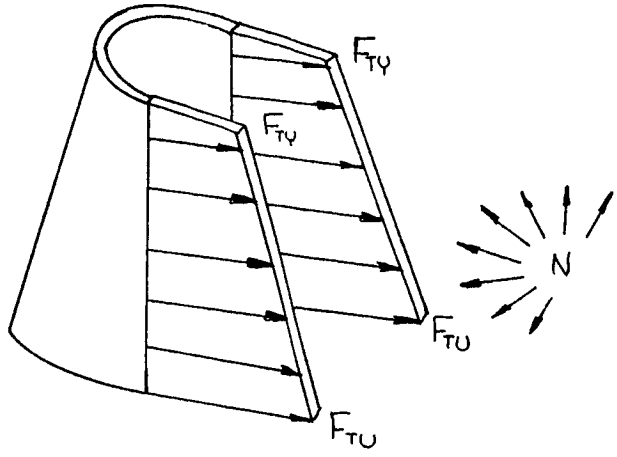

Fig. 12

Pictorial Cross-Section of Tube on Conical Die at Rupture Showing Assumed Circumfrential Stresses

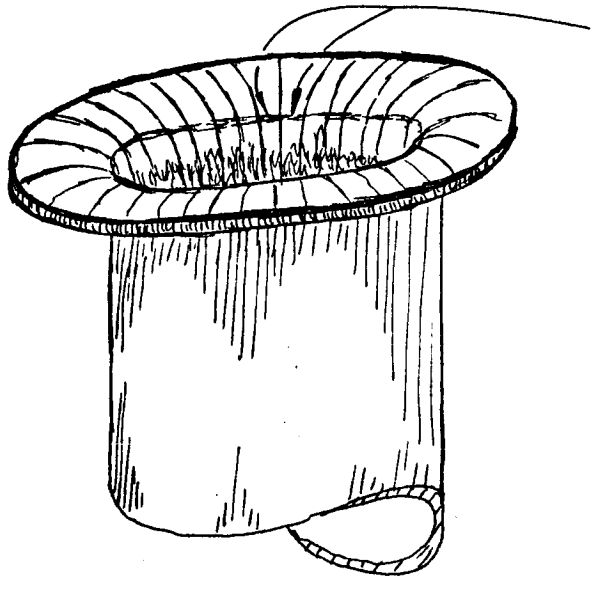

Fig. 13

Observed Mode of Initial Failure

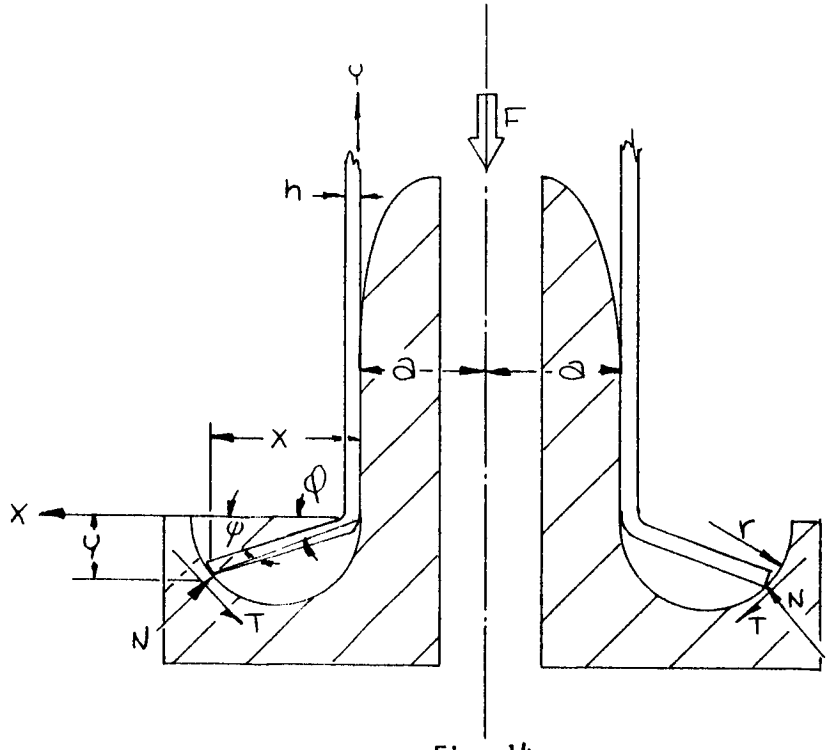

Fig. 14
Cross-Sectional View of Tube and Die Prior to $F=F_1$
(Final Analysis)

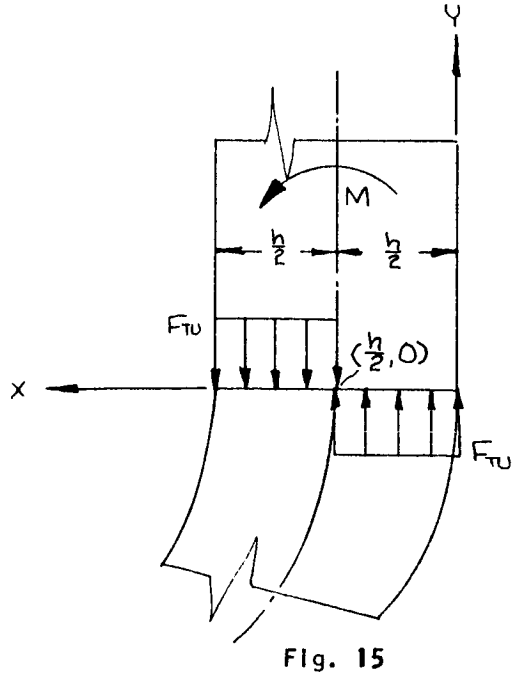

Fig. 15

Assumed Maximum Stress
Condition at $F-F_1$

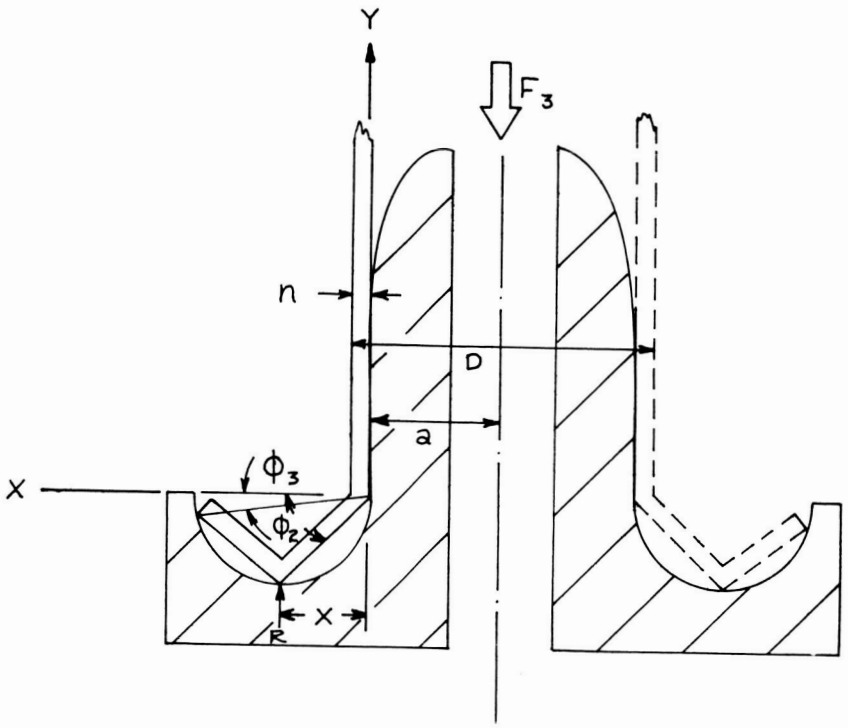

Fig. 16

Cross Sectional View of Tube and Die at $F = F_3$

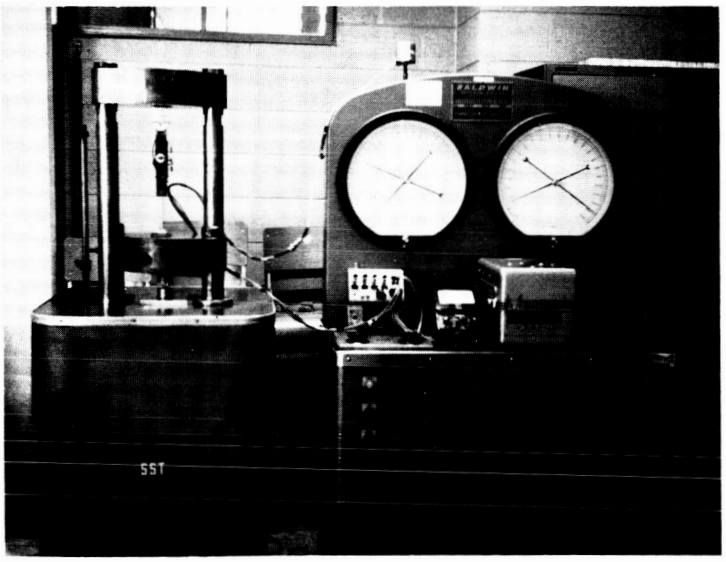

Fig. 17

Static Test of Frangible Tube Showing Load and Displacement Instrumentation

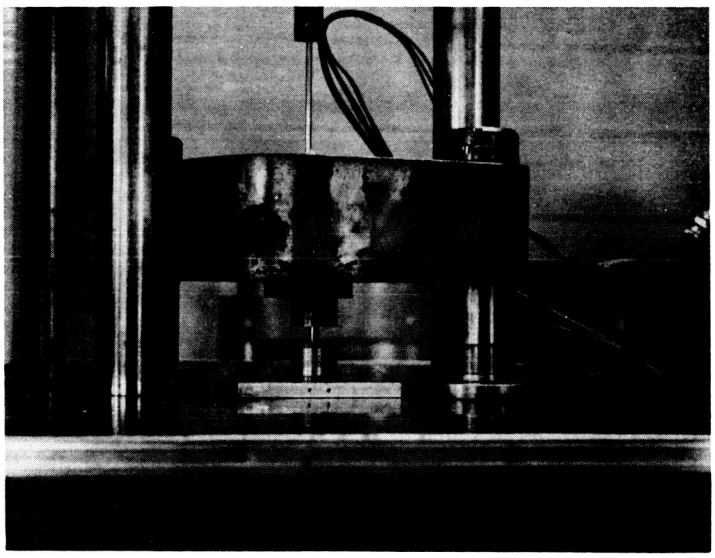

Figure 18.

Static Test of Frangible Tube System.

TABLE 1

COMPARISON OF ACTUAL AND THEORECTICAL
INITIAL PEAK FRAGMENTATION FORCES FOR ELEVEN
2024-T3 TUBE AND DIE GEOMETRIES

	a_t Tube Radius (inches)	h Tube Thickness (inches)	r Die Radius (inches)	Fi Theoretical (lbs)	Fi Actual (lbs)	Percent Error (%)
1)	.5000	.0650	.1625	7202	7225	- .30
2)	.5000	.0650	.1300	9026	8300	+ 8.75
3)	.2500	.0650	.1510	3241	3600	- 9.98
4)	.2500	.0470	.1092	2558	2830	- 9.97
5)	.2500	.0280	.0780	1421	1350	+27.50
6)	.2500	.0650	.1250	3654	3875	- 5.70
7)	.3750	.0650	.1510	5222	4500	+16.05
8)	.3468	.0530	.1105	4708	4150	+13.45
9)	.2370	.0505	.1261	2415	2400	+ .62
10)	.1250	.0200	.0465	642	630	+ 1.90
11)	.1250	.0200	.0400	748	950	-21.30

Average Percent
Error = $\pm$ 10.5%

TABLE 2

Values of the Average Fragmentation
Force for Seven Tube and Die Geometries Investigated
Experimentally

$f = 0.150$ $F_{tu} = 73$ KSI

Tube Size	h/r	h/D	F_{avg_t}	F_{avg}**	% Error
1" x .065"	.656	.0650	8167	6997	+16.7
3/4"x .049"	.449	.1530	2093	2195	- 4.6
*5/8" x .049"	.556 ±	.1275	2465	4416	-44.3*
1/2"x .065"	.585	.1300	2788	2645	+ 5.4
1/2" x .049"	.583	.0980	2506	2750	- 8.8
*1/2" x .028"	.470 ±	.0560	1245	1700	-26.8*
3/8" x .049"	.550	.1305	1545	1575	- 1.9

* Machining errors in fabrication of forming die crossection caused error in experimental values

** Average values for ten tests of each geometry

TABLE 3

Values of Average Fragmentation
Force for 25 Tube and Die Geometries (Ref. 1)

$f = 0.150$ $\quad F_{tu} = 65KSI$

h/D	h/r	h	F_{avgt}	F_{avg}	%Error
.030	.476	.020	1294	1416-	- 8.6
.088	.55	.022	696	550	+26.5
.088	.47	.022	485	443	+ 9.7
.088	.468	.022	478	426	+12.2
.056	.45	.028	964	950	+ 1.5
.058	.372	.029	692	733	- 5.5
.058	.558	.029	1588	1276	+24.4
.048	.300	.033	718	1080	-33.5
.079	.280	.035	433	620	-30.1
.062	.404	.044	1330	1750	-24.0
.104	.430	.047	962	1012	- 4.9
.070	.468	.051	1443	2516	-42.6
.112	.424	.053	1030	783	+31.5
.126	.420	.063	1148	1053	+ 9.0
.065	.400	.065	2189	2100	+ 4.2
.065	.500	.065	3328	3366	- 1.1
.065	.600	.065	5208	7100	-26.6
.065	.670	.065	7907	Buckled	
.130	.520	.065	1775	1500	+18.3
.130	.430	.065	1213	985	+23.1
.130	.504	.065	1657	1366	+21.3
.130	.335	.065	804	950	-15.3
.087	.430	.065	1840	1750	+ 5.1
.086	.600	.065	3915	4800	-18.4
.033	.430	.065	4945	4866	+ 1.6
.065	.430	.065	2482	2300	+ 7.9

TABLE 4

VALUES OF AVERAGE FRAGMENTATION FORCE OVER
ULTIMATE TENSILE STRESS FOR D/H= 3.75.

R2\H	0.022	0.028	0.035	0.049	0.058	0.065	0.083	0.095
.200	0.00066	0.00092	0.00124	0.00199	0.00253	0.00298	0.00426	0.00522
.225	0.00077	0.00107	0.00145	0.00231	0.00294	0.00346	0.00495	0.00605
.250	0.00089	0.00123	0.00167	0.00266	0.00337	0.00397	0.00568	0.00694
.275	0.00102	0.00141	0.00190	0.00303	0.00384	0.00453	0.00646	0.00789
.300	0.00116	0.00160	0.00216	0.00343	0.00435	0.00512	0.00730	0.00891
.325	0.00131	0.00180	0.00243	0.00387	0.00490	0.00576	0.00820	0.01001
.350	0.00147	0.00203	0.00273	0.00434	0.00549	0.00646	0.00918	0.01120
.375	0.00165	0.00227	0.00306	0.00485	0.00614	0.00722	0.01025	0.01248
.400	0.00185	0.00254	0.00343	0.00542	0.00685	0.00804	0.01141	0.01389
.425	0.00207	0.00284	0.00383	0.00605	0.00764	0.00896	0.01269	0.01543
.450	0.00232	0.00318	0.00427	0.00674	0.00850	0.00997	0.01410	0.01713
.475	0.00260	0.00355	0.00477	0.00751	0.00947	0.01110	0.01566	0.01901
.500	0.00291	0.00398	0.00534	0.00839	0.01056	0.01236	0.01742	0.02113
.525	0.	0.00447	0.00599	0.00938	0.01180	0.01380	0.01941	0.02351
.550	0.	0.00503	0.00673	0.01053	0.01322	0.01545	0.02169	0.02624
.575	0.	0.	0.00760	0.01186	0.01488	0.01737	0.02433	0.02939
.600	0.	0.	0.	0.01343	0.01683	0.01963	0.02743	0.03309
.625	0.	0.	0.	0.01533	0.01918	0.02234	0.03114	0.03751
.650	0.	0.	0.	0.	0.02206	0.02567	0.03568	0.04291
.675	0.	0.	0.	0.	0.	0.	0.04140	0.04969
.700	0.	0.	0.	0.	0.	0.	0.	0.05852
.725	0.	0.	0.	0.	0.	0.	0.	0.
.750	0.	0.	0.	0.	0.	0.	0.	0.
.775	0.	0.	0.	0.	0.	0.	0.	0.
.800	0.	0.	0.	0.	0.	0.	0.	0.

TABLE 5

VALUES OF AVERAGE FRAGMENTATION FORCE OVER
ULTIMATE TENSILE STRESS FOR D/H= 5.00.

R2\H	0.022	0.028	0.035	0.049	0.058	0.065	0.083	0.095
.200	0.00090	0.00124	0.00169	0.00271	0.00346	0.00408	0.00587	0.00720
.225	0.00105	0.00145	0.00197	0.00315	0.00402	0.00474	0.00681	0.00834
.250	0.00121	0.00167	0.00226	0.00363	0.00462	0.00544	0.00781	0.00957
.275	0.00138	0.00191	0.00258	0.00413	0.00526	0.00620	0.00888	0.01087
.300	0.00157	0.00216	0.00293	0.00468	0.00595	0.00701	0.01003	0.01227
.325	0.00177	0.00244	0.00330	0.00527	0.00669	0.00788	0.01127	0.01378
.350	0.00199	0.00274	0.00371	0.00591	0.00750	0.00883	0.01260	0.01540
.375	0.00223	0.00307	0.00416	0.00661	0.00838	0.00986	0.01406	0.01716
.400	0.00250	0.00344	0.00465	0.00738	0.00935	0.01099	0.01564	0.01908
.425	0.00280	0.00384	0.00519	0.00822	0.01041	0.01223	0.01738	0.02118
.450	0.00313	0.00430	0.00579	0.00916	0.01158	0.01360	0.01929	0.02349
.475	0.00350	0.00480	0.00646	0.01021	0.01289	0.01512	0.02142	0.02605
.500	0.00392	0.00537	0.00722	0.01138	0.01436	0.01684	0.02381	0.02892
.525	0.00440	0.00603	0.00809	0.01273	0.01604	0.01878	0.02650	0.03216
.550	0.	0.00678	0.00909	0.01427	0.01795	0.02101	0.02958	0.03585
.575	0.	0.	0.01026	0.01606	0.02018	0.02359	0.03314	0.04011
.600	0.	0.	0.01164	0.01818	0.02281	0.02664	0.03732	0.04510
.625	0.	0.	0.	0.02072	0.02596	0.03028	0.04232	0.05106
.650	0.	0.	0.	0.	0.02984	0.03476	0.04843	0.05833
.675	0.	0.	0.	0.	0.	0.04040	0.05611	0.06745
.700	0.	0.	0.	0.	0.	0.	0.06611	0.07930
.725	0.	0.	0.	0.	0.	0.	0.	0.
.750	0.	0.	0.	0.	0.	0.	0.	0.
.775	0.	0.	0.	0.	0.	0.	0.	0.
.800	0.	0.	0.	0.	0.	0.	0.	0.

TABLE 6

VALUES OF AVERAGE FRAGMENTATION FORCE OVER
ULTIMATE TENSILE STRESS FOR D/H= 6.25.

R2\H	0.022	0.028	0.035	0.049	0.058	0.065	0.083	0.095
.200	0.00113	0.00157	0.00214	0.00344	0.00439	0.00519	0.00747	0.00918
.225	0.00132	0.00183	0.00249	0.00400	0.00510	0.00602	0.00867	0.01064
.250	0.00152	0.00211	0.00286	0.00459	0.00586	0.00692	0.00994	0.01219
.275	0.00174	0.00240	0.00327	0.00524	0.00667	0.00787	0.01130	0.01385
.300	0.00197	0.00273	0.00370	0.00593	0.00754	0.00890	0.01276	0.01563
.325	0.00223	0.00308	0.00417	0.00667	0.00849	0.01000	0.01433	0.01754
.350	0.00251	0.00346	0.00469	0.00748	0.00951	0.01120	0.01602	0.01960
.375	0.00281	0.00388	0.00525	0.00836	0.01062	0.01251	0.01786	0.02183
.400	0.00315	0.00434	0.00586	0.00933	0.01184	0.01393	0.01987	0.02426
.425	0.00352	0.00485	0.00654	0.01040	0.01318	0.01549	0.02207	0.02692
.450	0.00393	0.00541	0.00730	0.01158	0.01466	0.01722	0.02449	0.02985
.475	0.00440	0.00605	0.00815	0.01290	0.01631	0.01915	0.02718	0.03309
.500	0.00493	0.00676	0.00911	0.01438	0.01817	0.02131	0.03019	0.03672
.525	0.00553	0.00758	0.01020	0.01607	0.02027	0.02376	0.03359	0.04081
.550	0.	0.00853	0.01145	0.01800	0.02268	0.02657	0.03747	0.04546
.575	0.	0.00963	0.01292	0.02026	0.02549	0.02982	0.04196	0.05083
.600	0.	0.	0.01465	0.02292	0.02879	0.03364	0.04722	0.05712
.625	0.	0.	0.	0.02611	0.03275	0.03822	0.05350	0.06462
.650	0.	0.	0.	0.03004	0.03761	0.04384	0.06118	0.07375
.675	0.	0.	0.	0.	0.	0.05092	0.07082	0.08520
.700	0.	0.	0.	0.	0.	0.	0.08337	0.10007
.725	0.	0.	0.	0.	0.	0.	0.	0.
.750	0.	0.	0.	0.	0.	0.	0.	0.
.775	0.	0.	0.	0.	0.	0.	0.	0.
.800	0.	0.	0.	0.	0.	0.	0.	0.

TABLE 7

VALUES OF AVERAGE FRAGMENTATION FORCE OVER
ULTIMATE TENSILE STRESS FOR D/H= 7.50.

R2\H	0.022	0.028	0.035	0.049	0.058	0.065	0.083	0.095
.200	0.00137	0.00190	0.00258	0.00417	0.00532	0.00629	0.00908	0.01116
.225	0.00159	0.00221	0.00301	0.00484	0.00618	0.00731	0.01053	0.01293
.250	0.00183	0.00254	0.00346	0.00556	0.00710	0.00839	0.01207	0.01482
.275	0.00210	0.00290	0.00395	0.00634	0.00808	0.00954	0.01372	0.01683
.300	0.00238	0.00329	0.00447	0.00717	0.00914	0.01079	0.01549	0.01899
.325	0.00269	0.00372	0.00504	0.00807	0.01028	0.01212	0.01739	0.02131
.350	0.00302	0.00418	0.00566	0.00905	0.01151	0.01357	0.01944	0.02380
.375	0.00339	0.00468	0.00634	0.01012	0.01286	0.01515	0.02167	0.02651
.400	0.00379	0.00523	0.00708	0.01129	0.01433	0.01687	0.02410	0.02945
.425	0.00424	0.00585	0.00790	0.01257	0.01595	0.01876	0.02676	0.03267
.450	0.00474	0.00653	0.00881	0.01400	0.01774	0.02085	0.02969	0.03621
.475	0.00530	0.00729	0.00984	0.01559	0.01973	0.02318	0.03294	0.04014
.500	0.00594	0.00816	0.01099	0.01738	0.02197	0.02579	0.03658	0.04452
.525	0.00667	0.00914	0.01230	0.01941	0.02451	0.02874	0.04068	0.04945
.550	0.00750	0.01028	0.01381	0.02174	0.02742	0.03212	0.04536	0.05507
.575	0.	0.01161	0.01558	0.02446	0.03079	0.03604	0.05077	0.06155
.600	0.	0.	0.01766	0.02766	0.03477	0.04065	0.05712	0.06914
.625	0.	0.	0.	0.03150	0.03954	0.04617	0.06469	0.07817
.650	0.	0.	0.	0.03623	0.04538	0.05292	0.07393	0.08917
.675	0.	0.	0.	0.	0.05276	0.06143	0.08553	0.10296
.700	0.	0.	0.	0.	0.	0.	0.10062	0.12085
.725	0.	0.	0.	0.	0.	0.	0.	0.
.750	0.	0.	0.	0.	0.	0.	0.	0.
.775	0.	0.	0.	0.	0.	0.	0.	0.
.800	0.	0.	0.	0.	0.	0.	0.	0.

TABLE 8

VALUES OF AVERAGE FRAGMENTATION FORCE OVER
ULTIMATE TENSILE STRESS FOR D/H= 8.75.

R2\H	0.022	0.028	0.035	0.049	0.058	0.065	0.083	0.095
.200	0.00160	0.00222	0.00303	0.00489	0.00625	0.00740	0.01068	0.01314
.225	0.00187	0.00259	0.00353	0.00568	0.00726	0.00859	0.01239	0.01523
.250	0.00215	0.00298	0.00406	0.00653	0.00834	0.00986	0.01420	0.01744
.275	0.00245	0.00340	0.00463	0.00744	0.00949	0.01121	0.01614	0.01981
.300	0.00279	0.00386	0.00524	0.00842	0.01073	0.01267	0.01822	0.02235
.325	0.00315	0.00435	0.00591	0.00948	0.01207	0.01425	0.02045	0.02507
.350	0.00354	0.00489	0.00664	0.01062	0.01352	0.01595	0.02286	0.02801
.375	0.00397	0.00548	0.00743	0.01187	0.01510	0.01780	0.02548	0.03118
.400	0.00444	0.00613	0.00830	0.01324	0.01682	0.01981	0.02833	0.03464
.425	0.00497	0.00685	0.00926	0.01475	0.01872	0.02203	0.03145	0.03842
.450	0.00555	0.00764	0.01033	0.01642	0.02081	0.02448	0.03488	0.04257
.475	0.00621	0.00854	0.01152	0.01828	0.02315	0.02721	0.03870	0.04718
.500	0.00695	0.00955	0.01287	0.02038	0.02577	0.03026	0.04296	0.05231
.525	0.00780	0.01070	0.01441	0.02275	0.02874	0.03372	0.04777	0.05810
.550	0.00878	0.01203	0.01617	0.02548	0.03215	0.03768	0.05325	0.06469
.575	0.	0.01358	0.01823	0.02866	0.03610	0.04226	0.05959	0.07227
.600	0.	0.	0.02067	0.03240	0.04075	0.04765	0.06701	0.08115
.625	0.	0.	0.	0.03689	0.04632	0.05411	0.07587	0.09173
.650	0.	0.	0.	0.04242	0.05316	0.06201	0.08668	0.10460
.675	0.	0.	0.	0.	0.06177	0.07195	0.10024	0.12071
.700	0.	0.	0.	0.	0.	0.	0.11787	0.14163
.725	0.	0.	0.	0.	0.	0.	0.	0.
.750	0.	0.	0.	0.	0.	0.	0.	0.
.775	0.	0.	0.	0.	0.	0.	0.	0.
.800	0.	0.	0.	0.	0.	0.	0.	0.

TABLE 9

VALUES OF AVERAGE FRAGMENTATION FORCE OVER
ULTIMATE TENSILE STRESS FOR D/H=10.00.

R2\H	0.022	0.028	0.035	0.049	0.058	0.065	0.083	0.095
.200	0.00184	0.00255	0.00348	0.00562	0.00719	0.00851	0.01229	0.01512
.225	0.00214	0.00297	0.00405	0.00653	0.00834	0.00987	0.01425	0.01752
.250	0.00246	0.00342	0.00466	0.00750	0.00958	0.01133	0.01633	0.02007
.275	0.00281	0.00390	0.00531	0.00854	0.01090	0.01289	0.01856	0.02279
.300	0.00319	0.00442	0.00602	0.00967	0.01233	0.01456	0.02095	0.02571
.325	0.00360	0.00499	0.00678	0.01088	0.01386	0.01637	0.02351	0.02884
.350	0.00405	0.00561	0.00761	0.01220	0.01553	0.01832	0.02628	0.03221
.375	0.00455	0.00628	0.00852	0.01363	0.01734	0.02044	0.02929	0.03586
.400	0.00509	0.00703	0.00952	0.01520	0.01931	0.02276	0.03256	0.03983
.425	0.00569	0.00785	0.01062	0.01692	0.02149	0.02530	0.03614	0.04416
.450	0.00636	0.00876	0.01184	0.01884	0.02389	0.02811	0.04008	0.04893
.475	0.00711	0.00978	0.01321	0.02097	0.02657	0.03123	0.04445	0.05422
.500	0.00796	0.01094	0.01475	0.02337	0.02957	0.03474	0.04934	0.06011
.525	0.00893	0.01226	0.01651	0.02610	0.03298	0.03870	0.05486	0.06675
.550	0.01005	0.01378	0.01853	0.02922	0.03688	0.04323	0.06115	0.07430
.575	0.	0.01556	0.02089	0.03286	0.04140	0.04849	0.06840	0.08300
.600	0.	0.	0.02368	0.03714	0.04672	0.05466	0.07691	0.09317
.625	0.	0.	0.	0.04229	0.05311	0.06205	0.08705	0.10528
.650	0.	0.	0.	0.04860	0.06093	0.07109	0.09943	0.12002
.675	0.	0.	0.	0.	0.07079	0.08247	0.11495	0.13847
.700	0.	0.	0.	0.	0.	0.	0.13513	0.16240
.725	0.	0.	0.	0.	0.	0.	0.	0.19498
.750	0.	0.	0.	0.	0.	0.	0.	0.
.775	0.	0.	0.	0.	0.	0.	0.	0.
.800	0.	0.	0.	0.	0.	0.	0.	0.

TABLE 10

VALUES OF AVERAGE FRAGMENTATION FORCE OVER
ULTIMATE TENSILE STRESS FOR D/H=11.25.

R2\H	0.022	0.028	0.035	0.049	0.058	0.065	0.083	0.095
.200	0.00207	0.00288	0.00393	0.00635	0.00812	0.00961	0.01390	0.01710
.225	0.00241	0.00335	0.00457	0.00737	0.00943	0.01115	0.01611	0.01981
.250	0.00278	0.00386	0.00525	0.00847	0.01082	0.01280	0.01846	0.02270
.275	0.00317	0.00440	0.00599	0.00965	0.01232	0.01456	0.02098	0.02577
.300	0.00360	0.00499	0.00679	0.01091	0.01392	0.01645	0.02368	0.02907
.325	0.00406	0.00563	0.00765	0.01228	0.01566	0.01849	0.02658	0.03260
.350	0.00457	0.00632	0.00859	0.01377	0.01753	0.02069	0.02971	0.03641
.375	0.00513	0.00709	0.00961	0.01538	0.01957	0.02309	0.03310	0.04053
.400	0.00574	0.00792	0.01074	0.01715	0.02181	0.02570	0.03679	0.04501
.425	0.00641	0.00885	0.01198	0.01910	0.02426	0.02857	0.04083	0.04991
.450	0.00717	0.00988	0.01335	0.02126	0.02697	0.03174	0.04528	0.05530
.475	0.00801	0.01103	0.01490	0.02366	0.02999	0.03526	0.05021	0.06126
.500	0.00897	0.01233	0.01664	0.02637	0.03337	0.03921	0.05573	0.06791
.525	0.01006	0.01382	0.01862	0.02944	0.03721	0.04368	0.06195	0.07539
.550	0.01133	0.01553	0.02089	0.03296	0.04161	0.04879	0.06904	0.08391
.575	0.	0.01754	0.02355	0.03705	0.04670	0.05471	0.07722	0.09372
.600	0.	0.	0.02669	0.04188	0.05270	0.06166	0.08680	0.10519
.625	0.	0.	0.	0.04768	0.05989	0.06999	0.09824	0.11884
.650	0.	0.	0.	0.05479	0.06870	0.08017	0.11218	0.13544
.675	0.	0.	0.	0.	0.07980	0.09299	0.12966	0.15623
.700	0.	0.	0.	0.	0.	0.	0.15238	0.18318
.725	0.	0.	0.	0.	0.	0.	0.	0.21985
.750	0.	0.	0.	0.	0.	0.	0.	0.
.775	0.	0.	0.	0.	0.	0.	0.	0.
.800	0.	0.	0.	0.	0.	0.	0.	0.

TABLE 11

VALUES OF AVERAGE FRAGMENTATION FORCE OVER
ULTIMATE TENSILE STRESS FOR D/H=12.50.

R2\H	0.022	0.028	0.035	0.049	0.058	0.065	0.083	0.095
.200	0.00230	0.00320	0.00437	0.00707	0.00905	0.01072	0.01550	0.01908
.225	0.00268	0.00373	0.00509	0.00822	0.01051	0.01244	0.01797	0.02211
.250	0.00309	0.00429	0.00585	0.00944	0.01206	0.01427	0.02060	0.02532
.275	0.00353	0.00490	0.00667	0.01075	0.01373	0.01623	0.02340	0.02875
.300	0.00401	0.00556	0.00756	0.01216	0.01552	0.01834	0.02641	0.03243
.325	0.00452	0.00627	0.00852	0.01369	0.01745	0.02061	0.02964	0.03637
.350	0.00509	0.00704	0.00956	0.01534	0.01954	0.02306	0.03313	0.04061
.375	0.00570	0.00789	0.01070	0.01714	0.02181	0.02573	0.03690	0.04521
.400	0.00638	0.00882	0.01195	0.01911	0.02430	0.02864	0.04102	0.05020
.425	0.00714	0.00985	0.01333	0.02128	0.02703	0.03184	0.04552	0.05566
.450	0.00797	0.01099	0.01487	0.02368	0.03005	0.03537	0.05047	0.06166
.475	0.00891	0.01228	0.01658	0.02635	0.03341	0.03929	0.05597	0.06830
.500	0.00998	0.01373	0.01852	0.02937	0.03718	0.04369	0.06211	0.07570
.525	0.01120	0.01538	0.02072	0.03278	0.04145	0.04866	0.06904	0.08404
.550	0.01260	0.01729	0.02326	0.03670	0.04634	0.05435	0.07693	0.09352
.575	0.	0.01951	0.02621	0.04125	0.05201	0.06093	0.08603	0.10444
.600	0.	0.	0.02970	0.04662	0.05868	0.06867	0.09670	0.11720
.625	0.	0.	0.03391	0.05307	0.06668	0.07793	0.10942	0.13239
.650	0.	0.	0.	0.06098	0.07647	0.08926	0.12493	0.15087
.675	0.	0.	0.	0.	0.08881	0.10351	0.14437	0.17398
.700	0.	0.	0.	0.	0.	0.	0.16963	0.20395
.725	0.	0.	0.	0.	0.	0.	0.	0.24473
.750	0.	0.	0.	0.	0.	0.	0.	0.
.775	0.	0.	0.	0.	0.	0.	0.	0.
.800	0.	0.	0.	0.	0.	0.	0.	0.

TABLE 12

VALUES OF AVERAGE FRAGMENTATION FORCE OVER
ULTIMATE TENSILE STRESS FOR D/H=13.75.

R2\H	0.022	0.028	0.035	0.049	0.058	0.065	0.083	0.095
.200	0.00254	0.00353	0.00482	0.00780	0.00998	0.01182	0.01711	0.02106
.225	0.00296	0.00411	0.00561	0.00906	0.01159	0.01372	0.01983	0.02440
.250	0.00341	0.00473	0.00645	0.01041	0.01330	0.01574	0.02273	0.02795
.275	0.00389	0.00540	0.00735	0.01185	0.01514	0.01790	0.02582	0.03173
.300	0.00441	0.00612	0.00833	0.01341	0.01711	0.02023	0.02914	0.03578
.325	0.00498	0.00690	0.00939	0.01509	0.01924	0.02273	0.03270	0.04013
.350	0.00560	0.00776	0.01054	0.01691	0.02155	0.02544	0.03655	0.04481
.375	0.00628	0.00869	0.01179	0.01889	0.02405	0.02838	0.04071	0.04988
.400	0.00703	0.00972	0.01317	0.02106	0.02679	0.03159	0.04524	0.05539
.425	0.00786	0.01085	0.01469	0.02345	0.02980	0.03511	0.05021	0.06141
.450	0.00878	0.01211	0.01638	0.02610	0.03312	0.03899	0.05567	0.06802
.475	0.00982	0.01352	0.01827	0.02905	0.03682	0.04332	0.06173	0.07534
.500	0.01099	0.01512	0.02040	0.03236	0.04098	0.04816	0.06849	0.08350
.525	0.01233	0.01694	0.02283	0.03613	0.04568	0.05364	0.07612	0.09269
.550	0.01387	0.01904	0.02562	0.04044	0.05107	0.05990	0.08482	0.10313
.575	0.	0.02149	0.02887	0.04545	0.05731	0.06715	0.09485	0.11516
.600	0.	0.	0.03272	0.05136	0.06466	0.07568	0.10660	0.12922
.625	0.	0.	0.03735	0.05846	0.07346	0.08587	0.12060	0.14595
.650	0.	0.	0.	0.06717	0.08425	0.09834	0.13768	0.16629
.675	0.	0.	0.	0.	0.09783	0.11402	0.15908	0.19174
.700	0.	0.	0.	0.	0.	0.	0.18689	0.22473
.725	0.	0.	0.	0.	0.	0.	0.	0.26961
.750	0.	0.	0.	0.	0.	0.	0.	0.
.775	0.	0.	0.	0.	0.	0.	0.	0.
.800	0.	0.	0.	0.	0.	0.	0.	0.

TABLE 13

VALUES OF AVERAGE FRAGMENTATION FORCE OVER
ULTIMATE TENSILE STRESS FOR D/H=15.00.

R2\H	0.022	0.028	0.035	0.049	0.058	0.065	0.083	0.095
.200	0.00277	0.00386	0.00527	0.00852	0.01091	0.01293	0.01871	0.02304
.225	0.00323	0.00449	0.00613	0.00990	0.01267	0.01500	0.02169	0.02669
.250	0.00372	0.00517	0.00705	0.01138	0.01454	0.01721	0.02486	0.03058
.275	0.00425	0.00590	0.00804	0.01296	0.01655	0.01958	0.02824	0.03472
.300	0.00482	0.00669	0.00910	0.01466	0.01871	0.02212	0.03187	0.03914
.325	0.00544	0.00754	0.01026	0.01649	0.02104	0.02485	0.03576	0.04390
.350	0.00612	0.00847	0.01151	0.01848	0.02355	0.02781	0.03997	0.04902
.375	0.00686	0.00949	0.01288	0.02065	0.02629	0.03102	0.04452	0.05456
.400	0.00768	0.01061	0.01439	0.02302	0.02928	0.03453	0.04947	0.06058
.425	0.00858	0.01185	0.01605	0.02563	0.03257	0.03838	0.05490	0.06715
.450	0.00959	0.01323	0.01789	0.02852	0.03620	0.04262	0.06087	0.07438
.475	0.01072	0.01477	0.01996	0.03174	0.04024	0.04734	0.06749	0.08238
.500	0.01200	0.01651	0.02228	0.03536	0.04478	0.05264	0.07488	0.09130
.525	0.01346	0.01850	0.02493	0.03947	0.04992	0.05862	0.08321	0.10133
.550	0.01515	0.02079	0.02798	0.04418	0.05580	0.06546	0.09271	0.11275
.575	0.	0.02346	0.03153	0.04965	0.06262	0.07338	0.10367	0.12588
.600	0.	0.	0.03573	0.05610	0.07064	0.08268	0.11649	0.14124
.625	0.	0.	0.04078	0.06385	0.08025	0.09381	0.13179	0.15950
.650	0.	0.	0.	0.07335	0.09202	0.10742	0.15043	0.18171
.675	0.	0.	0.	0.	0.10684	0.12454	0.17379	0.20949
.700	0.	0.	0.	0.	0.	0.	0.20414	0.24550
.725	0.	0.	0.	0.	0.	0.	0.	0.29448
.750	0.	0.	0.	0.	0.	0.	0.	0.
.775	0.	0.	0.	0.	0.	0.	0.	0.
.800	0.	0.	0.	0.	0.	0.	0.	0.

TABLE 14

VALUES OF AVERAGE FRAGMENTATION FORCE OVER
ULTIMATE TENSILE STRESS FOR D/H=16.25.

R2\H	0.022	0.028	0.035	0.049	0.058	0.065	0.083	0.095
.200	0.00301	0.00418	0.00571	0.00925	0.01185	0.01403	0.02032	0.02502
.225	0.00350	0.00487	0.00665	0.01075	0.01375	0.01628	0.02355	0.02899
.250	0.00403	0.00561	0.00764	0.01234	0.01579	0.01868	0.02699	0.03320
.275	0.00461	0.00640	0.00872	0.01406	0.01796	0.02125	0.03066	0.03770
.300	0.00523	0.00725	0.00987	0.01590	0.02030	0.02400	0.03460	0.04250
.325	0.00590	0.00818	0.01113	0.01789	0.02283	0.02697	0.03882	0.04766
.350	0.00664	0.00919	0.01249	0.02005	0.02556	0.03018	0.04339	0.05322
.375	0.00744	0.01029	0.01398	0.02240	0.02853	0.03367	0.04833	0.05923
.400	0.00833	0.01151	0.01561	0.02497	0.03177	0.03747	0.05370	0.06576
.425	0.00931	0.01285	0.01741	0.02780	0.03534	0.04164	0.05959	0.07290
.450	0.01040	0.01434	0.01941	0.03094	0.03928	0.04625	0.06606	0.08074
.475	0.01162	0.01601	0.02164	0.03443	0.04366	0.05137	0.07324	0.08942
.500	0.01301	0.01790	0.02417	0.03836	0.04858	0.05711	0.08126	0.09909
.525	0.01459	0.02006	0.02704	0.04281	0.05415	0.06360	0.09030	0.10998
.550	0.01642	0.02254	0.03034	0.04792	0.06053	0.07102	0.10060	0.12236
.575	0.	0.02544	0.03419	0.05385	0.06792	0.07960	0.11248	0.13661
.600	0.	0.02887	0.03874	0.06084	0.07662	0.08969	0.12639	0.15325
.625	0.	0.	0.04422	0.06924	0.08703	0.10175	0.14297	0.17305
.650	0.	0.	0.	0.07954	0.09979	0.11651	0.16318	0.19714
.675	0.	0.	0.	0.	0.11586	0.13506	0.18850	0.22725
.700	0.	0.	0.	0.	0.	0.	0.22140	0.26628
.725	0.	0.	0.	0.	0.	0.	0.	0.31936
.750	0.	0.	0.	0.	0.	0.	0.	0.
.775	0.	0.	0.	0.	0.	0.	0.	0.
.800	0.	0.	0.	0.	0.	0.	0.	0.

TABLE 15

VALUES OF AVERAGE FRAGMENTATION FORCE OVER
ULTIMATE TENSILE STRESS FOR D/H=17.50.

R2\H	0.022	0.028	0.035	0.049	0.058	0.065	0.083	0.095
.200	0.00324	0.00451	0.00616	0.00998	0.01278	0.01514	0.02192	0.02700
.225	0.00377	0.00525	0.00717	0.01159	0.01483	0.01756	0.02541	0.03128
.250	0.00435	0.00604	0.00824	0.01331	0.01703	0.02015	0.02912	0.03583
.275	0.00497	0.00690	0.00940	0.01516	0.01938	0.02292	0.03308	0.04068
.300	0.00563	0.00782	0.01065	0.01715	0.02190	0.02589	0.03733	0.04586
.325	0.00636	0.00882	0.01200	0.01930	0.02462	0.02909	0.04189	0.05143
.350	0.00715	0.00991	0.01346	0.02162	0.02757	0.03255	0.04681	0.05742
.375	0.00802	0.01110	0.01507	0.02416	0.03077	0.03631	0.05213	0.06390
.400	0.00897	0.01240	0.01683	0.02693	0.03427	0.04041	0.05793	0.07095
.425	0.01003	0.01385	0.01877	0.02998	0.03811	0.04491	0.06428	0.07865
.450	0.01121	0.01546	0.02092	0.03336	0.04236	0.04988	0.07126	0.08710
.475	0.01253	0.01726	0.02333	0.03712	0.04708	0.05540	0.07900	0.09646
.500	0.01402	0.01929	0.02605	0.04135	0.05239	0.06159	0.08765	0.10689
.525	0.01573	0.02162	0.02914	0.04615	0.05839	0.06858	0.09739	0.11863
.550	0.01770	0.02429	0.03270	0.05166	0.06526	0.07657	0.10849	0.13197
.575	0.	0.02741	0.03684	0.05805	0.07323	0.08582	0.12130	0.14733
.600	0.	0.03111	0.04175	0.06559	0.08260	0.09669	0.13629	0.16527
.625	0.	0.	0.04765	0.07463	0.09382	0.10969	0.15415	0.18661
.650	0.	0.	0.	0.08573	0.10757	0.12559	0.17593	0.21256
.675	0.	0.	0.	0.	0.12487	0.14558	0.20321	0.24500
.700	0.	0.	0.	0.	0.	0.	0.23865	0.28706
.725	0.	0.	0.	0.	0.	0.	0.	0.34424
.750	0.	0.	0.	0.	0.	0.	0.	0.
.775	0.	0.	0.	0.	0.	0.	0.	0.
.800	0.	0.	0.	0.	0.	0.	0.	0.

TABLE 16

VALUES OF AVERAGE FRAGMENTATION FORCE OVER
ULTIMATE TENSILE STRESS FOR D/H=18.75.

R2\H	0.022	0.028	0.035	0.049	0.058	0.065	0.083	0.095
.200	0.00348	0.00484	0.00661	0.01070	0.01371	0.01624	0.02353	0.02898
.225	0.00405	0.00563	0.00769	0.01243	0.01591	0.01885	0.02727	0.03357
.250	0.00466	0.00648	0.00884	0.01428	0.01827	0.02162	0.03125	0.03845
.275	0.00532	0.00740	0.01008	0.01626	0.02079	0.02459	0.03550	0.04366
.300	0.00604	0.00838	0.01142	0.01840	0.02350	0.02778	0.04006	0.04922
.325	0.00682	0.00946	0.01287	0.02070	0.02641	0.03121	0.04495	0.05519
.350	0.00767	0.01062	0.01444	0.02319	0.02957	0.03493	0.05023	0.06162
.375	0.00860	0.01190	0.01616	0.02591	0.03301	0.03896	0.05594	0.06858
.400	0.00962	0.01330	0.01804	0.02888	0.03676	0.04336	0.06216	0.07614
.425	0.01075	0.01485	0.02012	0.03215	0.04088	0.04818	0.06897	0.08439
.450	0.01201	0.01657	0.02243	0.03578	0.04543	0.05351	0.07646	0.09347
.475	0.01343	0.01851	0.02502	0.03981	0.05050	0.05943	0.08476	0.10350
.500	0.01503	0.02069	0.02793	0.04435	0.05619	0.06606	0.09403	0.11469
.525	0.01686	0.02317	0.03125	0.04950	0.06263	0.07356	0.10448	0.12727
.550	0.01897	0.02604	0.03506	0.05540	0.06999	0.08213	0.11638	0.14158
.575	0.	0.02939	0.03950	0.06225	0.07853	0.09205	0.13011	0.15805
.600	0.	0.03335	0.04476	0.07033	0.08857	0.10370	0.14618	0.17729
.625	0.	0.	0.05109	0.08002	0.10060	0.11763	0.16534	0.20016
.650	0.	0.	0.	0.09192	0.11534	0.13467	0.18868	0.22798
.675	0.	0.	0.	0.	0.13389	0.15610	0.21792	0.26276
.700	0.	0.	0.	0.	0.	0.	0.25590	0.30783
.725	0.	0.	0.	0.	0.	0.	0.	0.36911
.750	0.	0.	0.	0.	0.	0.	0.	0.
.775	0.	0.	0.	0.	0.	0.	0.	0.
.800	0.	0.	0.	0.	0.	0.	0.	0.

TABLE 17

VALUES OF AVERAGE FRAGMENTATION FORCE OVER
ULTIMATE TENSILE STRESS FOR D/H=20.00.

R2\H	0.022	0.028	0.035	0.049	0.058	0.065	0.083	0.095
.200	0.00371	0.00516	0.00706	0.01143	0.01464	0.01735	0.02513	0.03097
.225	0.00432	0.00601	0.00821	0.01328	0.01700	0.02013	0.02913	0.03587
.250	0.00498	0.00692	0.00944	0.01525	0.01951	0.02309	0.03338	0.04108
.275	0.00568	0.00790	0.01076	0.01737	0.02220	0.02627	0.03792	0.04664
.300	0.00645	0.00895	0.01219	0.01964	0.02509	0.02967	0.04279	0.05258
.325	0.00728	0.01009	0.01374	0.02210	0.02821	0.03334	0.04801	0.05896
.350	0.00818	0.01134	0.01542	0.02477	0.03158	0.03730	0.05365	0.06583
.375	0.00918	0.01270	0.01725	0.02767	0.03525	0.04160	0.05975	0.07325
.400	0.01027	0.01420	0.01926	0.03084	0.03925	0.04630	0.06639	0.08132
.425	0.01148	0.01585	0.02148	0.03433	0.04365	0.05145	0.07366	0.09014
.450	0.01282	0.01769	0.02395	0.03820	0.04851	0.05714	0.08165	0.09983
.475	0.01433	0.01975	0.02671	0.04250	0.05392	0.06345	0.09052	0.11054
.500	0.01604	0.02208	0.02981	0.04735	0.05999	0.07053	0.10041	0.12249
.525	0.01799	0.02473	0.03335	0.05284	0.06686	0.07854	0.11157	0.13592
.550	0.02024	0.02779	0.03742	0.05914	0.07472	0.08769	0.12428	0.15119
.575	0.	0.03136	0.04216	0.06645	0.08383	0.09827	0.13893	0.16877
.600	0.	0.03559	0.04777	0.07507	0.09455	0.11070	0.15608	0.18930
.625	0.	0.	0.05452	0.08541	0.10739	0.12557	0.17652	0.21372
.650	0.	0.	0.	0.09810	0.12311	0.14376	0.20143	0.24341
.675	0.	0.	0.	0.	0.14290	0.16662	0.23263	0.28052
.700	0.	0.	0.	0.	0.	0.	0.27316	0.32861
.725	0.	0.	0.	0.	0.	0.	0.	0.39399
.750	0.	0.	0.	0.	0.	0.	0.	0.
.775	0.	0.	0.	0.	0.	0.	0.	0.
.800	0.	0.	0.	0.	0.	0.	0.	0.

TABLE 18

VALUES OF AVERAGE FRAGMENTATION FORCE OVER
ULTIMATE TENSILE STRESS FOR D/H=21.25.

R2\H	0.022	0.028	0.035	0.049	0.058	0.065	0.083	0.095
.200	0.00394	0.00549	0.00750	0.01216	0.01557	0.01846	0.02674	0.03295
.225	0.00459	0.00639	0.00873	0.01412	0.01808	0.02141	0.03099	0.03816
.250	0.00529	0.00736	0.01004	0.01622	0.02075	0.02457	0.03551	0.04371
.275	0.00604	0.00839	0.01144	0.01847	0.02361	0.02794	0.04034	0.04962
.300	0.00686	0.00952	0.01296	0.02089	0.02669	0.03156	0.04552	0.05594
.325	0.00774	0.01073	0.01460	0.02350	0.03000	0.03546	0.05107	0.06272
.350	0.00870	0.01206	0.01639	0.02634	0.03359	0.03967	0.05707	0.07003
.375	0.00975	0.01350	0.01834	0.02942	0.03748	0.04425	0.06356	0.07793
.400	0.01091	0.01509	0.02048	0.03279	0.04174	0.04924	0.07062	0.08651
.425	0.01220	0.01685	0.02284	0.03651	0.04642	0.05472	0.07835	0.09589
.450	0.01363	0.01881	0.02546	0.04062	0.05159	0.06076	0.08685	0.10619
.475	0.01523	0.02100	0.02839	0.04520	0.05734	0.06748	0.09627	0.11758
.500	0.01705	0.02347	0.03170	0.05034	0.06379	0.07501	0.10680	0.13028
.525	0.01912	0.02629	0.03546	0.05618	0.07110	0.08352	0.11866	0.14457
.550	0.02152	0.02954	0.03978	0.06288	0.07945	0.09324	0.13217	0.16081
.575	0.	0.03334	0.04482	0.07065	0.08914	0.10449	0.14774	0.17949
.600	0.	0.03783	0.05078	0.07981	0.10053	0.11771	0.16598	0.20132
.625	0.	0.	0.05796	0.09080	0.11418	0.13351	0.18770	0.22727
.650	0.	0.	0.	0.10429	0.13088	0.15284	0.21418	0.25883
.675	0.	0.	0.	0.	0.15192	0.17713	0.24734	0.29827
.700	0.	0.	0.	0.	0.	0.	0.29041	0.34938
.725	0.	0.	0.	0.	0.	0.	0.	0.41887
.750	0.	0.	0.	0.	0.	0.	0.	0.
.775	0.	0.	0.	0.	0.	0.	0.	0.
.800	0.	0.	0.	0.	0.	0.	0.	0.

TABLE 19

VALUES OF AVERAGE FRAGMENTATION FORCE OVER
ULTIMATE TENSILE STRESS FOR D/H=22.50.

R2\H	0.022	0.028	0.035	0.049	0.058	0.065	0.083	0.095
.200	0.00418	0.00582	0.00795	0.01288	0.01651	0.01956	0.02834	0.03493
.225	0.00487	0.00677	0.00925	0.01496	0.01916	0.02269	0.03285	0.04045
.250	0.00560	0.00779	0.01063	0.01719	0.02199	0.02604	0.03765	0.04633
.275	0.00640	0.00889	0.01212	0.01957	0.02502	0.02961	0.04276	0.05260
.300	0.00726	0.01008	0.01373	0.02214	0.02828	0.03345	0.04825	0.05930
.325	0.00820	0.01137	0.01547	0.02491	0.03179	0.03758	0.05413	0.06649
.350	0.00922	0.01277	0.01737	0.02791	0.03559	0.04204	0.06049	0.07423
.375	0.01033	0.01431	0.01943	0.03118	0.03972	0.04689	0.06736	0.08260
.400	0.01156	0.01599	0.02170	0.03475	0.04424	0.05218	0.07485	0.09170
.425	0.01292	0.01785	0.02420	0.03868	0.04919	0.05799	0.08304	0.10163
.450	0.01444	0.01992	0.02697	0.04304	0.05467	0.06439	0.09205	0.11255
.475	0.01614	0.02224	0.03008	0.04789	0.06076	0.07151	0.10203	0.12462
.500	0.01806	0.02486	0.03358	0.05334	0.06759	0.07948	0.11318	0.13808
.525	0.02026	0.02785	0.03756	0.05953	0.07533	0.08850	0.12575	0.15321
.550	0.02279	0.03129	0.04214	0.06662	0.08418	0.09880	0.14006	0.17042
.575	0.	0.03531	0.04748	0.07485	0.09444	0.11072	0.15656	0.19021
.600	0.	0.04007	0.05379	0.08455	0.10651	0.12472	0.17587	0.21334
.625	0.	0.	0.06139	0.09619	0.12096	0.14146	0.19889	0.24083
.650	0.	0.	0.	0.11048	0.13866	0.16192	0.22693	0.27425
.675	0.	0.	0.	0.	0.16093	0.18765	0.26205	0.31603
.700	0.	0.	0.	0.	0.	0.	0.30766	0.37016
.725	0.	0.	0.	0.	0.	0.	0.	0.44374
.750	0.	0.	0.	0.	0.	0.	0.	0.
.775	0.	0.	0.	0.	0.	0.	0.	0.
.800	0.	0.	0.	0.	0.	0.	0.	0.

TABLE 20

VALUES OF AVERAGE FRAGMENTATION FORCE OVER
ULTIMATE TENSILE STRESS FOR D/H=23.75.

R2\H	0.022	0.028	0.035	0.049	0.058	0.065	0.083	0.095
.200	0.00441	0.00614	0.00840	0.01361	0.01744	0.02067	0.02995	0.03691
.225	0.00514	0.00715	0.00977	0.01581	0.02024	0.02398	0.03471	0.04275
.250	0.00592	0.00823	0.01123	0.01816	0.02323	0.02751	0.03978	0.04896
.275	0.00676	0.00939	0.01281	0.02068	0.02644	0.03128	0.04518	0.05558
.300	0.00767	0.01065	0.01450	0.02338	0.02988	0.03534	0.05098	0.06266
.325	0.00866	0.01201	0.01634	0.02631	0.03359	0.03970	0.05720	0.07025
.350	0.00973	0.01349	0.01834	0.02948	0.03760	0.04442	0.06391	0.07843
.375	0.01091	0.01511	0.02052	0.03293	0.04196	0.04954	0.07117	0.08728
.400	0.01221	0.01689	0.02292	0.03671	0.04673	0.05513	0.07908	0.09689
.425	0.01364	0.01885	0.02556	0.04086	0.05196	0.06126	0.08773	0.10738
.450	0.01524	0.02104	0.02849	0.04545	0.05774	0.06802	0.09725	0.11891
.475	0.01704	0.02349	0.03177	0.05058	0.06418	0.07554	0.10779	0.13166
.500	0.01907	0.02626	0.03546	0.05634	0.07140	0.08396	0.11957	0.14588
.525	0.02139	0.02941	0.03967	0.06287	0.07957	0.09348	0.13284	0.16186
.550	0.02407	0.03304	0.04450	0.07035	0.08892	0.10436	0.14795	0.18003
.575	0.	0.03729	0.05014	0.07905	0.09975	0.11694	0.16537	0.20094
.600	0.	0.04231	0.05680	0.08929	0.11249	0.13172	0.18577	0.22535
.625	0.	0.	0.06482	0.10158	0.12775	0.14940	0.21007	0.25438
.650	0.	0.	0.	0.11666	0.14643	0.17101	0.23968	0.28968
.675	0.	0.	0.	0.	0.16995	0.19817	0.27676	0.33378
.700	0.	0.	0.	0.	0.	0.	0.32492	0.39093
.725	0.	0.	0.	0.	0.	0.	0.	0.46862
.750	0.	0.	0.	0.	0.	0.	0.	0.
.775	0.	0.	0.	0.	0.	0.	0.	0.
.800	0.	0.	0.	0.	0.	0.	0.	0.

TABLE 21

VALUES OF AVERAGE FRAGMENTATION FORCE OVER
ULTIMATE TENSILE STRESS FOR D/H=25.00.

R2\H	0.022	0.028	0.035	0.049	0.058	0.065	0.083	0.095
.200	0.00465	0.00647	0.00884	0.01434	0.01837	0.02177	0.03155	0.03889
.225	0.00541	0.00753	0.01029	0.01665	0.02132	0.02526	0.03657	0.04504
.250	0.00623	0.00867	0.01183	0.01913	0.02447	0.02898	0.04191	0.05158
.275	0.00712	0.00989	0.01349	0.02178	0.02785	0.03296	0.04760	0.05856
.300	0.00808	0.01121	0.01528	0.02463	0.03147	0.03722	0.05371	0.06602
.325	0.00912	0.01265	0.01721	0.02771	0.03538	0.04182	0.06026	0.07402
.350	0.01025	0.01420	0.01932	0.03105	0.03961	0.04679	0.06733	0.08263
.375	0.01149	0.01591	0.02161	0.03468	0.04420	0.05218	0.07498	0.09195
.400	0.01286	0.01778	0.02413	0.03866	0.04922	0.05807	0.08331	0.10207
.425	0.01437	0.01985	0.02691	0.04303	0.05473	0.06452	0.09242	0.11313
.450	0.01605	0.02216	0.03000	0.04787	0.06082	0.07165	0.10244	0.12527
.475	0.01794	0.02474	0.03345	0.05327	0.06760	0.07957	0.11355	0.13870
.500	0.02008	0.02765	0.03734	0.05933	0.07520	0.08843	0.12595	0.15367
.525	0.02252	0.03097	0.04177	0.06621	0.08380	0.09846	0.13993	0.17051
.550	0.02534	0.03480	0.04686	0.07409	0.09365	0.10991	0.15584	0.18964
.575	0.	0.03926	0.05280	0.08325	0.10505	0.12316	0.17419	0.21166
.600	0.	0.04455	0.05981	0.09403	0.11847	0.13873	0.19567	0.23737
.625	0.	0.	0.06826	0.10697	0.13453	0.15734	0.22125	0.26794
.650	0.	0.	0.	0.12285	0.15420	0.18009	0.25243	0.30510
.675	0.	0.	0.	0.	0.17896	0.20869	0.29147	0.35154
.700	0.	0.	0.	0.	0.	0.	0.34217	0.41171
.725	0.	0.	0.	0.	0.	0.	0.	0.49350
.750	0.	0.	0.	0.	0.	0.	0.	0.
.775	0.	0.	0.	0.	0.	0.	0.	0.
.800	0.	0.	0.	0.	0.	0.	0.	0.

TABLE 22

VALUES OF AVERAGE FRAGMENTATION FORCE OVER
ULTIMATE TENSILE STRESS FOR D/H=26.25.

R2\H	0.022	0.028	0.035	0.049	0.058	0.065	0.083	0.095
.200	0.00488	0.00680	0.00929	0.01506	0.01930	0.02288	0.03316	0.04087
.225	0.00568	0.00791	0.01081	0.01750	0.02240	0.02654	0.03843	0.04734
.250	0.00655	0.00911	0.01243	0.02009	0.02571	0.03045	0.04404	0.05421
.275	0.00748	0.01039	0.01417	0.02288	0.02926	0.03463	0.05003	0.06154
.300	0.00848	0.01178	0.01605	0.02588	0.03307	0.03911	0.05643	0.06938
.325	0.00958	0.01328	0.01808	0.02911	0.03717	0.04394	0.06332	0.07778
.350	0.01077	0.01492	0.02029	0.03262	0.04161	0.04916	0.07075	0.08684
.375	0.01207	0.01671	0.02271	0.03644	0.04644	0.05483	0.07879	0.09663
.400	0.01350	0.01868	0.02535	0.04062	0.05171	0.06101	0.08754	0.10726
.425	0.01509	0.02085	0.02827	0.04521	0.05750	0.06779	0.09711	0.11888
.450	0.01686	0.02327	0.03151	0.05029	0.06390	0.07528	0.10764	0.13163
.475	0.01885	0.02598	0.03514	0.05596	0.07102	0.08359	0.11931	0.14574
.500	0.02109	0.02904	0.03923	0.06233	0.07900	0.09291	0.13233	0.16147
.525	0.02365	0.03253	0.04388	0.06955	0.08804	0.10344	0.14701	0.17916
.550	0.02661	0.03655	0.04923	0.07783	0.09838	0.11547	0.16373	0.19925
.575	0.	0.04124	0.05546	0.08745	0.11036	0.12939	0.18301	0.22238
.600	0.	0.04679	0.06282	0.09877	0.12445	0.14573	0.20556	0.24939
.625	0.	0.	0.07169	0.11236	0.14132	0.16528	0.23244	0.28149
.650	0.	0.	0.	0.12904	0.16197	0.18917	0.26518	0.32052
.675	0.	0.	0.	0.	0.18798	0.21921	0.30618	0.36930
.700	0.	0.	0.	0.	0.	0.	0.35942	0.43248
.725	0.	0.	0.	0.	0.	0.	0.	0.51837
.750	0.	0.	0.	0.	0.	0.	0.	0.
.775	0.	0.	0.	0.	0.	0.	0.	0.
.800	0.	0.	0.	0.	0.	0.	0.	0.

TABLE 23

VALUES OF AVERAGE FRAGMENTATION FORCE OVER
ULTIMATE TENSILE STRESS FOR D/H=27.50.

R2\H	0.022	0.028	0.035	0.049	0.058	0.065	0.083	0.095
.200	0.00512	0.00712	0.00974	0.01579	0.02024	0.02398	0.03477	0.04285
.225	0.00596	0.00829	0.01132	0.01834	0.02349	0.02782	0.04029	0.04963
.250	0.00686	0.00954	0.01302	0.02106	0.02696	0.03192	0.04617	0.05684
.275	0.00784	0.01089	0.01485	0.02398	0.03067	0.03630	0.05245	0.06452
.300	0.00889	0.01234	0.01682	0.02713	0.03466	0.04100	0.05916	0.07273
.325	0.01003	0.01392	0.01895	0.03052	0.03896	0.04606	0.06638	0.08155
.350	0.01128	0.01564	0.02127	0.03419	0.04362	0.05153	0.07417	0.09104
.375	0.01265	0.01751	0.02380	0.03819	0.04868	0.05747	0.08260	0.10130
.400	0.01415	0.01958	0.02657	0.04257	0.05420	0.06395	0.09177	0.11245
.425	0.01581	0.02185	0.02963	0.04739	0.06027	0.07106	0.10180	0.12462
.450	0.01767	0.02439	0.03303	0.05271	0.06698	0.07890	0.11284	0.13800
.475	0.01975	0.02723	0.03683	0.05865	0.07444	0.08762	0.12506	0.15278
.500	0.02210	0.03043	0.04111	0.06533	0.08280	0.09738	0.13872	0.16927
.525	0.02479	0.03409	0.04598	0.07290	0.09227	0.10842	0.15410	0.18780
.550	0.02789	0.03830	0.05159	0.08157	0.10311	0.12102	0.17162	0.20887
.575	0.	0.04321	0.05811	0.09164	0.11566	0.13561	0.19182	0.23310
.600	0.	0.04903	0.06583	0.10351	0.13042	0.15274	0.21546	0.26140
.625	0.	0.	0.07513	0.11776	0.14810	0.17322	0.24362	0.29505
.650	0.	0.	0.	0.13523	0.16975	0.19825	0.27793	0.33594
.675	0.	0.	0.	0.	0.19699	0.22972	0.32089	0.38705
.700	0.	0.	0.	0.	0.	0.	0.37668	0.45326
.725	0.	0.	0.	0.	0.	0.	0.	0.54325
.750	0.	0.	0.	0.	0.	0.	0.	0.
.775	0.	0.	0.	0.	0.	0.	0.	0.
.800	0.	0.	0.	0.	0.	0.	0.	0.

TABLE 24

VALUES OF AVERAGE FRAGMENTATION FORCE OVER
ULTIMATE TENSILE STRESS FOR D/H=28.75.

R2\H	0.022	0.028	0.035	0.049	0.058	0.065	0.083	0.095
.200	0.00535	0.00745	0.01019	0.01652	0.02117	0.02509	0.03637	0.04483
.225	0.00623	0.00867	0.01184	0.01918	0.02457	0.02911	0.04215	0.05192
.250	0.00718	0.00998	0.01362	0.02203	0.02820	0.03339	0.04830	0.05946
.275	0.00819	0.01139	0.01553	0.02509	0.03208	0.03797	0.05487	0.06750
.300	0.00930	0.01291	0.01759	0.02837	0.03626	0.04289	0.06189	0.07609
.325	0.01049	0.01456	0.01982	0.03192	0.04076	0.04818	0.06944	0.08531
.350	0.01180	0.01635	0.02224	0.03576	0.04563	0.05391	0.07759	0.09524
.375	0.01323	0.01832	0.02489	0.03995	0.05092	0.06012	0.08640	0.10598
.400	0.01480	0.02047	0.02779	0.04453	0.05670	0.06690	0.09600	0.11764
.425	0.01654	0.02285	0.03099	0.04956	0.06304	0.07433	0.10649	0.13037
.450	0.01848	0.02550	0.03454	0.05513	0.07005	0.08253	0.11803	0.14436
.475	0.02065	0.02847	0.03851	0.06135	0.07785	0.09165	0.13082	0.15983
.500	0.02311	0.03183	0.04299	0.06832	0.08660	0.10186	0.14510	0.17706
.525	0.02592	0.03565	0.04809	0.07624	0.09651	0.11340	0.16119	0.19645
.550	0.02916	0.04005	0.05395	0.08531	0.10784	0.12658	0.17951	0.21848
.575	0.	0.04519	0.06077	0.09584	0.12097	0.14183	0.20064	0.24382
.600	0.	0.05127	0.06884	0.10825	0.13640	0.15974	0.22535	0.27342
.625	0.	0.	0.07856	0.12315	0.15489	0.18116	0.25480	0.30860
.650	0.	0.	0.	0.14141	0.17752	0.20734	0.29068	0.35137
.675	0.	0.	0.	0.	0.20601	0.24024	0.33560	0.40481
.700	0.	0.	0.	0.	0.	0.28311	0.39393	0.47404
.725	0.	0.	0.	0.	0.	0.	0.	0.56813
.750	0.	0.	0.	0.	0.	0.	0.	0.
.775	0.	0.	0.	0.	0.	0.	0.	0.
.800	0.	0.	0.	0.	0.	0.	0.	0.

TABLE 25

VALUES OF AVERAGE FRAGMENTATION FORCE OVER
ULTIMATE TENSILE STRESS FOR D/H=30.00.

R2\H	0.022	0.028	0.035	0.049	0.058	0.065	0.083	0.095
.200	0.00558	0.00778	0.01063	0.01724	0.02210	0.02619	0.03798	0.04681
.225	0.00650	0.00905	0.01236	0.02003	0.02565	0.03039	0.04401	0.05422
.250	0.00749	0.01042	0.01422	0.02300	0.02944	0.03486	0.05043	0.06209
.275	0.00855	0.01189	0.01621	0.02619	0.03350	0.03964	0.05729	0.07048
.300	0.00970	0.01348	0.01836	0.02962	0.03785	0.04478	0.06462	0.07945
.325	0.01095	0.01520	0.02069	0.03332	0.04255	0.05030	0.07251	0.08908
.350	0.01231	0.01707	0.02322	0.03734	0.04763	0.05628	0.08101	0.09944
.375	0.01380	0.01912	0.02598	0.04170	0.05316	0.06276	0.09021	0.11065
.400	0.01545	0.02137	0.02901	0.04648	0.05919	0.06984	0.10023	0.12282
.425	0.01726	0.02386	0.03235	0.05174	0.06581	0.07760	0.11118	0.13612
.450	0.01928	0.02662	0.03605	0.05755	0.07313	0.08616	0.12323	0.15072
.475	0.02155	0.02972	0.04020	0.06404	0.08127	0.09568	0.13658	0.16687
.500	0.02412	0.03322	0.04487	0.07132	0.09041	0.10633	0.15149	0.18486
.525	0.02705	0.03721	0.05019	0.07958	0.10074	0.11838	0.16828	0.20510
.550	0.03044	0.04180	0.05631	0.08905	0.11257	0.13214	0.18740	0.22809
.575	0.	0.04716	0.06343	0.10004	0.12627	0.14806	0.20945	0.25455
.600	0.	0.05352	0.07185	0.11300	0.14238	0.16675	0.23525	0.28544
.625	0.	0.	0.08200	0.12854	0.16167	0.18910	0.26599	0.32216
.650	0.	0.	0.	0.14760	0.18529	0.21642	0.30343	0.36679
.675	0.	0.	0.	0.	0.21502	0.25076	0.35031	0.42256
.700	0.	0.	0.	0.	0.	0.29550	0.41119	0.49481
.725	0.	0.	0.	0.	0.	0.	0.	0.59300
.750	0.	0.	0.	0.	0.	0.	0.	0.
.775	0.	0.	0.	0.	0.	0.	0.	0.
.800	0.	0.	0.	0.	0.	0.	0.	0.

TABLE 26

VALUES OF AVERAGE FRAGMENTATION FORCE OVER
ULTIMATE TENSILE STRESS FOR D/H=31.25.

R2\H	0.022	0.028	0.035	0.049	0.058	0.065	0.083	0.095
.200	0.00582	0.00810	0.01108	0.01797	0.02303	0.02730	0.03958	0.04879
.225	0.00678	0.00943	0.01288	0.02087	0.02673	0.03167	0.04587	0.05651
.250	0.00780	0.01086	0.01482	0.02397	0.03068	0.03633	0.05256	0.06471
.275	0.00891	0.01239	0.01690	0.02729	0.03491	0.04132	0.05971	0.07346
.300	0.01011	0.01404	0.01914	0.03087	0.03945	0.04667	0.06735	0.08281
.325	0.01141	0.01583	0.02156	0.03473	0.04434	0.05243	0.07557	0.09284
.350	0.01283	0.01779	0.02419	0.03891	0.04964	0.05865	0.08443	0.10365
.375	0.01438	0.01992	0.02707	0.04346	0.05539	0.06541	0.09402	0.11532
.400	0.01609	0.02226	0.03022	0.04844	0.06168	0.07278	0.10445	0.12801
.425	0.01798	0.02486	0.03370	0.05391	0.06858	0.08087	0.11587	0.14186
.450	0.02009	0.02774	0.03757	0.05997	0.07621	0.08979	0.12843	0.15708
.475	0.02246	0.03097	0.04189	0.06673	0.08469	0.09970	0.14234	0.17391
.500	0.02513	0.03461	0.04676	0.07432	0.09421	0.11081	0.15787	0.19266
.525	0.02819	0.03876	0.05230	0.08293	0.10498	0.12336	0.17537	0.21374
.550	0.03171	0.04355	0.05867	0.09279	0.11730	0.13769	0.19530	0.23770
.575	0.	0.04914	0.06609	0.10424	0.13157	0.15428	0.21827	0.26527
.600	0.	0.05576	0.07487	0.11774	0.14836	0.17376	0.24515	0.29745
.625	0.	0.	0.08543	0.13393	0.16846	0.19704	0.27717	0.33571
.650	0.	0.	0.	0.15379	0.19307	0.22550	0.31618	0.38221
.675	0.	0.	0.	0.	0.22404	0.26128	0.36502	0.44032
.700	0.	0.	0.	0.	0.	0.30788	0.42844	0.51559
.725	0.	0.	0.	0.	0.	0.	0.	0.61788
.750	0.	0.	0.	0.	0.	0.	0.	0.
.775	0.	0.	0.	0.	0.	0.	0.	0.
.800	0.	0.	0.	0.	0.	0.	0.	0.

TABLE 27

VALUES OF AVERAGE FRAGMENTATION FORCE OVER
ULTIMATE TENSILE STRESS FOR D/H=32.50.

R2\H	0.022	0.028	0.035	0.049	0.058	0.065	0.083	0.095
.200	0.00605	0.00843	0.01153	0.01870	0.02396	0.02841	0.04119	0.05077
.225	0.00705	0.00981	0.01340	0.02171	0.02781	0.03295	0.04773	0.05880
.250	0.00812	0.01129	0.01542	0.02494	0.03192	0.03780	0.05469	0.06734
.275	0.00927	0.01289	0.01758	0.02840	0.03632	0.04299	0.06213	0.07644
.300	0.01052	0.01461	0.01991	0.03211	0.04104	0.04855	0.07008	0.08617
.325	0.01187	0.01647	0.02243	0.03613	0.04614	0.05455	0.07863	0.09661
.350	0.01335	0.01850	0.02517	0.04048	0.05164	0.06102	0.08785	0.10785
.375	0.01496	0.02072	0.02816	0.04521	0.05763	0.06805	0.09783	0.12000
.400	0.01674	0.02316	0.03144	0.05039	0.06417	0.07572	0.10868	0.13320
.425	0.01871	0.02586	0.03506	0.05609	0.07135	0.08414	0.12056	0.14761
.450	0.02090	0.02885	0.03908	0.06239	0.07929	0.09342	0.13362	0.16344
.475	0.02336	0.03221	0.04357	0.06942	0.08811	0.10373	0.14810	0.18095
.500	0.02614	0.03600	0.04864	0.07732	0.09801	0.11528	0.16425	0.20045
.525	0.02932	0.04032	0.05440	0.08627	0.10921	0.12834	0.18246	0.22239
.550	0.03298	0.04530	0.06103	0.09653	0.12203	0.14325	0.20319	0.24731
.575	0.	0.05111	0.06875	0.10844	0.13688	0.16050	0.22708	0.27599
.600	0.	0.05800	0.07788	0.12248	0.15434	0.18076	0.25504	0.30947
.625	0.	0.	0.08886	0.13932	0.17525	0.20498	0.28835	0.34927
.650	0.	0.	0.	0.15998	0.20084	0.23459	0.32893	0.39764
.675	0.	0.	0.	0.	0.23305	0.27180	0.37974	0.45808
.700	0.	0.	0.	0.	0.	0.32027	0.44569	0.53636
.725	0.	0.	0.	0.	0.	0.	0.	0.64276
.750	0.	0.	0.	0.	0.	0.	0.	0.
.775	0.	0.	0.	0.	0.	0.	0.	0.
.800	0.	0.	0.	0.	0.	0.	0.	0.

TABLE 28

VALUES OF AVERAGE FRAGMENTATION FORCE OVER
ULTIMATE TENSILE STRESS FOR D/H=33.75.

R2\H	0.022	0.028	0.035	0.049	0.058	0.065	0.083	0.095
.200	0.00629	0.00876	0.01197	0.01942	0.02490	0.02951	0.04279	0.05275
.225	0.00732	0.01019	0.01392	0.02256	0.02889	0.03424	0.04959	0.06110
.250	0.00843	0.01173	0.01601	0.02591	0.03316	0.03927	0.05683	0.06997
.275	0.00963	0.01339	0.01826	0.02950	0.03773	0.04466	0.06455	0.07942
.300	0.01092	0.01517	0.02068	0.03336	0.04264	0.05044	0.07281	0.08953
.325	0.01233	0.01711	0.02330	0.03753	0.04793	0.05667	0.08169	0.10037
.350	0.01386	0.01922	0.02614	0.04205	0.05365	0.06340	0.09127	0.11205
.375	0.01554	0.02152	0.02925	0.04697	0.05987	0.07070	0.10163	0.12467
.400	0.01739	0.02406	0.03266	0.05235	0.06666	0.07867	0.11291	0.13839
.425	0.01943	0.02686	0.03642	0.05826	0.07412	0.08740	0.12525	0.15336
.450	0.02171	0.02997	0.04059	0.06481	0.08236	0.09705	0.13882	0.16980
.475	0.02426	0.03346	0.04526	0.07211	0.09153	0.10776	0.15385	0.18799
.500	0.02715	0.03739	0.05052	0.08031	0.10181	0.11976	0.17064	0.20825
.525	0.03045	0.04188	0.05651	0.08961	0.11345	0.13332	0.18955	0.23104
.550	0.03426	0.04705	0.06339	0.10027	0.12676	0.14881	0.21108	0.25693
.575	0.	0.05309	0.07141	0.11264	0.14218	0.16673	0.23590	0.28671
.600	0.	0.06024	0.08089	0.12722	0.16032	0.18777	0.26494	0.32149
.625	0.	0.	0.09230	0.14471	0.18203	0.21292	0.29954	0.36282
.650	0.	0.	0.	0.16616	0.20861	0.24367	0.34168	0.41306
.675	0.	0.	0.	0.	0.24207	0.28232	0.39445	0.47583
.700	0.	0.	0.	0.	0.	0.33266	0.46295	0.55714
.725	0.	0.	0.	0.	0.	0.	0.	0.66763
.750	0.	0.	0.	0.	0.	0.	0.	0.
.775	0.	0.	0.	0.	0.	0.	0.	0.
.800	0.	0.	0.	0.	0.	0.	0.	0.

TABLE 29

VALUES OF AVERAGE FRAGMENTATION FORCE OVER
ULTIMATE TENSILE STRESS FOR D/H=35.00.

R2\H	0.022	0.028	0.035	0.049	0.058	0.065	0.083	0.095
.200	0.00652	0.00908	0.01242	0.02015	0.02583	0.03062	0.04440	0.05473
.225	0.00759	0.01057	0.01444	0.02340	0.02998	0.03552	0.05145	0.06339
.250	0.00875	0.01217	0.01661	0.02688	0.03440	0.04074	0.05896	0.07259
.275	0.00999	0.01388	0.01894	0.03060	0.03914	0.04633	0.06697	0.08240
.300	0.01133	0.01574	0.02145	0.03461	0.04423	0.05233	0.07554	0.09289
.325	0.01279	0.01775	0.02417	0.03893	0.04972	0.05879	0.08475	0.10414
.350	0.01438	0.01994	0.02712	0.04362	0.05566	0.06577	0.09469	0.11625
.375	0.01612	0.02233	0.03034	0.04872	0.06211	0.07334	0.10544	0.12935
.400	0.01803	0.02495	0.03388	0.05430	0.06916	0.08161	0.11714	0.14357
.425	0.02015	0.02786	0.03778	0.06044	0.07689	0.09067	0.12994	0.15911
.450	0.02252	0.03109	0.04211	0.06723	0.08544	0.10067	0.14402	0.17616
.475	0.02516	0.03470	0.04695	0.07480	0.09495	0.11179	0.15961	0.19503
.500	0.02816	0.03879	0.05240	0.08331	0.10561	0.12423	0.17702	0.21605
.525	0.03158	0.04344	0.05861	0.09295	0.11768	0.13830	0.19664	0.23968
.550	0.03553	0.04880	0.06575	0.10401	0.13149	0.15436	0.21897	0.26654
.575	0.	0.05506	0.07407	0.11684	0.14749	0.17295	0.24471	0.29743
.600	0.	0.06248	0.08390	0.13196	0.16630	0.19477	0.27484	0.33350
.625	0.	0.	0.09573	0.15010	0.18882	0.22086	0.31072	0.37638
.650	0.	0.	0.	0.17235	0.21638	0.25275	0.35442	0.42848
.675	0.	0.	0.	0.	0.25108	0.29283	0.40916	0.49359
.700	0.	0.	0.	0.	0.	0.34504	0.48020	0.57791
.725	0.	0.	0.	0.	0.	0.	0.	0.69251
.750	0.	0.	0.	0.	0.	0.	0.	0.
.775	0.	0.	0.	0.	0.	0.	0.	0.
.800	0.	0.	0.	0.	0.	0.	0.	0.

TABLE 30

VALUES OF AVERAGE FRAGMENTATION FORCE OVER
ULTIMATE TENSILE STRESS FOR D/H=36.25.

R2\H	0.022	0.028	0.035	0.049	0.058	0.065	0.083	0.095
.200	0.00675	0.00941	0.01287	0.02088	0.02676	0.03172	0.04600	0.05671
.225	0.00787	0.01095	0.01496	0.02424	0.03106	0.03680	0.05331	0.06568
.250	0.00906	0.01261	0.01721	0.02784	0.03564	0.04222	0.06109	0.07522
.275	0.01035	0.01438	0.01962	0.03170	0.04056	0.04801	0.06939	0.08538
.300	0.01174	0.01630	0.02222	0.03586	0.04583	0.05422	0.07827	0.09625
.325	0.01325	0.01839	0.02504	0.04034	0.05151	0.06091	0.08782	0.10790
.350	0.01490	0.02065	0.02810	0.04519	0.05766	0.06814	0.09811	0.12045
.375	0.01670	0.02313	0.03143	0.05048	0.06435	0.07599	0.10925	0.13402
.400	0.01868	0.02585	0.03510	0.05626	0.07165	0.08455	0.12137	0.14876
.425	0.02088	0.02886	0.03914	0.06262	0.07966	0.09394	0.13463	0.16485
.450	0.02332	0.03220	0.04362	0.06965	0.08852	0.10430	0.14921	0.18253
.475	0.02607	0.03595	0.04864	0.07749	0.09837	0.11581	0.16537	0.20207
.500	0.02917	0.04018	0.05429	0.08631	0.10942	0.12871	0.18341	0.22385
.525	0.03272	0.04500	0.06072	0.09630	0.12192	0.14328	0.20373	0.24833
.550	0.03681	0.05056	0.06811	0.10775	0.13622	0.15992	0.22686	0.27615
.575	0.	0.05704	0.07673	0.12104	0.15279	0.17917	0.25353	0.30816
.600	0.	0.06472	0.08691	0.13670	0.17227	0.20178	0.28473	0.34552
.625	0.	0.	0.09917	0.15549	0.19560	0.22880	0.32190	0.38993
.650	0.	0.	0.	0.17854	0.22416	0.26184	0.36717	0.44391
.675	0.	0.	0.	0.	0.26010	0.30335	0.42387	0.51134
.700	0.	0.	0.	0.	0.	0.35743	0.49745	0.59869
.725	0.	0.	0.	0.	0.	0.	0.	0.71739
.750	0.	0.	0.	0.	0.	0.	0.	0.
.775	0.	0.	0.	0.	0.	0.	0.	0.
.800	0.	0.	0.	0.	0.	0.	0.	0.

TABLE 31

VALUES OF AVERAGE FRAGMENTATION FORCE OVER
ULTIMATE TENSILE STRESS FOR D/H=37.50.

R2\H	0.022	0.028	0.035	0.049	0.058	0.065	0.083	0.095
.200	0.00699	0.00974	0.01332	0.02160	0.02769	0.03283	0.04761	0.05869
.225	0.00814	0.01133	0.01548	0.02509	0.03214	0.03808	0.05517	0.06798
.250	0.00937	0.01304	0.01781	0.02881	0.03689	0.04369	0.06322	0.07784
.275	0.01071	0.01488	0.02030	0.03281	0.04197	0.04968	0.07181	0.08836
.300	0.01215	0.01687	0.02299	0.03710	0.04742	0.05611	0.08100	0.09961
.325	0.01371	0.01902	0.02591	0.04174	0.05331	0.06303	0.09088	0.11167
.350	0.01541	0.02137	0.02907	0.04676	0.05967	0.07051	0.10153	0.12466
.375	0.01728	0.02393	0.03253	0.05223	0.06659	0.07864	0.11306	0.13870
.400	0.01933	0.02675	0.03631	0.05821	0.07414	0.08749	0.12560	0.15395
.425	0.02160	0.02986	0.04049	0.06479	0.08243	0.09721	0.13932	0.17060
.450	0.02413	0.03332	0.04513	0.07207	0.09160	0.10793	0.15441	0.18889
.475	0.02697	0.03719	0.05032	0.08019	0.10179	0.11984	0.17113	0.20911
.500	0.03018	0.04157	0.05617	0.08930	0.11322	0.13318	0.18979	0.23164
.525	0.03385	0.04656	0.06282	0.09964	0.12616	0.14826	0.21082	0.25698
.550	0.03808	0.05231	0.07047	0.11149	0.14095	0.16548	0.23475	0.28576
.575	0.	0.05901	0.07938	0.12524	0.15810	0.18540	0.26235	0.31888
.600	0.	0.06696	0.08992	0.14144	0.17825	0.20878	0.29463	0.35754
.625	0.	0.	0.10260	0.16088	0.20239	0.23674	0.33309	0.40349
.650	0.	0.	0.	0.18473	0.23193	0.27092	0.37992	0.45933
.675	0.	0.	0.	0.	0.26911	0.31387	0.43858	0.52910
.700	0.	0.	0.	0.	0.	0.36982	0.51471	0.61946
.725	0.	0.	0.	0.	0.	0.	0.	0.74227
.750	0.	0.	0.	0.	0.	0.	0.	0.
.775	0.	0.	0.	0.	0.	0.	0.	0.
.800	0.	0.	0.	0.	0.	0.	0.	0.

TABLE 32

VALUES OF AVERAGE FRAGMENTATION FORCE OVER
ULTIMATE TENSILE STRESS FOR D/H=38.75.

R2\H	0.022	0.028	0.035	0.049	0.058	0.065	0.083	0.095
.200	0.00722	0.01007	0.01376	0.02233	0.02862	0.03393	0.04921	0.06067
.225	0.00841	0.01171	0.01600	0.02593	0.03322	0.03937	0.05703	0.07027
.250	0.00969	0.01348	0.01840	0.02978	0.03813	0.04516	0.06535	0.08047
.275	0.01106	0.01538	0.02098	0.03391	0.04338	0.05135	0.07423	0.09134
.300	0.01255	0.01744	0.02377	0.03835	0.04902	0.05800	0.08373	0.10297
.325	0.01417	0.01966	0.02678	0.04314	0.05510	0.06515	0.09394	0.11543
.350	0.01593	0.02208	0.03005	0.04833	0.06168	0.07289	0.10495	0.12886
.375	0.01786	0.02473	0.03362	0.05399	0.06883	0.08128	0.11687	0.14337
.400	0.01998	0.02764	0.03753	0.06017	0.07663	0.09044	0.12983	0.15914
.425	0.02232	0.03086	0.04185	0.06697	0.08520	0.10048	0.14401	0.17635
.450	0.02494	0.03444	0.04665	0.07449	0.09467	0.11156	0.15961	0.19525
.475	0.02787	0.03844	0.05201	0.08288	0.10521	0.12387	0.17689	0.21615
.500	0.03119	0.04296	0.05805	0.09230	0.11702	0.13765	0.19617	0.23944
.525	0.03498	0.04812	0.06493	0.10298	0.13039	0.15324	0.21790	0.26562
.550	0.03935	0.05406	0.07283	0.11523	0.14568	0.17103	0.24264	0.29538
.575	0.	0.06099	0.08204	0.12944	0.16340	0.19162	0.27116	0.32960
.600	0.	0.06920	0.09293	0.14618	0.18423	0.21579	0.30453	0.36955
.625	0.	0.	0.10604	0.16627	0.20917	0.24469	0.34427	0.41704
.650	0.	0.	0.	0.19091	0.23970	0.28000	0.39267	0.47475
.675	0.	0.	0.	0.	0.27813	0.32439	0.45329	0.54686
.700	0.	0.	0.	0.	0.	0.38220	0.53196	0.64024
.725	0.	0.	0.	0.	0.	0.	0.	0.76714
.750	0.	0.	0.	0.	0.	0.	0.	0.
.775	0.	0.	0.	0.	0.	0.	0.	0.
.800	0.	0.	0.	0.	0.	0.	0.	0.

TABLE 33

VALUES OF AVERAGE FRAGMENTATION FORCE OVER
ULTIMATE TENSILE STRESS FOR D/H=40.00.

R2\H	0.022	0.028	0.035	0.049	0.058	0.065	0.083	0.095
.200	0.00746	0.01039	0.01421	0.02305	0.02956	0.03504	0.05082	0.06266
.225	0.00868	0.01209	0.01652	0.02678	0.03430	0.04065	0.05889	0.07256
.250	0.01000	0.01392	0.01900	0.03075	0.03937	0.04663	0.06748	0.08310
.275	0.01142	0.01588	0.02167	0.03501	0.04479	0.05302	0.07665	0.09432
.300	0.01296	0.01800	0.02454	0.03960	0.05062	0.05988	0.08646	0.10632
.325	0.01463	0.02030	0.02765	0.04454	0.05689	0.06727	0.09700	0.11920
.350	0.01644	0.02280	0.03102	0.04991	0.06368	0.07526	0.10837	0.13306
.375	0.01843	0.02554	0.03471	0.05574	0.07107	0.08393	0.12067	0.14805
.400	0.02062	0.02854	0.03875	0.06212	0.07913	0.09338	0.13406	0.16432
.425	0.02305	0.03186	0.04321	0.06914	0.08797	0.10375	0.14870	0.18209
.450	0.02575	0.03555	0.04816	0.07691	0.09775	0.11519	0.16480	0.20161
.475	0.02878	0.03969	0.05370	0.08557	0.10863	0.12790	0.18264	0.22319
.500	0.03220	0.04436	0.05994	0.09530	0.12082	0.14213	0.20256	0.24724
.525	0.03611	0.04968	0.06703	0.10632	0.13463	0.15821	0.22499	0.27427
.550	0.04063	0.05581	0.07519	0.11897	0.15042	0.17659	0.25053	0.30499
.575	0.	0.06296	0.08470	0.13364	0.16870	0.19784	0.27998	0.34032
.600	0.	0.07144	0.09594	0.15092	0.19021	0.22280	0.31442	0.38157
.625	0.	0.	0.10947	0.17166	0.21596	0.25263	0.35545	0.43060
.650	0.	0.	0.	0.19710	0.24748	0.28909	0.40542	0.49018
.675	0.	0.	0.	0.	0.28714	0.33491	0.46800	0.56461
.700	0.	0.	0.	0.	0.	0.39459	0.54922	0.66102
.725	0.	0.	0.	0.	0.	0.	0.	0.79202
.750	0.	0.	0.	0.	0.	0.	0.	0.
.775	0.	0.	0.	0.	0.	0.	0.	0.
.800	0.	0.	0.	0.	0.	0.	0.	0.

TABLE 34

VALUES OF AVERAGE FRAGMENTATION FORCE OVER
ULTIMATE TENSILE STRESS FOR D/H=41.25.

R2\H	0.022	0.028	0.035	0.049	0.058	0.065	0.083	0.095
.200	0.00769	0.01072	0.01466	0.02378	0.03049	0.03615	0.05243	0.06464
.225	0.00896	0.01247	0.01704	0.02762	0.03538	0.04193	0.06075	0.07486
.250	0.01032	0.01435	0.01960	0.03172	0.04061	0.04810	0.06961	0.08572
.275	0.01178	0.01638	0.02235	0.03612	0.04620	0.05470	0.07907	0.09730
.300	0.01337	0.01857	0.02531	0.04084	0.05221	0.06177	0.08919	0.10968
.325	0.01509	0.02094	0.02851	0.04595	0.05869	0.06939	0.10006	0.12296
.350	0.01696	0.02352	0.03200	0.05148	0.06569	0.07763	0.11179	0.13726
.375	0.01901	0.02634	0.03580	0.05750	0.07330	0.08657	0.12448	0.15272
.400	0.02127	0.02944	0.03997	0.06408	0.08162	0.09632	0.13829	0.16951
.425	0.02377	0.03286	0.04457	0.07132	0.09075	0.10702	0.15339	0.18784
.450	0.02655	0.03667	0.04967	0.07933	0.10083	0.11882	0.17000	0.20797
.475	0.02968	0.04093	0.05538	0.08826	0.11205	0.13192	0.18840	0.23023
.500	0.03321	0.04575	0.06182	0.09829	0.12463	0.14660	0.20894	0.25503
.525	0.03725	0.05124	0.06914	0.10967	0.13886	0.16319	0.23208	0.28292
.550	0.04190	0.05756	0.07756	0.12270	0.15515	0.18215	0.25843	0.31460
.575	0.	0.06494	0.08736	0.13784	0.17401	0.20407	0.28879	0.35104
.600	0.	0.07368	0.09895	0.15567	0.19619	0.22980	0.32432	0.39359
.625	0.	0.	0.11290	0.17705	0.22274	0.26057	0.36664	0.44415
.650	0.	0.	0.	0.20329	0.25525	0.29817	0.41817	0.50560
.675	0.	0.	0.	0.	0.29616	0.34542	0.48271	0.58237
.700	0.	0.	0.	0.	0.	0.40698	0.56647	0.68179
.725	0.	0.	0.	0.	0.	0.	0.	0.81690
.750	0.	0.	0.	0.	0.	0.	0.	0.
.775	0.	0.	0.	0.	0.	0.	0.	0.
.800	0.	0.	0.	0.	0.	0.	0.	0.

TABLE 35

VALUES OF AVERAGE FRAGMENTATION FORCE OVER
ULTIMATE TENSILE STRESS FOR D/H=42.50.

R2\H	0.022	0.028	0.035	0.049	0.058	0.065	0.083	0.095
.200	0.00793	0.01105	0.01510	0.02451	0.03142	0.03725	0.05403	0.06662
.225	0.00923	0.01285	0.01756	0.02846	0.03647	0.04321	0.06261	0.07715
.250	0.01063	0.01479	0.02020	0.03269	0.04185	0.04957	0.07174	0.08835
.275	0.01214	0.01688	0.02303	0.03722	0.04761	0.05637	0.08149	0.10028
.300	0.01377	0.01913	0.02608	0.04209	0.05381	0.06366	0.09192	0.11304
.325	0.01555	0.02158	0.02938	0.04735	0.06048	0.07151	0.10313	0.12673
.350	0.01748	0.02423	0.03297	0.05305	0.06770	0.08000	0.11521	0.14147
.375	0.01959	0.02714	0.03689	0.05925	0.07554	0.08922	0.12829	0.15740
.400	0.02192	0.03033	0.04119	0.06603	0.08411	0.09926	0.14252	0.17470
.425	0.02449	0.03386	0.04593	0.07349	0.09352	0.11028	0.15808	0.19359
.450	0.02736	0.03778	0.05119	0.08175	0.10391	0.12244	0.17520	0.21433
.475	0.03058	0.04218	0.05707	0.09095	0.11547	0.13595	0.19416	0.23727
.500	0.03422	0.04714	0.06370	0.10129	0.12843	0.15108	0.21533	0.26283
.525	0.03838	0.05280	0.07124	0.11301	0.14310	0.16817	0.23917	0.29156
.550	0.04318	0.05931	0.07992	0.12644	0.15988	0.18770	0.26632	0.32421
.575	0.	0.06691	0.09002	0.14204	0.17931	0.21029	0.29761	0.36176
.600	0.	0.07592	0.10196	0.16041	0.20217	0.23681	0.33421	0.40560
.625	0.	0.	0.11634	0.18244	0.22953	0.26851	0.37782	0.45771
.650	0.	0.	0.	0.20947	0.26302	0.30725	0.43092	0.52102
.675	0.	0.	0.	0.	0.30517	0.35594	0.49742	0.60012
.700	0.	0.	0.	0.	0.	0.41936	0.58372	0.70257
.725	0.	0.	0.	0.	0.	0.	0.	0.84177
.750	0.	0.	0.	0.	0.	0.	0.	0.
.775	0.	0.	0.	0.	0.	0.	0.	0.
.800	0.	0.	0.	0.	0.	0.	0.	0.

TABLE 36

VALUES OF AVERAGE FRAGMENTATION FORCE OVER
ULTIMATE TENSILE STRESS FOR D/H=43.75.

R2\H	0.022	0.028	0.035	0.049	0.058	0.065	0.083	0.095
.200	0.00816	0.01137	0.01555	0.02523	0.03235	0.03836	0.05564	0.06860
.225	0.00950	0.01323	0.01808	0.02931	0.03755	0.04449	0.06447	0.07944
.250	0.01095	0.01523	0.02080	0.03366	0.04309	0.05104	0.07387	0.09097
.275	0.01250	0.01738	0.02371	0.03832	0.04903	0.05804	0.08391	0.10326
.300	0.01418	0.01970	0.02685	0.04334	0.05540	0.06555	0.09465	0.11640
.325	0.01600	0.02221	0.03025	0.04875	0.06227	0.07364	0.10619	0.13049
.350	0.01799	0.02495	0.03395	0.05462	0.06970	0.08237	0.11863	0.14567
.375	0.02017	0.02794	0.03798	0.06100	0.07778	0.09186	0.13210	0.16207
.400	0.02257	0.03123	0.04240	0.06799	0.08660	0.10221	0.14675	0.17988
.425	0.02522	0.03486	0.04728	0.07567	0.09629	0.11355	0.16277	0.19933
.450	0.02817	0.03890	0.05270	0.08417	0.10698	0.12607	0.18039	0.22069
.475	0.03148	0.04342	0.05876	0.09364	0.11888	0.13998	0.19992	0.24431
.500	0.03523	0.04853	0.06558	0.10429	0.13223	0.15555	0.22171	0.27063
.525	0.03951	0.05435	0.07335	0.11635	0.14733	0.17315	0.24626	0.30021
.550	0.04445	0.06106	0.08228	0.13018	0.16461	0.19326	0.27421	0.33382
.575	0.	0.06889	0.09268	0.14624	0.18462	0.21651	0.30642	0.37249
.600	0.	0.07816	0.10497	0.16515	0.20815	0.24381	0.34411	0.41762
.625	0.	0.	0.11977	0.18783	0.23631	0.27645	0.38900	0.47126
.650	0.	0.	0.	0.21566	0.27079	0.31634	0.44367	0.53644
.675	0.	0.	0.	0.	0.31419	0.36646	0.51213	0.61788
.700	0.	0.	0.	0.	0.	0.43175	0.60098	0.72334
.725	0.	0.	0.	0.	0.	0.	0.	0.86665
.750	0.	0.	0.	0.	0.	0.	0.	0.
.775	0.	0.	0.	0.	0.	0.	0.	0.
.800	0.	0.	0.	0.	0.	0.	0.	0.

TABLE 37

VALUES OF AVERAGE FRAGMENTATION FORCE OVER
ULTIMATE TENSILE STRESS FOR D/H=45.00.

R2\H	0.022	0.028	0.035	0.049	0.058	0.065	0.083	0.095
.200	0.00839	0.01170	0.01600	0.02596	0.03328	0.03946	0.05724	0.07058
.225	0.00978	0.01361	0.01860	0.03015	0.03863	0.04578	0.06633	0.08174
.250	0.01126	0.01567	0.02139	0.03463	0.04433	0.05251	0.07601	0.09360
.275	0.01286	0.01788	0.02439	0.03942	0.05044	0.05971	0.08633	0.10624
.300	0.01459	0.02026	0.02762	0.04459	0.05700	0.06744	0.09738	0.11976
.325	0.01646	0.02285	0.03112	0.05016	0.06406	0.07576	0.10925	0.13426
.350	0.01851	0.02567	0.03492	0.05619	0.07171	0.08475	0.12205	0.14987
.375	0.02075	0.02874	0.03907	0.06276	0.08002	0.09451	0.13590	0.16674
.400	0.02321	0.03213	0.04362	0.06994	0.08909	0.10515	0.15098	0.18507
.425	0.02594	0.03586	0.04864	0.07785	0.09906	0.11682	0.16746	0.20508
.450	0.02898	0.04002	0.05421	0.08659	0.11006	0.12970	0.18559	0.22706
.475	0.03239	0.04467	0.06044	0.09634	0.12230	0.14401	0.20567	0.25135
.500	0.03624	0.04992	0.06747	0.10728	0.13603	0.16003	0.22809	0.27842
.525	0.04064	0.05591	0.07545	0.11970	0.15157	0.17813	0.25335	0.30886
.550	0.04572	0.06281	0.08464	0.13392	0.16934	0.19881	0.28210	0.34344
.575	0.	0.07086	0.09534	0.15043	0.18992	0.22274	0.31524	0.38321
.600	0.	0.08040	0.10798	0.16989	0.21412	0.25082	0.35401	0.42964
.625	0.	0.	0.12321	0.19323	0.24310	0.28439	0.40019	0.48482
.650	0.	0.	0.	0.22185	0.27857	0.32542	0.45642	0.55187
.675	0.	0.	0.	0.	0.32320	0.37698	0.52684	0.63564
.700	0.	0.	0.	0.	0.	0.44413	0.61823	0.74412
.725	0.	0.	0.	0.	0.	0.	0.	0.89153
.750	0.	0.	0.	0.	0.	0.	0.	0.
.775	0.	0.	0.	0.	0.	0.	0.	0.
.800	0.	0.	0.	0.	0.	0.	0.	0.

TABLE 37

VALUES OF AVERAGE FRAGMENTATION FORCE OVER
ULTIMATE TENSILE STRESS FOR D/H=45.00.

R2\H	0.022	0.028	0.035	0.049	0.058	0.065	0.083	0.095
.200	0.00839	0.01170	0.01600	0.02596	0.03328	0.03946	0.05724	0.07058
.225	0.00978	0.01361	0.01860	0.03015	0.03863	0.04578	0.06633	0.08174
.250	0.01126	0.01567	0.02139	0.03463	0.04433	0.05251	0.07601	0.09360
.275	0.01286	0.01788	0.02439	0.03942	0.05044	0.05971	0.08633	0.10624
.300	0.01459	0.02026	0.02762	0.04459	0.05700	0.06744	0.09738	0.11976
.325	0.01646	0.02285	0.03112	0.05016	0.06406	0.07576	0.10925	0.13426
.350	0.01851	0.02567	0.03492	0.05619	0.07171	0.08475	0.12205	0.14987
.375	0.02075	0.02874	0.03907	0.06276	0.08002	0.09451	0.13590	0.16674
.400	0.02321	0.03213	0.04362	0.06994	0.08909	0.10515	0.15098	0.18507
.425	0.02594	0.03586	0.04864	0.07785	0.09906	0.11682	0.16746	0.20508
.450	0.02898	0.04002	0.05421	0.08659	0.11006	0.12970	0.18559	0.22706
.475	0.03239	0.04467	0.06044	0.09634	0.12230	0.14401	0.20567	0.25135
.500	0.03624	0.04992	0.06747	0.10728	0.13603	0.16003	0.22809	0.27842
.525	0.04064	0.05591	0.07545	0.11970	0.15157	0.17813	0.25335	0.30886
.550	0.04572	0.06281	0.08464	0.13392	0.16934	0.19881	0.28210	0.34344
.575	0.	0.07086	0.09534	0.15043	0.18992	0.22274	0.31524	0.38321
.600	0.	0.08040	0.10798	0.16989	0.21412	0.25082	0.35401	0.42964
.625	0.	0.	0.12321	0.19323	0.24310	0.28439	0.40019	0.48482
.650	0.	0.	0.	0.22185	0.27857	0.32542	0.45642	0.55187
.675	0.	0.	0.	0.	0.32320	0.37698	0.52684	0.63564
.700	0.	0.	0.	0.	0.	0.44413	0.61823	0.74412
.725	0.	0.	0.	0.	0.	0.	0.	0.89153
.750	0.	0.	0.	0.	0.	0.	0.	0.
.775	0.	0.	0.	0.	0.	0.	0.	0.
.800	0.	0.	0.	0.	0.	0.	0.	0.

TABLE 38

VALUES OF AVERAGE FRAGMENTATION FORCE OVER
ULTIMATE TENSILE STRESS FOR D/H=46.25.

R2\H	0.022	0.028	0.035	0.049	0.058	0.065	0.083	0.095
.200	0.00863	0.01203	0.01645	0.02669	0.03422	0.04057	0.05885	0.07256
.225	0.01005	0.01399	0.01912	0.03099	0.03971	0.04706	0.06819	0.08403
.250	0.01157	0.01610	0.02199	0.03559	0.04557	0.05398	0.07814	0.09623
.275	0.01322	0.01838	0.02507	0.04053	0.05185	0.06138	0.08875	0.10922
.300	0.01499	0.02083	0.02840	0.04583	0.05859	0.06933	0.10011	0.12312
.325	0.01692	0.02349	0.03199	0.05156	0.06586	0.07788	0.11231	0.13803
.350	0.01903	0.02638	0.03590	0.05776	0.07372	0.08712	0.12547	0.15407
.375	0.02133	0.02955	0.04016	0.06451	0.08226	0.09715	0.13971	0.17142
.400	0.02386	0.03302	0.04484	0.07190	0.09159	0.10809	0.15521	0.19026
.425	0.02666	0.03686	0.05000	0.08002	0.10183	0.12009	0.17215	0.21083
.450	0.02979	0.04113	0.05573	0.08901	0.11314	0.13333	0.19079	0.23342
.475	0.03329	0.04592	0.06213	0.09903	0.12572	0.14803	0.21143	0.25839
.500	0.03725	0.05132	0.06935	0.11028	0.13983	0.16450	0.23448	0.28622
.525	0.04178	0.05747	0.07756	0.12304	0.15580	0.18311	0.26044	0.31751
.550	0.04700	0.06456	0.08700	0.13766	0.17407	0.20437	0.28999	0.35305
.575	0.	0.07284	0.09799	0.15463	0.19523	0.22896	0.32405	0.39393
.600	0.	0.08264	0.11099	0.17463	0.22010	0.25782	0.36390	0.44165
.625	0.	0.	0.12664	0.19862	0.24989	0.29233	0.41137	0.49837
.650	0.	0.	0.	0.22804	0.28634	0.33450	0.46917	0.56729
.675	0.	0.	0.	0.	0.33222	0.38750	0.54155	0.65339
.700	0.	0.	0.	0.	0.	0.45652	0.63548	0.76489
.725	0.	0.	0.	0.	0.	0.	0.	0.91640
.750	0.	0.	0.	0.	0.	0.	0.	0.
.775	0.	0.	0.	0.	0.	0.	0.	0.
.800	0.	0.	0.	0.	0.	0.	0.	0.

TABLE 39

VALUES OF AVERAGE FRAGMENTATION FORCE OVER
ULTIMATE TENSILE STRESS FOR D/H=47.50.

R2\H	0.022	0.028	0.035	0.049	0.058	0.065	0.083	0.095
.200	0.00886	0.01235	0.01689	0.02741	0.03515	0.04167	0.06045	0.07454
.225	0.01032	0.01437	0.01964	0.03184	0.04079	0.04834	0.07005	0.08633
.250	0.01189	0.01654	0.02259	0.03656	0.04681	0.05545	0.08027	0.09885
.275	0.01358	0.01888	0.02575	0.04163	0.05326	0.06306	0.09117	0.11221
.300	0.01540	0.02140	0.02917	0.04708	0.06019	0.07122	0.10284	0.12648
.325	0.01738	0.02413	0.03286	0.05296	0.06765	0.08000	0.11537	0.14179
.350	0.01954	0.02710	0.03687	0.05933	0.07572	0.08949	0.12889	0.15827
.375	0.02191	0.03035	0.04125	0.06627	0.08450	0.09980	0.14352	0.17609
.400	0.02451	0.03392	0.04606	0.07386	0.09408	0.11104	0.15944	0.19545
.425	0.02739	0.03786	0.05136	0.08220	0.10460	0.12336	0.17684	0.21658
.450	0.03059	0.04225	0.05724	0.09143	0.11622	0.13696	0.19598	0.23978
.475	0.03419	0.04716	0.06382	0.10172	0.12914	0.15206	0.21719	0.26543
.500	0.03826	0.05271	0.07123	0.11328	0.14364	0.16898	0.24086	0.29402
.525	0.04291	0.05903	0.07966	0.12638	0.16004	0.18809	0.26753	0.32615
.550	0.04827	0.06632	0.08936	0.14140	0.17880	0.20993	0.29788	0.36266
.575	0.	0.07482	0.10065	0.15883	0.20053	0.23518	0.33287	0.40465
.600	0.	0.08488	0.11400	0.17937	0.22608	0.26483	0.37380	0.45367
.625	0.	0.	0.13008	0.20401	0.25667	0.30027	0.42255	0.51193
.650	0.	0.	0.	0.23422	0.29411	0.34359	0.48192	0.58271
.675	0.	0.	0.	0.	0.34123	0.39801	0.55626	0.67115
.700	0.	0.	0.	0.	0.	0.46891	0.65274	0.78567
.725	0.	0.	0.	0.	0.	0.	0.	0.94128
.750	0.	0.	0.	0.	0.	0.	0.	0.
.775	0.	0.	0.	0.	0.	0.	0.	0.
.800	0.	0.	0.	0.	0.	0.	0.	0.

TABLE 40

VALUES OF AVERAGE FRAGMENTATION FORCE OVER
ULTIMATE TENSILE STRESS FOR D/H=48.75.

R2\H	0.022	0.028	0.035	0.049	0.058	0.065	0.083	0.095
.200	0.00910	0.01268	0.01734	0.02814	0.03608	0.04278	0.06206	0.07652
.225	0.01059	0.01475	0.02016	0.03268	0.04187	0.04962	0.07191	0.08862
.250	0.01220	0.01698	0.02319	0.03753	0.04806	0.05692	0.08240	0.10148
.275	0.01393	0.01938	0.02644	0.04273	0.05467	0.06473	0.09359	0.11519
.300	0.01581	0.02196	0.02994	0.04833	0.06178	0.07310	0.10557	0.12984
.325	0.01784	0.02476	0.03373	0.05436	0.06944	0.08212	0.11844	0.14556
.350	0.02006	0.02782	0.03785	0.06090	0.07773	0.09186	0.13231	0.16248
.375	0.02248	0.03115	0.04235	0.06802	0.08674	0.10244	0.14733	0.18077
.400	0.02515	0.03481	0.04728	0.07581	0.09657	0.11398	0.16366	0.20063
.425	0.02811	0.03886	0.05272	0.08437	0.10737	0.12663	0.18153	0.22232
.450	0.03140	0.04337	0.05875	0.09385	0.11929	0.14058	0.20118	0.24614
.475	0.03510	0.04841	0.06551	0.10441	0.13256	0.15609	0.22295	0.27247
.500	0.03927	0.05410	0.07311	0.11627	0.14744	0.17345	0.24725	0.30181
.525	0.04404	0.06059	0.08177	0.12972	0.16427	0.19307	0.27462	0.33480
.550	0.04955	0.06807	0.09172	0.14514	0.18353	0.21548	0.30577	0.37227
.575	0.	0.07679	0.10331	0.16303	0.20584	0.24140	0.34168	0.41537
.600	0.	0.08712	0.11702	0.18411	0.23206	0.27184	0.38370	0.46569
.625	0.	0.	0.13351	0.20940	0.26346	0.30821	0.43374	0.52548
.650	0.	0.	0.	0.24041	0.30188	0.35267	0.49467	0.59814
.675	0.	0.	0.	0.	0.35025	0.40853	0.57097	0.68890
.700	0.	0.	0.	0.	0.	0.48129	0.66999	0.80644
.725	0.	0.	0.	0.	0.	0.	0.	0.96616
.750	0.	0.	0.	0.	0.	0.	0.	0.
.775	0.	0.	0.	0.	0.	0.	0.	0.
.800	0.	0.	0.	0.	0.	0.	0.	0.

TABLE 41

VALUES OF AVERAGE FRAGMENTATION FORCE OVER
ULTIMATE TENSILE STRESS FOR D/H=50.00.

R2\H	0.022	0.028	0.035	0.049	0.058	0.065	0.083	0.095
.200	0.00933	0.01301	0.01779	0.02887	0.03701	0.04388	0.06366	0.07850
.225	0.01087	0.01513	0.02068	0.03352	0.04295	0.05091	0.07377	0.09091
.250	0.01252	0.01742	0.02378	0.03850	0.04930	0.05839	0.08453	0.10411
.275	0.01429	0.01987	0.02712	0.04384	0.05609	0.06640	0.09601	0.11817
.300	0.01621	0.02253	0.03071	0.04957	0.06338	0.07499	0.10830	0.13320
.325	0.01830	0.02540	0.03460	0.05577	0.07124	0.08424	0.12150	0.14932
.350	0.02057	0.02853	0.03883	0.06248	0.07974	0.09424	0.13573	0.16668
.375	0.02306	0.03195	0.04344	0.06978	0.08897	0.10509	0.15114	0.18544
.400	0.02580	0.03571	0.04850	0.07777	0.09906	0.11692	0.16789	0.20582
.425	0.02883	0.03986	0.05407	0.08655	0.11014	0.12990	0.18622	0.22807
.450	0.03221	0.04448	0.06027	0.09627	0.12237	0.14421	0.20638	0.25250
.475	0.03600	0.04965	0.06719	0.10710	0.13598	0.16012	0.22871	0.27951
.500	0.04028	0.05549	0.07500	0.11927	0.15124	0.17793	0.25363	0.30961
.525	0.04517	0.06215	0.08387	0.13307	0.16851	0.19805	0.28171	0.34345
.550	0.05082	0.06982	0.09408	0.14888	0.18826	0.22104	0.31366	0.38188
.575	0.	0.07877	0.10597	0.16723	0.21114	0.24763	0.35050	0.42610
.600	0.	0.08936	0.12003	0.18885	0.23804	0.27884	0.39359	0.47770
.625	0.	0.	0.13695	0.21479	0.27024	0.31615	0.44492	0.53904
.650	0.	0.	0.	0.24660	0.30966	0.36175	0.50742	0.61356
.675	0.	0.	0.	0.	0.35926	0.41905	0.58568	0.70666
.700	0.	0.	0.	0.	0.	0.49368	0.68724	0.82722
.725	0.	0.	0.	0.	0.	0.	0.	0.99103
.750	0.	0.	0.	0.	0.	0.	0.	0.
.775	0.	0.	0.	0.	0.	0.	0.	0.
.800	0.	0.	0.	0.	0.	0.	0.	0.

TABLE 42

VALUES OF AVERAGE FRAGMENTATION FORCE OVER
ULTIMATE TENSILE STRESS FOR D/H=51.25.

R2\H	0.022	0.028	0.035	0.049	0.058	0.065	0.083	0.095
.200	0.00957	0.01333	0.01823	0.02959	0.03794	0.04499	0.06527	0.08048
.225	0.01114	0.01551	0.02120	0.03437	0.04404	0.05219	0.07563	0.09321
.250	0.01283	0.01785	0.02438	0.03947	0.05054	0.05987	0.08666	0.10673
.275	0.01465	0.02037	0.02780	0.04494	0.05750	0.06807	0.09843	0.12115
.300	0.01662	0.02309	0.03148	0.05082	0.06497	0.07688	0.11103	0.13656
.325	0.01876	0.02604	0.03547	0.05717	0.07303	0.08636	0.12456	0.15309
.350	0.02109	0.02925	0.03980	0.06405	0.08174	0.09661	0.13915	0.17088
.375	0.02364	0.03275	0.04453	0.07153	0.09121	0.10773	0.15494	0.19012
.400	0.02645	0.03661	0.04971	0.07972	0.10155	0.11986	0.17212	0.21101
.425	0.02956	0.04086	0.05543	0.08873	0.11291	0.13317	0.19091	0.23382
.450	0.03302	0.04560	0.06178	0.09869	0.12545	0.14784	0.21157	0.25886
.475	0.03690	0.05090	0.06888	0.10979	0.13940	0.16414	0.23446	0.28656
.500	0.04129	0.05689	0.07688	0.12227	0.15504	0.18240	0.26001	0.31741
.525	0.04631	0.06371	0.08598	0.13641	0.17274	0.20303	0.28879	0.35209
.550	0.05209	0.07157	0.09644	0.15262	0.19299	0.22660	0.32156	0.39150
.575	0.	0.08074	0.10863	0.17143	0.21644	0.25385	0.35932	0.43682
.600	0.	0.09160	0.12304	0.19359	0.24402	0.28585	0.40349	0.48972
.625	0.	0.	0.14038	0.22018	0.27703	0.32409	0.45610	0.55259
.650	0.	0.	0.	0.25279	0.31743	0.37083	0.52017	0.62898
.675	0.	0.	0.	0.	0.36828	0.42957	0.60039	0.72441
.700	0.	0.	0.	0.	0.	0.50607	0.70450	0.84800
.725	0.	0.	0.	0.	0.	0.	0.	1.01591
.750	0.	0.	0.	0.	0.	0.	0.	0.
.775	0.	0.	0.	0.	0.	0.	0.	0.
.800	0.	0.	0.	0.	0.	0.	0.	0.

TABLE 43

VALUES OF AVERAGE FRAGMENTATION FORCE OVER
ULTIMATE TENSILE STRESS FOR D/H=52.50.

R2\H	0.022	0.028	0.035	0.049	0.058	0.065	0.083	0.095
.200	0.00980	0.01366	0.01868	0.03032	0.03888	0.04610	0.06687	0.08246
.225	0.01141	0.01589	0.02172	0.03521	0.04512	0.05347	0.07749	0.09550
.250	0.01314	0.01829	0.02498	0.04044	0.05178	0.06134	0.08879	0.10936
.275	0.01501	0.02087	0.02848	0.04604	0.05891	0.06975	0.10085	0.12413
.300	0.01703	0.02366	0.03225	0.05207	0.06657	0.07877	0.11376	0.13992
.325	0.01922	0.02668	0.03634	0.05857	0.07482	0.08848	0.12762	0.15685
.350	0.02161	0.02996	0.04078	0.06562	0.08375	0.09898	0.14257	0.17508
.375	0.02422	0.03356	0.04562	0.07329	0.09345	0.11038	0.15875	0.19479
.400	0.02710	0.03750	0.05093	0.08168	0.10405	0.12281	0.17635	0.21620
.425	0.03028	0.04187	0.05679	0.09090	0.11568	0.13643	0.19560	0.23956
.450	0.03383	0.04671	0.06329	0.10111	0.12853	0.15147	0.21677	0.26523
.475	0.03780	0.05215	0.07057	0.11249	0.14282	0.16817	0.24022	0.29360
.500	0.04230	0.05828	0.07876	0.12526	0.15884	0.18688	0.26640	0.32520
.525	0.04744	0.06527	0.08808	0.13975	0.17698	0.20801	0.29588	0.36074
.550	0.05337	0.07332	0.09880	0.15636	0.19772	0.23215	0.32945	0.40111
.575	0.	0.08272	0.11129	0.17563	0.22175	0.26007	0.36813	0.44754
.600	0.	0.09384	0.12605	0.19833	0.25000	0.29285	0.41339	0.50174
.625	0.	0.	0.14381	0.22557	0.28381	0.33203	0.46729	0.56615
.650	0.	0.	0.	0.25897	0.32520	0.37992	0.53292	0.64441
.675	0.	0.	0.	0.	0.37729	0.44009	0.61510	0.74217
.700	0.	0.	0.	0.	0.	0.51845	0.72175	0.86877
.725	0.	0.	0.	0.	0.	0.	0.	1.04079
.750	0.	0.	0.	0.	0.	0.	0.	0.
.775	0.	0.	0.	0.	0.	0.	0.	0.
.800	0.	0.	0.	0.	0.	0.	0.	0.

TABLE 44

VALUES OF AVERAGE FRAGMENTATION FORCE OVER
ULTIMATE TENSILE STRESS FOR D/H=53.75.

R2\H	0.022	0.028	0.035	0.049	0.058	0.065	0.083	0.095
.200	0.01003	0.01399	0.01913	0.03105	0.03981	0.04720	0.06848	0.08444
.225	0.01169	0.01627	0.02224	0.03605	0.04620	0.05475	0.07935	0.09779
.250	0.01346	0.01873	0.02558	0.04141	0.05302	0.06281	0.09092	0.11198
.275	0.01537	0.02137	0.02916	0.04714	0.06032	0.07142	0.10327	0.12711
.300	0.01744	0.02422	0.03303	0.05331	0.06816	0.08066	0.11649	0.14327
.325	0.01968	0.02732	0.03721	0.05997	0.07661	0.09060	0.13068	0.16062
.350	0.02212	0.03068	0.04175	0.06719	0.08576	0.10135	0.14599	0.17928
.375	0.02480	0.03436	0.04671	0.07504	0.09569	0.11302	0.16256	0.19947
.400	0.02774	0.03840	0.05215	0.08363	0.10654	0.12575	0.18058	0.22138
.425	0.03100	0.04287	0.05815	0.09308	0.11845	0.13970	0.20029	0.24531
.450	0.03463	0.04783	0.06481	0.10353	0.13160	0.15510	0.22197	0.27159
.475	0.03871	0.05339	0.07225	0.11518	0.14624	0.17220	0.24598	0.30064
.500	0.04331	0.05967	0.08064	0.12826	0.16265	0.19135	0.27278	0.33300
.525	0.04857	0.06683	0.09019	0.14310	0.18121	0.21299	0.30297	0.36939
.550	0.05464	0.07507	0.10116	0.16010	0.20245	0.23771	0.33734	0.41072
.575	0.	0.08469	0.11395	0.17983	0.22705	0.26630	0.37695	0.45826
.600	0.	0.09609	0.12906	0.20308	0.25597	0.29986	0.42328	0.51375
.625	0.	0.	0.14725	0.23096	0.29060	0.33997	0.47847	0.57970
.650	0.	0.	0.	0.26516	0.33298	0.38900	0.54567	0.65983
.675	0.	0.	0.	0.	0.38631	0.45061	0.62981	0.75993
.700	0.	0.	0.	0.	0.	0.53084	0.73901	0.88955
.725	0.	0.	0.	0.	0.	0.	0.	1.06566
.750	0.	0.	0.	0.	0.	0.	0.	0.
.775	0.	0.	0.	0.	0.	0.	0.	0.
.800	0.	0.	0.	0.	0.	0.	0.	0.

TABLE 45

VALUES OF AVERAGE FRAGMENTATION FORCE OVER
ULTIMATE TENSILE STRESS FOR D/H=55.00.

R2\H	0.022	0.028	0.035	0.049	0.058	0.065	0.083	0.095
.200	0.01027	0.01431	0.01958	0.03177	0.04074	0.04831	0.07008	0.08642
.225	0.01196	0.01665	0.02276	0.03690	0.04728	0.05604	0.08121	0.10009
.250	0.01377	0.01917	0.02618	0.04238	0.05426	0.06428	0.09306	0.11461
.275	0.01573	0.02187	0.02984	0.04825	0.06173	0.07309	0.10569	0.13009
.300	0.01784	0.02479	0.03380	0.05456	0.06976	0.08255	0.11922	0.14663
.325	0.02014	0.02795	0.03808	0.06138	0.07841	0.09273	0.13375	0.16438
.350	0.02264	0.03140	0.04273	0.06876	0.08776	0.10373	0.14941	0.18349
.375	0.02538	0.03516	0.04780	0.07680	0.09793	0.11567	0.16637	0.20414
.400	0.02839	0.03930	0.05337	0.08559	0.10903	0.12869	0.18481	0.22657
.425	0.03173	0.04387	0.05951	0.09525	0.12122	0.14297	0.20498	0.25106
.450	0.03544	0.04895	0.06632	0.10595	0.13468	0.15873	0.22717	0.27795
.475	0.03961	0.05464	0.07394	0.11787	0.14966	0.17623	0.25174	0.30768
.500	0.04432	0.06106	0.08253	0.13126	0.16645	0.19583	0.27917	0.34080
.525	0.04970	0.06839	0.09229	0.14644	0.18545	0.21797	0.31006	0.37803
.550	0.05592	0.07682	0.10353	0.16384	0.20718	0.24327	0.34523	0.42033
.575	0.	0.08667	0.11661	0.18403	0.23236	0.27252	0.38576	0.46898
.600	0.	0.09833	0.13207	0.20782	0.26195	0.30686	0.43318	0.52577
.625	0.	0.	0.15068	0.23635	0.29738	0.34792	0.48965	0.59326
.650	0.	0.	0.	0.27135	0.34075	0.39808	0.55842	0.67525
.675	0.	0.	0.	0.	0.39532	0.46112	0.64452	0.77768
.700	0.	0.	0.	0.	0.	0.54323	0.75626	0.91032
.725	0.	0.	0.	0.	0.	0.	0.	1.09054
.750	0.	0.	0.	0.	0.	0.	0.	0.
.775	0.	0.	0.	0.	0.	0.	0.	0.
.800	0.	0.	0.	0.	0.	0.	0.	0.

TABLE 46

VALUES OF AVERAGE FRAGMENTATION FORCE OVER
ULTIMATE TENSILE STRESS FOR D/H=56.25.

R2\H	0.022	0.028	0.035	0.049	0.058	0.065	0.083	0.095
.200	0.01050	0.01464	0.02002	0.03250	0.04167	0.04941	0.07169	0.08840
.225	0.01223	0.01703	0.02328	0.03774	0.04836	0.05732	0.08307	0.10238
.250	0.01409	0.01960	0.02677	0.04335	0.05550	0.06575	0.09519	0.11724
.275	0.01609	0.02237	0.03053	0.04935	0.06315	0.07476	0.10811	0.13307
.300	0.01825	0.02536	0.03457	0.05581	0.07135	0.08443	0.12195	0.14999
.325	0.02060	0.02859	0.03895	0.06278	0.08020	0.09485	0.13681	0.16815
.350	0.02316	0.03211	0.04370	0.07033	0.08977	0.10610	0.15283	0.18769
.375	0.02596	0.03596	0.04889	0.07855	0.10017	0.11831	0.17017	0.20882
.400	0.02904	0.04019	0.05459	0.08754	0.11152	0.13163	0.18904	0.23176
.425	0.03245	0.04487	0.06086	0.09743	0.12399	0.14624	0.20967	0.25681
.450	0.03625	0.05006	0.06783	0.10837	0.13776	0.16235	0.23236	0.28431
.475	0.04051	0.05588	0.07563	0.12056	0.15308	0.18026	0.25750	0.31472
.500	0.04533	0.06246	0.08441	0.13425	0.17025	0.20030	0.28555	0.34860
.525	0.05084	0.06994	0.09440	0.14978	0.18969	0.22295	0.31715	0.38668
.550	0.05719	0.07857	0.10589	0.16758	0.21191	0.24882	0.35312	0.42994
.575	0.	0.08864	0.11926	0.18823	0.23766	0.27874	0.39458	0.47970
.600	0.	0.10057	0.13508	0.21256	0.26793	0.31387	0.44308	0.53779
.625	0.	0.	0.15412	0.24174	0.30417	0.35586	0.50084	0.60681
.650	0.	0.	0.	0.27754	0.34852	0.40717	0.57117	0.69068
.675	0.	0.	0.	0.	0.40433	0.47164	0.65923	0.79544
.700	0.	0.	0.	0.	0.	0.55561	0.77351	0.93110
.725	0.	0.	0.	0.	0.	0.	0.	1.11542
.750	0.	0.	0.	0.	0.	0.	0.	0.
.775	0.	0.	0.	0.	0.	0.	0.	0.
.800	0.	0.	0.	0.	0.	0.	0.	0.

TABLE 47

VALUES OF AVERAGE FRAGMENTATION FORCE OVER
ULTIMATE TENSILE STRESS FOR D/H=57.50.

R2\H	0.022	0.028	0.035	0.049	0.058	0.065	0.083	0.095
.200	0.01074	0.01497	0.02047	0.03323	0.04260	0.05052	0.07330	0.09038
.225	0.01250	0.01741	0.02380	0.03859	0.04944	0.05860	0.08493	0.10467
.250	0.01440	0.02004	0.02737	0.04431	0.05674	0.06722	0.09732	0.11986
.275	0.01645	0.02287	0.03121	0.05045	0.06456	0.07644	0.11053	0.13605
.300	0.01866	0.02592	0.03534	0.05706	0.07295	0.08632	0.12468	0.15335
.325	0.02106	0.02923	0.03982	0.06418	0.08199	0.09697	0.13987	0.17191
.350	0.02367	0.03283	0.04468	0.07190	0.09178	0.10847	0.15625	0.19189
.375	0.02653	0.03677	0.04998	0.08031	0.10241	0.12096	0.17398	0.21349
.400	0.02969	0.04109	0.05580	0.08950	0.11402	0.13458	0.19327	0.23695
.425	0.03317	0.04587	0.06222	0.09960	0.12676	0.14951	0.21436	0.26255
.450	0.03706	0.05118	0.06935	0.11079	0.14084	0.16598	0.23756	0.29067
.475	0.04141	0.05713	0.07731	0.12325	0.15650	0.18428	0.26325	0.32176
.500	0.04634	0.06385	0.08629	0.13725	0.17405	0.20477	0.29193	0.35639
.525	0.05197	0.07150	0.09650	0.15312	0.19392	0.22793	0.32424	0.39533
.550	0.05846	0.08032	0.10825	0.17132	0.21665	0.25438	0.36101	0.43956
.575	0.06605	0.09062	0.12192	0.19243	0.24297	0.28497	0.40339	0.49043
.600	0.	0.10281	0.13809	0.21730	0.27391	0.32088	0.45297	0.54980
.625	0.	0.	0.15755	0.24713	0.31095	0.36380	0.51202	0.62037
.650	0.	0.	0.	0.28372	0.35629	0.41625	0.58392	0.70610
.675	0.	0.	0.	0.	0.41335	0.48216	0.67394	0.81319
.700	0.	0.	0.	0.	0.	0.56800	0.79077	0.95187
.725	0.	0.	0.	0.	0.	0.	0.	1.14029
.750	0.	0.	0.	0.	0.	0.	0.	0.
.775	0.	0.	0.	0.	0.	0.	0.	0.
.800	0.	0.	0.	0.	0.	0.	0.	0.

TABLE 48

VALUES OF AVERAGE FRAGMENTATION FORCE OVER
ULTIMATE TENSILE STRESS FOR D/H=58.75.

R2\H	0.022	0.028	0.035	0.049	0.058	0.065	0.083	0.095
.200	0.01097	0.01529	0.02092	0.03395	0.04354	0.05162	0.07490	0.09237
.225	0.01278	0.01780	0.02432	0.03943	0.05053	0.05988	0.08679	0.10697
.250	0.01472	0.02048	0.02797	0.04528	0.05799	0.06869	0.09945	0.12249
.275	0.01680	0.02337	0.03189	0.05156	0.06597	0.07811	0.11295	0.13903
.300	0.01906	0.02649	0.03611	0.05830	0.07454	0.08821	0.12741	0.15671
.325	0.02152	0.02987	0.04069	0.06558	0.08379	0.09909	0.14293	0.17568
.350	0.02419	0.03355	0.04565	0.07347	0.09378	0.11084	0.15967	0.19609
.375	0.02711	0.03757	0.05107	0.08206	0.10465	0.12360	0.17779	0.21816
.400	0.03033	0.04199	0.05702	0.09145	0.11651	0.13752	0.19750	0.24213
.425	0.03390	0.04687	0.06358	0.10178	0.12953	0.15278	0.21905	0.26830
.450	0.03787	0.05230	0.07086	0.11321	0.14391	0.16961	0.24276	0.29703
.475	0.04232	0.05838	0.07900	0.12594	0.15991	0.18831	0.26901	0.32880
.500	0.04735	0.06524	0.08817	0.14025	0.17785	0.20925	0.29832	0.36419
.525	0.05310	0.07306	0.09861	0.15647	0.19816	0.23291	0.33133	0.40397
.550	0.05974	0.08208	0.11061	0.17505	0.22138	0.25994	0.36890	0.44917
.575	0.06749	0.09259	0.12458	0.19663	0.24827	0.29119	0.41221	0.50115
.600	0.	0.10505	0.14110	0.22204	0.27989	0.32788	0.46287	0.56182
.625	0.	0.	0.16099	0.25252	0.31774	0.37174	0.52320	0.63392
.650	0.	0.	0.	0.28991	0.36407	0.42533	0.59667	0.72152
.675	0.	0.	0.	0.	0.42236	0.49268	0.68865	0.83095
.700	0.	0.	0.	0.	0.	0.58039	0.80802	0.97265
.725	0.	0.	0.	0.	0.	0.	0.	1.16517
.750	0.	0.	0.	0.	0.	0.	0.	0.
.775	0.	0.	0.	0.	0.	0.	0.	0.
.800	0.	0.	0.	0.	0.	0.	0.	0.

TABLE 49

VALUES OF AVERAGE FRAGMENTATION FORCE OVER
ULTIMATE TENSILE STRESS FOR D/H=60.00.

R2\H	0.022	0.028	0.035	0.049	0.058	0.065	0.083	0.095
.200	0.01121	0.01562	0.02136	0.03468	0.04447	0.05273	0.07651	0.09435
.225	0.01305	0.01818	0.02484	0.04027	0.05161	0.06117	0.08865	0.10926
.250	0.01503	0.02092	0.02857	0.04625	0.05923	0.07016	0.10158	0.12511
.275	0.01716	0.02387	0.03257	0.05266	0.06738	0.07978	0.11537	0.14201
.300	0.01947	0.02705	0.03689	0.05955	0.07614	0.09010	0.13014	0.16007
.325	0.02197	0.03051	0.04155	0.06699	0.08558	0.10121	0.14599	0.17944
.350	0.02470	0.03426	0.04663	0.07505	0.09579	0.11322	0.16309	0.20030
.375	0.02769	0.03837	0.05217	0.08382	0.10688	0.12625	0.18160	0.22284
.400	0.03098	0.04288	0.05824	0.09341	0.11900	0.14046	0.20173	0.24732
.425	0.03462	0.04787	0.06494	0.10396	0.13230	0.15605	0.22374	0.27405
.450	0.03867	0.05341	0.07238	0.11563	0.14699	0.17324	0.24795	0.30339
.475	0.04322	0.05962	0.08069	0.12863	0.16333	0.19234	0.27477	0.33584
.500	0.04836	0.06663	0.09006	0.14325	0.18166	0.21372	0.30470	0.37199
.525	0.05424	0.07462	0.10071	0.15981	0.20239	0.23789	0.33842	0.41262
.550	0.06101	0.08383	0.11297	0.17879	0.22611	0.26549	0.37679	0.45878
.575	0.06893	0.09457	0.12724	0.20083	0.25357	0.29741	0.42102	0.51187
.600	0.	0.10729	0.14411	0.22678	0.28587	0.33489	0.47276	0.57384
.625	0.	0.	0.16442	0.25791	0.32453	0.37968	0.53439	0.64748
.650	0.	0.	0.	0.29610	0.37184	0.43442	0.60942	0.73695
.675	0.	0.	0.	0.	0.43138	0.50320	0.70336	0.84871
.700	0.	0.	0.	0.	0.	0.59277	0.82527	0.99343
.725	0.	0.	0.	0.	0.	0.	0.	1.19005
.750	0.	0.	0.	0.	0.	0.	0.	0.
.775	0.	0.	0.	0.	0.	0.	0.	0.
.800	0.	0.	0.	0.	0.	0.	0.	0.

SPACE TECHNOLOGY PROJECT NO. 9

SOLUTIONS OF ELASTICITY PROBLEMS USING BOUNDARY CONDITIONS OBTAINED EXPERIMENTALLY

SOLUTIONS OF ELASTICITY PROBLEMS USING BOUNDARY CONDITIONS OBTAINED EXPERIMENTALLY

Principal Investigators

Dr. J. George H. Thompson, Professor of Mechanical Engineering

Mr. Bobby P. Long, Graduate Assistant

I. Introduction

The purpose of the research is to develop rapid methods of calculating stresses in irregularly shaped bodies. Space age developments demand that methods suit the need and cannot permit the design to be limited by existing methods of computation. This project, therefore, seeks to make simpler, more rapid, and far more flexible forms of well established ways of figuring stresses. The principles employed are basic and very well established. But the object is to use these basic principles in such new ways as will permit the fullest utilization of modern aids such as the digital computer. Furthermore, the object is to use quick, though admittedly approximate, experimental methods rather than the more precise analytical methods wherever the loss in accuracy will not be serious and the gain in time required will be substantial.

II. Present Status of the Research

A computer program has been developed and is in the process of being further refined.

Much progress has been made in the last three months in the use of the lateral extensometer as a device for determining boundary

conditions. This technique has been applied successfully to a more complicated problem than had been attempted before and detail comparisons of extensometer results with values determined by other means have verified the reliability of the method. Mr. Long has cleverly developed a new way to use the extensometer so as to greatly aid the computer work and to lead towards the solution of multiple connected shapes.

The conductive sheet technique has further been extended in the past three months. Mr. Long has developed ways of experimentally reducing fields involving certain kinds of singular points to equivalent fields not containing singular points. He has not only extended the field of application of the conductive sheet technique but has also compared the results of this technique with those produced by other methods.

The work has not yet gone to the point of developing novel and clearly superior ways in which conductive sheets are more attractive than existing methods. The research is moving in that direction, however, and now has progressed to the point where it is known, by actual demonstration, that the conductive sheet procedures are reliable.

Work is still continuing to the end of extending this activity further into the areas of multiple connected bodies and, later, into the field of three dimensional bodies.

A technical paper is now being written by Dr. Thompson (Ninth Mid-Western Mechanics Conference) based on the work of this project.

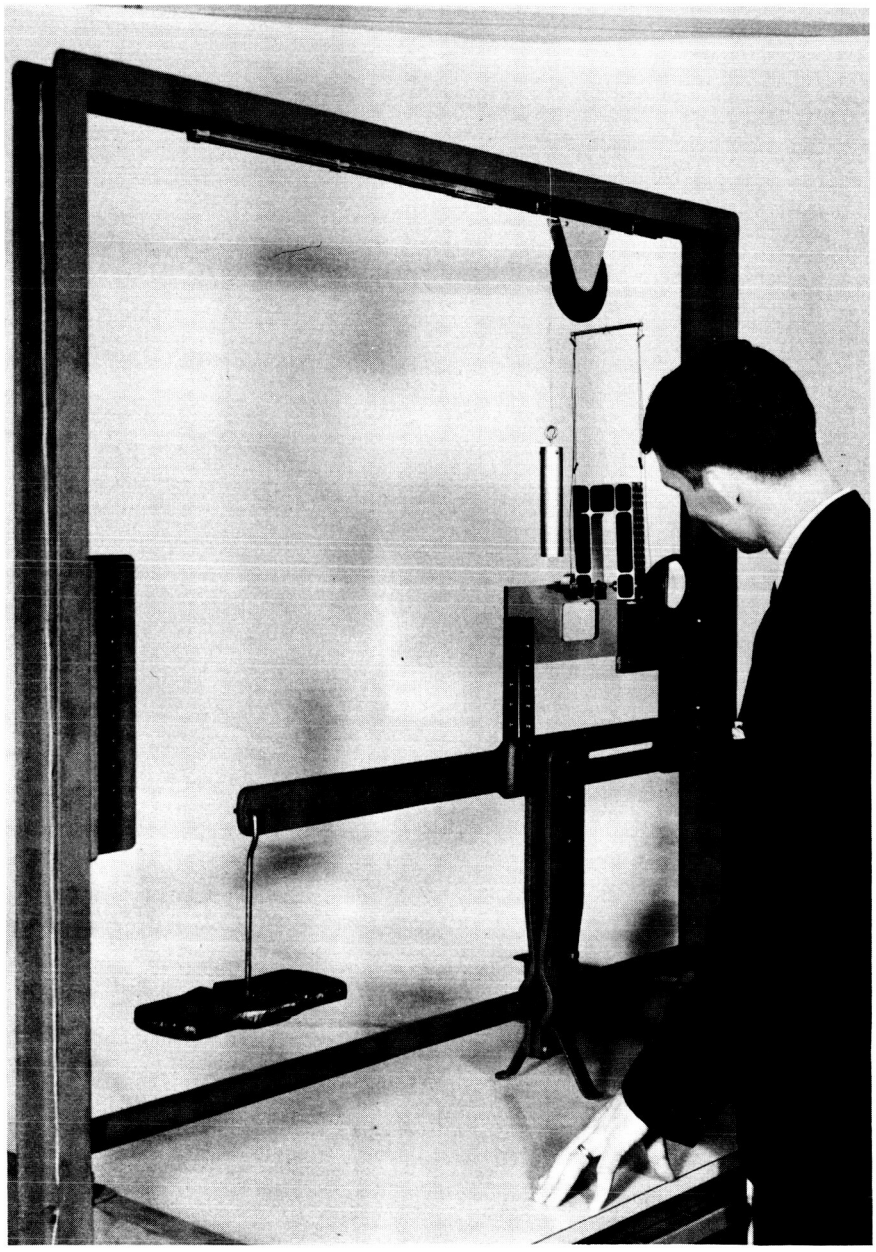

Figure 9-1

Mr. Bobby P. Long inspects test loading device and positioning of lateral extensometer.

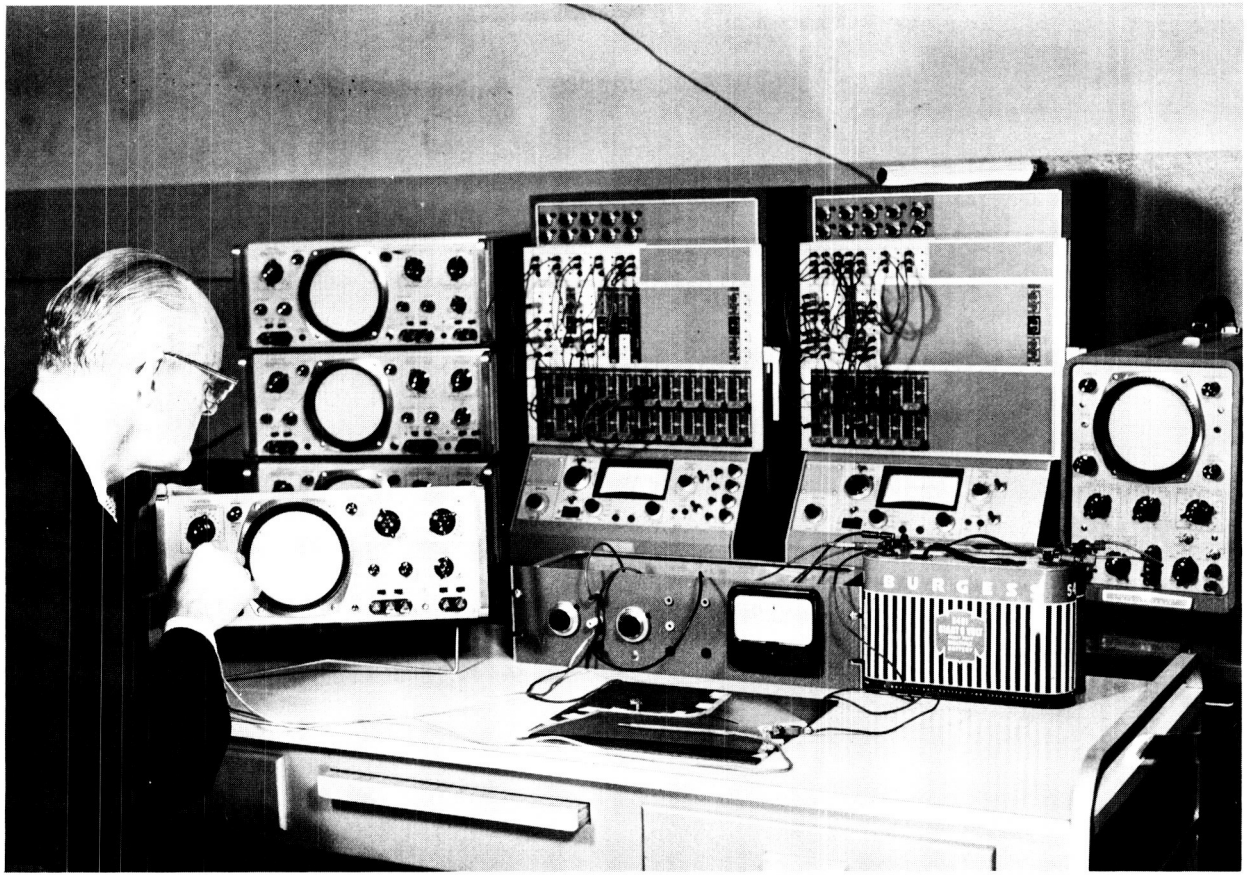

Figure 9-2

Dr. Thompson makes preliminary adjustment of conductive sheet apparatus.

A Master of Science Thesis has been completed as a result of the work of this project. This is titled "A Critical Comparison and Appraisal of Several Methods of Experimental Stress Analysis." It has been written by Mr. Bobby Paul Long. This is included as an appendix to the report on Project No. 9.

III. Procedure

Since the details of the descriptions of the several techniques and the theory behind them have repeatedly been discussed in previous reports, only general remarks will be entered into the record at this time.

The lateral extensometer measures the sum of the principal stresses at any desired point in a two dimensional stress problem. One could measure this value by applying the extensometer to each of the several thousand points involved in a given problem but this would take too long. Instead, the extensometer is used to find values at as many points as are desired on the periphery of a given domain. Then the computer is employed to quickly calculate all of the values at internal points within the field. It is possible to do this speedily since the sum of the principal stresses satisfies Laplace's equation over the field and common relaxation calculations may therefore be employed.

The preceding computations automatically satisfy the compatibility requirements of the theory of elasticity for the problems now being handled. Next, the computer employs approximate methods to

converge upon a solution of the equilibrium equations at each point of the field. Having done these things, the computer can now print out full stress information for all specified points in the field.

The conductive sheet procedure is being utilized as an alternate method and at this time it is impossible to say which procedure will more attractively lend itself to the desired end. A network of stress trajectories in a two-dimensional elastic field can often be constructed experimentally by tracing the equipotentials in the analogous uniform electric field. One of the two sets of orthogonal curves produced by the conductive sheet procedure measures the electric potential of the field. For many problems the lines of equal potential represent a family of stress trajectories. The orthogonal set of lines represents electrically, the intensity of the current in the electric field divided by the conductivity of the medium, and this set of curves, at all points orthogonal to the first set of curves, represents the second set of stress trajectories. It is anticipated that more complicated problems, for which the foregoing explanation may not be exactly true, will yield to future treatment.

IV. Conclusion

This research involves the novel feature of determining stress values at thousands of points in a field rather quickly rather than slowly computing stress intensities at only one point at a time, as is the usual procedure. The research seeks to develop flexible methods that will lend themselves to the treatment of irregular

shapes. This is in contrast to many existing methods of calculation in which the shape of the body itself is often introduced as a mathematical part of the solution.

This research seeks to employ the tremendous speed of the large digital computer. Though the creation and development of the computer program will be slow and will involve an intimate understanding of advanced theory, the practical use of the program will be fast and will not require highly trained personnel.

Emphasis is also being placed on the development of experimental methods for supplying information required by the digital computer. Here, as in the case of the computer program itself, much time and greatly detailed theoretical considerations enter into the effort, but the use of the perfected procedures will be relatively quick and will not require the use of highly trained personnel.

APPENDIX 9-1

Abstract

Three experimental stress analysis techniques are compared. Photoelastic precedure, lateral extensometer coupled with digital computer, and conductive sheet electric procedures are found to be in agreement. Each is found to have a place but the standard photoelastic procedure is the most universally applicable method. The lateral extensometer and the conductive sheet are each shown to be reliable but best employed as auxiliary procedures.

This thesis is based upon a photelastic study[1] of a simplification of a Ph.D. dissertation[2] and, in this thesis, lateral extensometer readings and conductive sheet results are found to be reasonably consistent with each other and with the photoelastic results.

Certain selected sheets of the thesis follow. These briefly reveal the nature of the work. Figure 7 shows the cantilever beam under study and indicates regions A & B which are scrutinized in

---

1 Schroeter, D. R., A Photoelastic Investigation of the Effects of Rectangular Openings at the Neutral Axis of Beams Subject to Both Bending and Shear, M. S. Thesis, Texas A&M University, August, 1964

2 Seyner, E. P., Jr., An Investigation of the Requirements for Reinforcement Around Rectangular Openings in the Webs of Wide-Flange Beams Subject to Bending Moment and Shear, Ph.D. Dissertatio Agricultural and Mechanical College of Texas, August, 1962, p. 6.

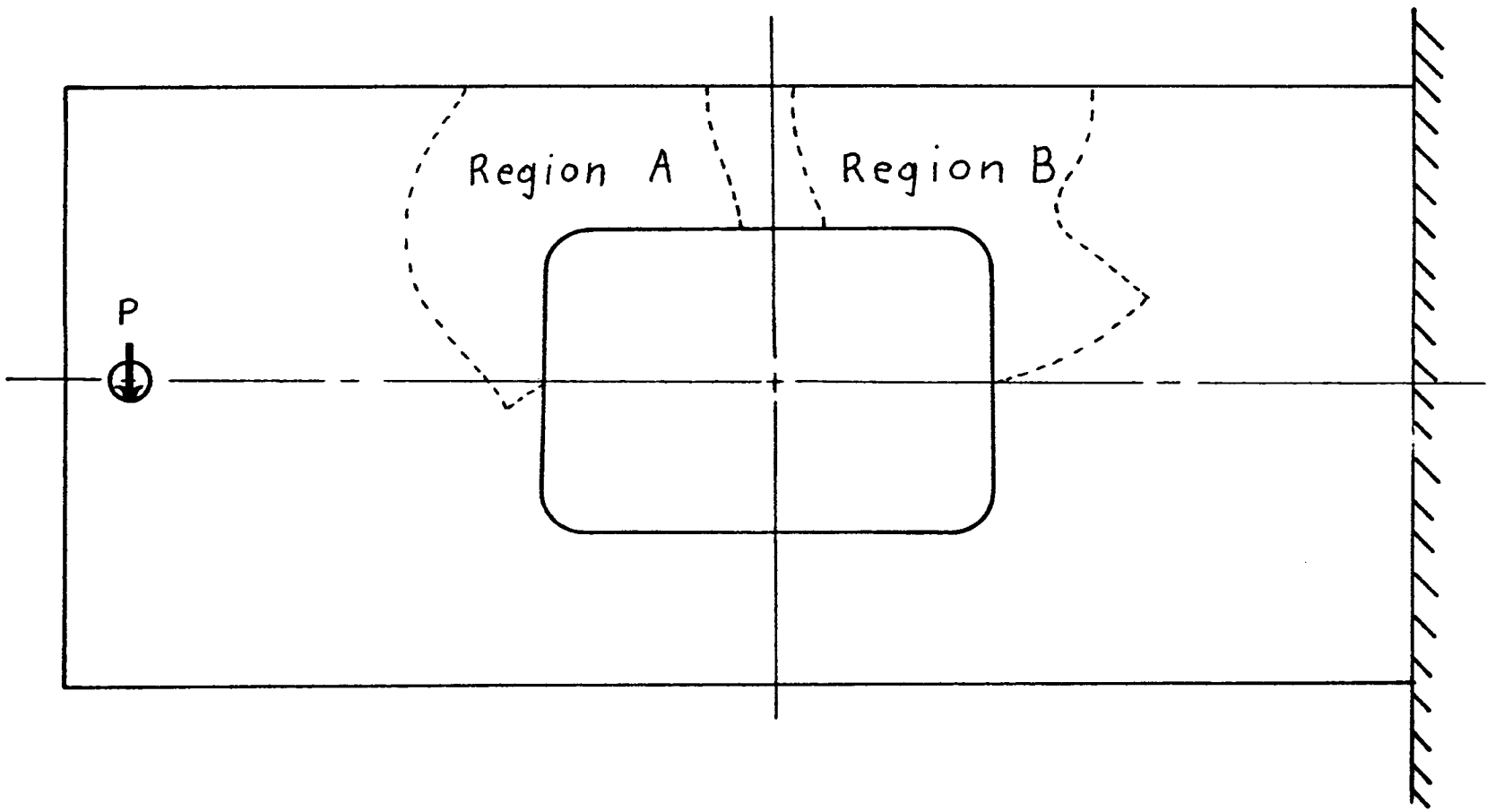

Figure 7. Division of Model for Electrical Analogy

detail to compare results of photoelastic and conductive techniques. Figures 16, 17, 18 and 19 indicate, in essence, the extent of agreement found between photoelasticity and conductive sheet procedures. Figure 13 compares the three methods and Figure 10 defines certain parameters. Finally, Table 1 summarizes principal stress values, in psi, obtained by each of the three methods.

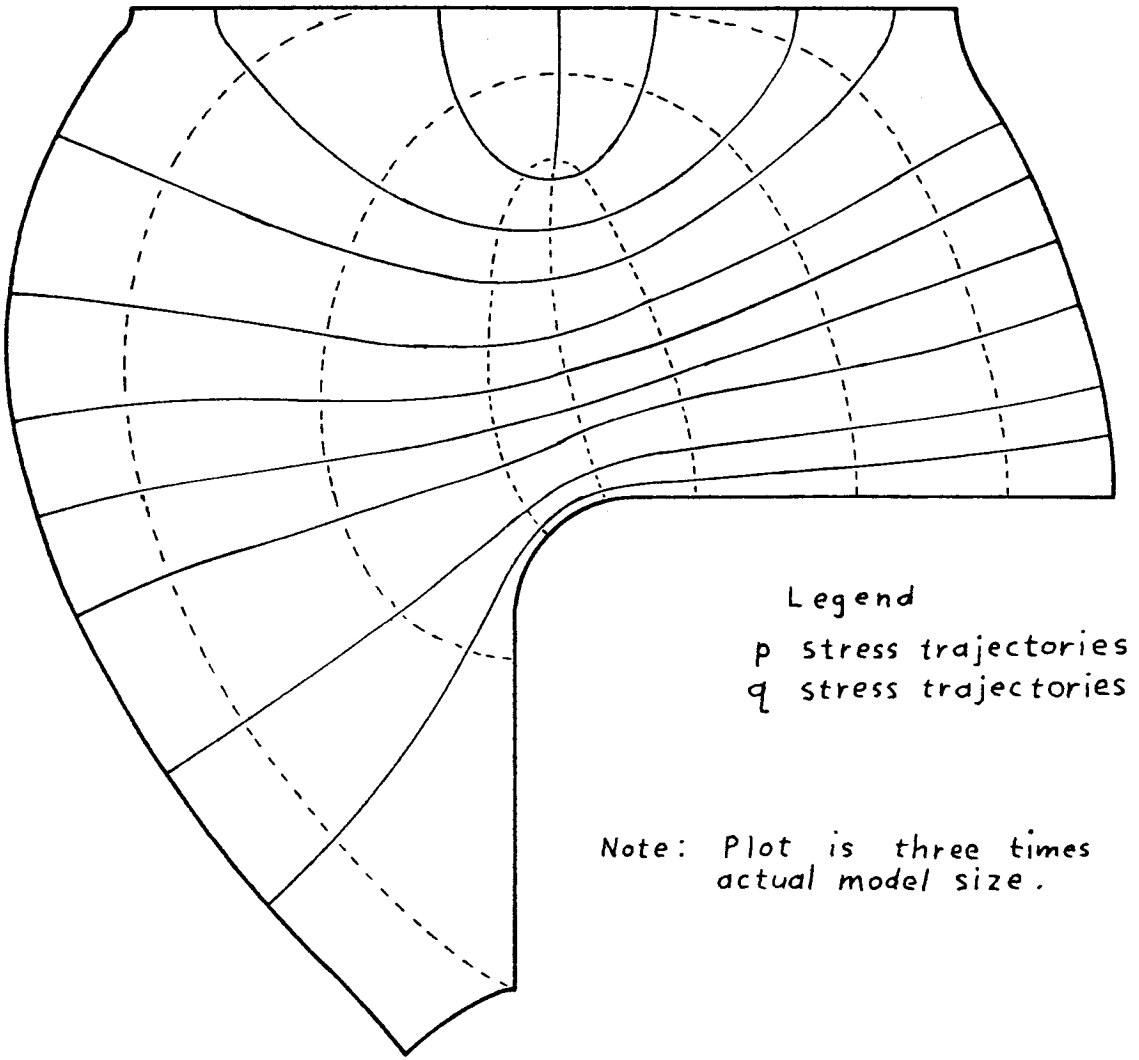

Figure 16. Stress Trajectories by Isoclinics for Region A

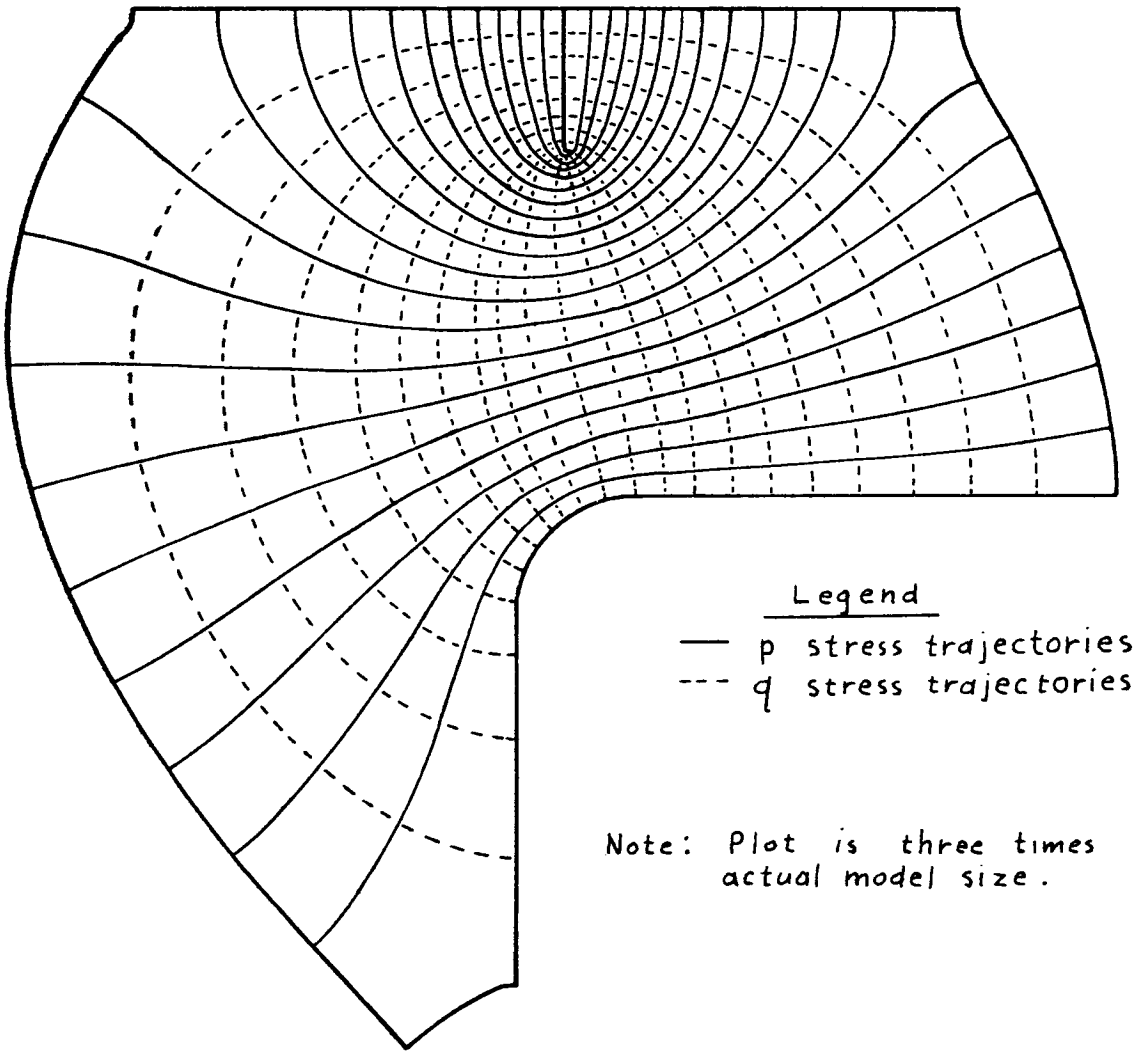

Figure 17. Stress Trajectories by Electrical Analogy for Region A

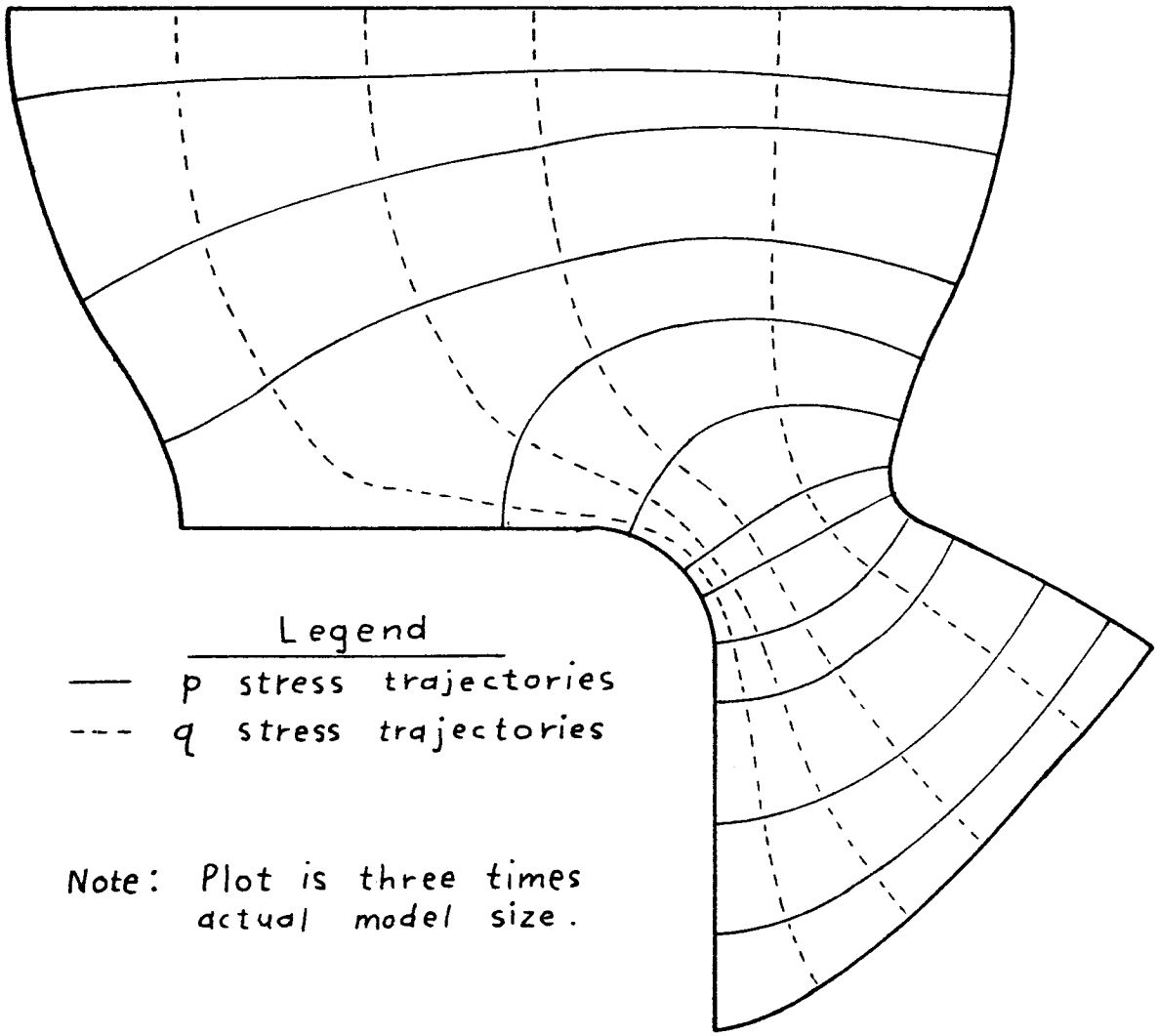

Figure 18. Stress Trajectories by Isoclinics for Region B

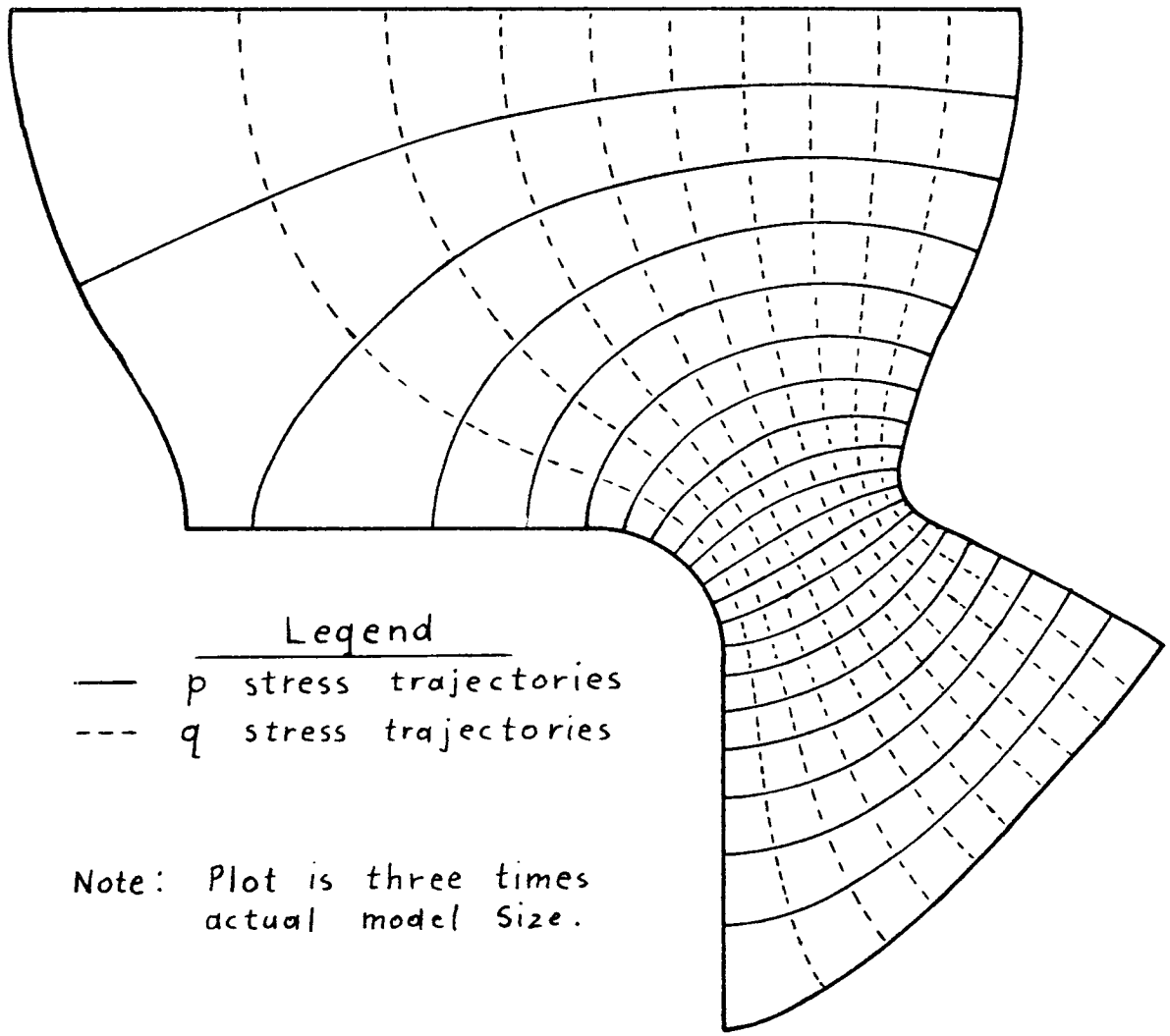

Figure 19. Stress Trajectories by Electrical Analogy for Region B

Figure 13. Comparison Chart of the Three Methods

METHOD I. (Photoelasticity)

A. Based upon isochromatic and isoclinic values developed experimentally.

B. This method involved isoclinic data.

C. Values calculated for only a few points.

D. Methods II and III agreed closely with each other but were grossly different from the results of this method.

METHOD II. (Lateral Extensometer and Digital Computer)

A. Based on photoelastically produced isochromatic values for many points in the field and on extensometer readings over the periphery of the designated field and computer manipulation to produce desired information at every indicated point within the field and on the periphery of the field.

B. This method did not involve isoclinic data.

C. Values calculated for hundreds of points.

D. Method III gave results very close to this method.

METHOD III. (Electrical Analogy)

A. Based on a few photoelastically produced stress trajectories, on photoelastically produced isochromatic values, and computational treatment involving the Lame-Maxwell equations along stress trajectories.

B. This method involved isoclinic data but was influenced less by isoclinic errors than was Method I.

C. Values calculated for only a few points.

D. Method II gave results very close to those of this method.

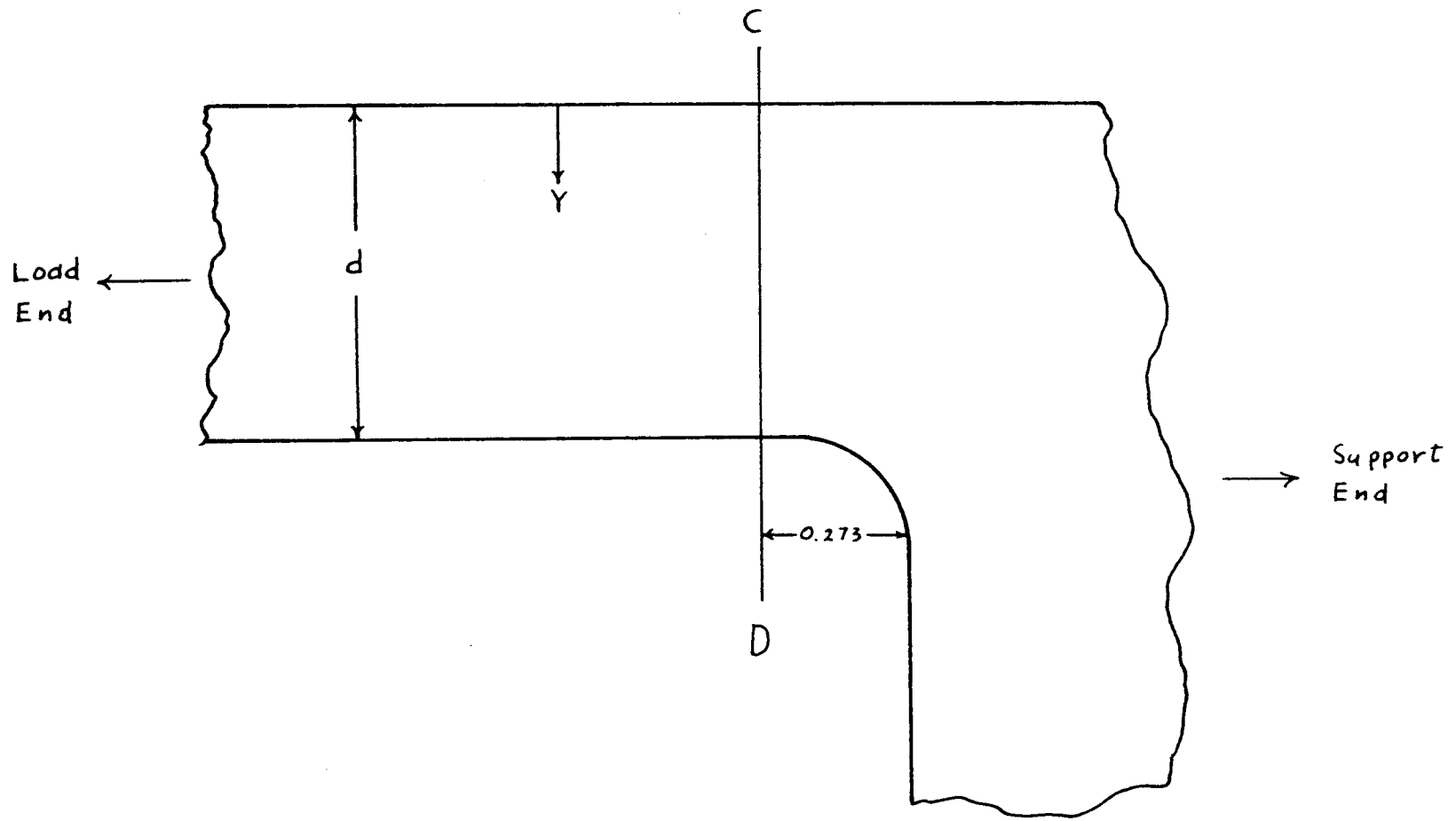

Figure 10. Sketch of Section CD and Related Parameters

Table 1. Principal Stresses Across Section CD* by the Different Methods

Point	Photoelasticity		Lateral Extensometer		Electrical Analogy	
Y/d	p	q	p	q	p	q
0.0	3143	0	3143	0	3143	0
0.1	2783	10	2805	11	2674	-120
0.2	2415	35	2323	-76	2198	-200
0.3	2108	76	1917	-131	1749	-300
0.4	1855	101	1526	-244	1390	-380
0.5	1616	113	1156	1357	1034	-480
0.6	1365	94	787	-492	701	-580
0.7	1025	-37	410	-662	351	-720
0.8	620	-373	80	-921	141	-860
0.9	247	-908	15	-1359	-16	-1180
1.0	0	-1862	0	-1862	0	-1862

SPACE TECHNOLOGY PROJECT # 10

THE RELATIONSHIP BETWEEN VISCOSITY AND CIRCULAR PIPE EXPERIMENTAL DATA FOR NON-NEWTONIAN FLOW

THE RELATIONSHIP BETWEEN VISCOSITY AND CIRCULAR PIPE EXPERIMENTAL DATA FOR NON-NEWTONIAN FLOW

Project Investigators

Dr. P. T. Eubank, Department of Chemical Engineering

Mr. B. F. Fort, Graduate Assistant

Mr. T. T. McConnell, Undergraduate Assistant

During the past six months considerable progress has been made on this project in both the experimental and theoretical phases.

I. Experimental

Data has been obtained from CMC solutions and also polyvinyl alcohol solutions (PVA) of various concentrations in water. Rotational viscometer data is represented by shear stress versus shear rate; pipe or capillary tube data appears as pressure drop versus volumetric flow rate. As discussed in previous reports, it is possible to convert rotational to pipe data by means of the Rabinowitsch Equation and numerical integration techniques. By taking both experimental rotational and pipe data, we may test the accuracy of such conversions.

A digital computer program has been written recently to reduce both rotational and pipe data to the desired form cited above. Several programs, which involve different numerical methods, have also been completed for rotational data conversion to pipe results.

All data has been taken for CMC and PVA solutions However, at this time, only the CMC data has been completely reduced and

conversion from rotational to pipe data calculated. The results from the latter are encouraging. Calculated and experimental pipe results agree to 3 - 4% for CMC solutions indicating that the numerical conversion techniques are sound but, no doubt, can be improved.

Sufficient experiment work has been completed for the Master of Science degree of Mr. Fort. As data on other solutions will be necessary for the Ph.D. work of Mr. Fort, some equipment revision is now planned. Both the rotational and pipe apparatus performed well during the current investigation. However, it was necessary to operate the pipe apparatus in a shear stress range above that anticipated. Enough overlap of the range of rotational and pipe data occured to allow comparison via the rotational data conversion technique. However, the two shear stress ranges should coincide for optimum use of data towards the goals of this project. Since the range of the pipe data cannot be lowered without greatly decreasing accuracy, an attempt to increase the range and flexibility of the rotational apparatus is planned.

II. Theoretical

Several numerical integration techniques have been studied for their usefulness in conversion of rotational to pipe flow results for non-Newtonian liquids. While it is best to check these numerical techniques with experimental data, it is interesting to assume that the liquid obeys a given model from which all results may be calculated.

Assuming such model liquids, the Newton-Coates numerical integration formulas were used. Results indicate that polynominals of degree from four to six can be used to fit most models to better than 0.5%. Models used were the power-law, Ellis, Reiner-Phillippoff, Eyring, and a power-law model with variable coefficients.

SPACE TECHNOLOGY PROJECT # 11

MAGNETIC PROPERTIES OF SOLIDS

MAGNETIC PROPERTIES OF SOLIDS

Project Investigators

Dr. Charles F. Squire, Associate Dean for Science, Principal Investigator

Mr. Tom W. Adair, III, NASA Graduate Fellow

Mr. E. Sharp, Graduate Fellow

Dr. J. L. Gammel, Professor, Department of Physics

A significant scientific contribution has resulted from the NASA supported studies described in the following paragraphs. The new experimental observation in our laboratory concerning the magnetic properties of defects in pure, single crystals of alkali halides has received the unbiased, critical scrutiny of the editors of The Physical Review and two papers accepted for publication in the January 18, 1965 issue. The following are the titles and abstracts of this work:

1. Magnetic Properties of Radiation-Damaged LiF
   T. W. Adair, III and C. F. Squire

   A right circular cylinder of a large single crystal of LiF was hung along its axis of symmetry to form a sensitive torsion pendulum. In a uniform magnetic field a torque was observed to act on the pendulum, which has been interpreted as arising from lattice defects caused by soft x radiation. Quantitative studies on the frequency of oscillation as a function of magnetic field orientation to the LiF crystal are reported.

2. Phenomenological Interpretation of Experiments on the Magnetic Properties of Radiation-Damaged LiF
   J. L. Gammel

   The experimental observations in the preceding paper by Adair and Squire have a reasonable phenomenological interpretation. There is a quantitative agreement between theory and experiment.

The magnetization due to radiation damage exhibits a residual value in zero external field and is described by a susceptibility tensor with off-diagonal terms in the presence of a magnetic field

The progress during the past several months has emphasized that our group has indeed discovered an interesting phenomenon. The following abstract for a scientific paper to be presented before The American Physical Society at Norman, Oklahoma on February 25-27, 1965 has been accepted:

Magnetic Properties of Lattice Defects in Alkali Halides*
T. W. Adair, III, E. J. Sharp, and C. F. Squire

Our Newly discovered evidence[1] for a magnetization in single crystals of LiF arising from lattice defects has been extended to single crystals of KCl and NaCl. The phenomenological interpretation by Professor Gammel given in a companion paper to reference 1 has been the basis of some quantitative experiments on the torque which acts on the torsion pendulum in a magnetic field.

[1]T. W. Adair, III and C. F. Squire, Physical Review, January 18, 1965 and companion paper by J. L. Gammel.

*Supported by NASA Institutional Grant

The central scientific problem before us is to prove <u>what is</u> the source of magnetization. If it be defects, does this mean electrons trapped at vacancy sights; does is mean F_2 ion formed with preferential orientation, or some other mechanism? Obviously we must investigate.

A request for a grant of $33,202 for one year to pursue this scientific effort with vigor has been submitted to NASA. At this writing, no decision has been taken by NASA on this request for support and the proposal has not been submitted to any other

Federal Agency or private research foundation. The cost of equipment and expendable items on the start up of this program were supplied by Texas A&M University and by The Robert A. Welch Foundation, Houston.

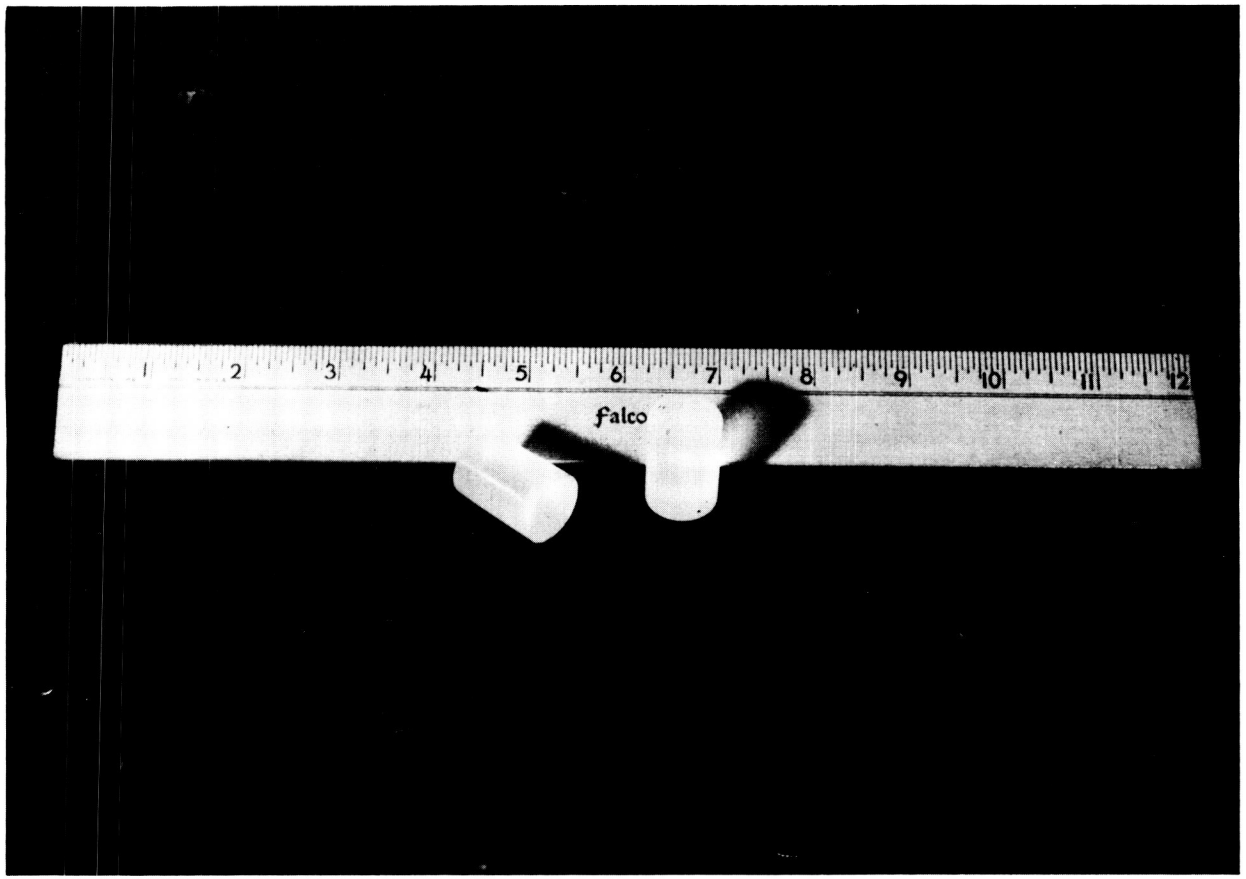

Figure 11-1

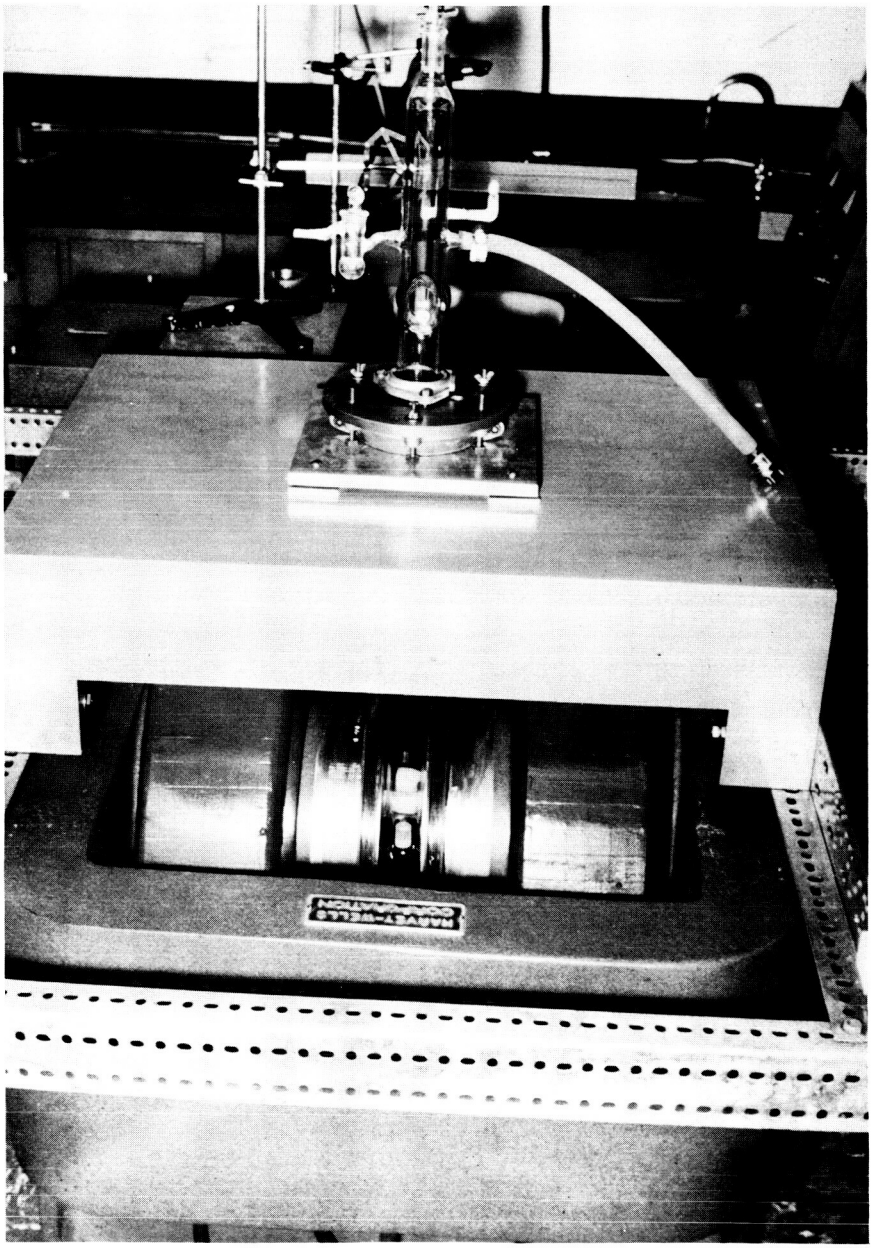

Figure 11-2

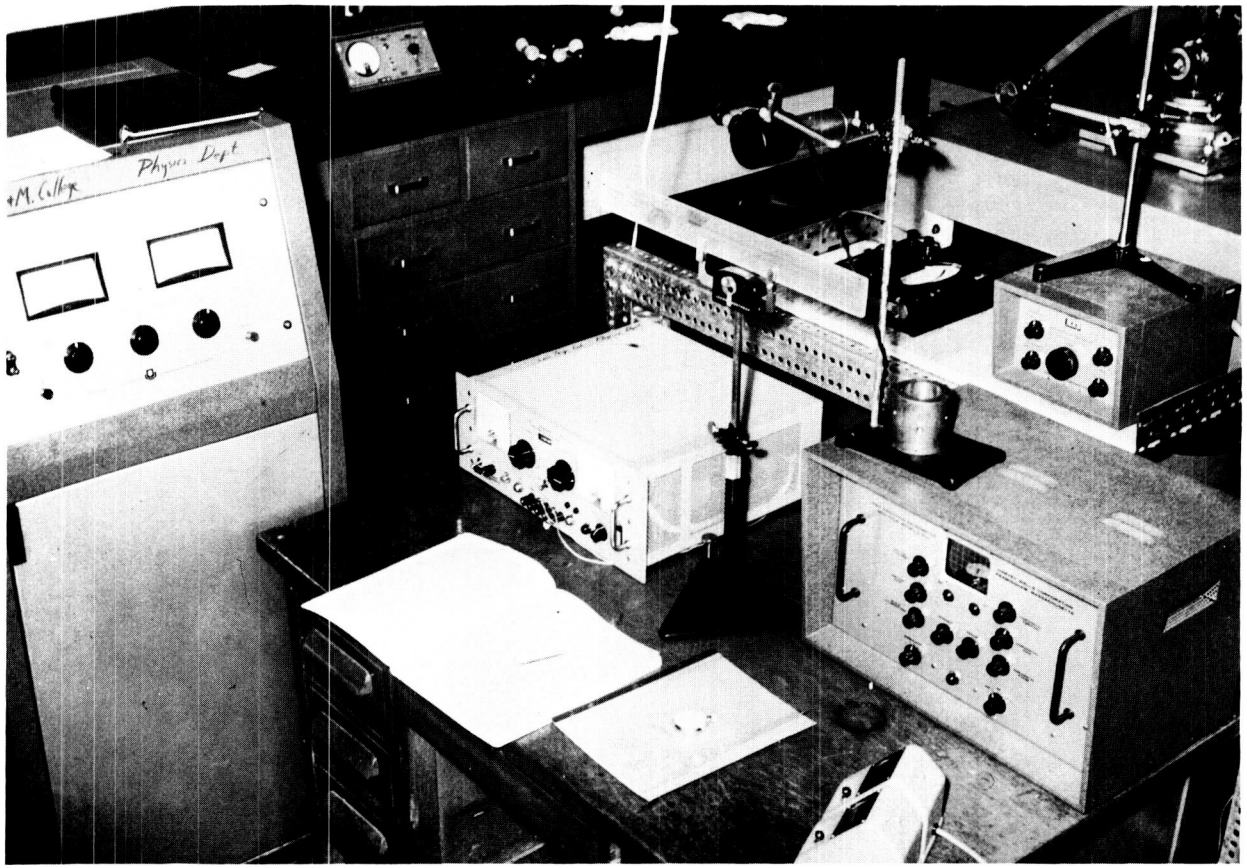

Figure 11-3

SPACE TECHNOLOGY PROJECT NO. 12

EFFECTS OF EXTERNAL IRRADIATION OF THE HEART ON CARDIAC OUTPUT VENOUS PRESSURE AND ARTERIAL PRESSURE

EFFECTS OF EXTERNAL IRRADIATION OF THE HEART ON CARDIAC OUTPUT VENOUS PRESSURE AND ARTERIAL PRESSURE

Project Investigator

Dr. V. S. Bishop, Department of Nuclear Engineering

I. Introduction

During the past several years we have produced chronic heart failure by exposing either the right or left ventricle to approximately 20,000r of Co^{60} gamma irradiation, Stone, Bishop and Guyton (8). In characterizing this type of heart failure, we have been interested both in the changes of the pumping ability of the heart and in the direct effects of ionizing radiation on the heart. In these studies we have evaluated the pressure changes which occur in the venous and arterial pressure systems following unilaterial exposure to 20,000r of Co^{60}. The venous pressures were found to begin to rise about 6 days post-irradiation and continue to increase until death. The arterial pressure was found to remain constant until just prior to death. Using these parameters in conjunction with microscopic examinations, we were able to obtain qualitative answers as to the degree of right or left heart failure.

In the present study we evaluated the resting cardiac output venous pressures, (both right and left atrial pressures) and arterial pressure changes following exposure of the right chest wall to 20,000r of Co^{60}. Since the effects of the exposure must be related to the actual dose, dosimetry measurements were made on the ventricles of the heart and throughout the thoracic cavity.

The results thus found indicate that resting cardiac output is maintained until just prior to death following exposure to 20,000r of Co^{60}. The dosimetry measurements indicate that with exposure doses of 20,000r only about 10,000r reaches the exposed ventricle.

II. Methods and Materials

a. Irradiation Technique

The technique used to irradiate the right ventricle has been previously described, Stone, Bishop and Guyton (8). Briefly, the animals were placed beneath a fluoroscope and the right heart (ventricle) shadow outlined on the lateral chest-wall. Then the animals were placed beneath a Co^{60} therapy unit and the 4 x 4 cm Co^{60} beam was centered directly over the shadow.

b. Instrumentation of the Dogs

Seven mongrel dogs were used in this portion of the study. In order to measure cardiac output, arterial pressure, right and left atrial pressure, the following technique was used in instrumenting the animals. This technique has also been described in previous publications, Bishop, Stone and Guyton (1). The general technique involves the implantation of an electromagnetic flow probe around the root of the aorta proximal to the brachiocephalic artery. During this same surgery, a polyvinyl catheter was inserted into the left atrium through the left atrial appendage. Another polyvinyl catheter was placed in the right atrium through the right jugular vein. The leads from the flow meter and the catheters were run under the skin and exteriorized from the back of the neck. The catheters were filled with heparin

solution and closed.

Control measurements consisting of right atrial pressure, left atrial pressure, femoral arterial pressure, body weight, pulse rate and cardiac output were made in all dogs during the two week recovery. All pressure measurements were recorded on a Grass polygraph using Statham pressure transducers. Measurements of cardiac output made by using a Medicon electromagnetic flow meter (Model K-2000, 400 CPS) and heart rates were recorded on the Grass polygraph along with the pressure measurements.

About 2-3 weeks following surgery the animals were irradiated using the above procedure. Mean right and left atrial pressure, arterial pressure, heart rate and ventricular output were followed periodically until death.

c. Dosimetry

Preliminary dosimetry measurements were made by using silver activated phosphate glass (7). A calibration curve was determined from Co^{60} irradiated glass needles. Victoreen ionization chambers which had been previously calibrated at the National Bureau of Standards were used to check the calibration curve. Both the calibrated needles and the needles used to measure the dose at various locations in the thoracic cavity were individually soaked and washed in reagent grade ethanol and acetone. After allowing them to air dry they were inspected for flaws. Prior to radiation exposures zero readings were established on each needle utilizing a G.K. Turner Model 11 Fluorometer. Four days post-irradiation the

needles were again carried through the cleaning procedure and the fluorescence of the needles recorded.

Each needle prior to implantation was sealed in small lengths of polyvinyl tubing. These needles were then placed in the following positions in a dog which had been sacrificed.

1) In the exposure beam at 35 cm (2 dosimeters)
2) Directly beneath the external chest in the center of the beam (1 dosimeter)
3) Directly upon the exposed ventricle (5 dosimeters)
4) Directly upon the Septum (2 dosimeters)
5) Directly upon the opposite ventricle (unexposed) (5 dosimeters)
6) Directly upon the diaphragm (1 dosimeter)
7) Directly upon the spine (1 dosimeter)

The needles were exposed at these positions when the extrapolated exposure dose of the Co^{60} therapy unit was set at 5,000r to right lateral chest wall, 1,000r to the right lateral chest wall, 5,000r to the left lateral chest wall and 1,000r to the left lateral chest wall.

III. Results

a. Changes in Ventricular Output, Stroke Volume and Arterial Pressures

Figure 1 shows the resting values of ventricular output, stroke volume, and arterial pressure plotted against the time prior to and following irradiation of the right ventricle with 20,000r Co^{60}.

Heart rate, right and left atrial pressures were also measured, but they were found to be consistent with changes previously described by Stone, Bishop and Guyton (8).

The animals used in this study reclined quietly unrestrained during the measurement of ventricular output. However, it should be noticed in Figure 1 that there was a variation in resting ventricular output prior to irradiation. This variation continues following irradiation. Generally, the resting ventricular output remained within the normal range until 4-6 days prior to death. The animal represented by the triangles in Figure 1 had a reduction in resting ventricular output approximately 10 days prior to death. Most of the animals used in this study displayed a reduction in resting ventricular output 4-6 days prior to death and the variation in time could usually be related to the amount of muscle damage determined at autopsy.

The changes in resting stroke volume followed very closely the changes in resting ventricular output. This point can be seen by comparing the points of Figure 1.

The arterial pressure was maintained essentially constant by all animals in this study as illustrated in the upper portion of Figure 1. In a few cases a slight decline could be noted 2 or 3 days prior to death. However, it is usually well regulated.

b. Dosimetry

The doses measured by the silver activated glass phosphate dosimetry as related to the extrapolated exposure dose (EED), i.e.,

previous calibrated dose corrected for decay, are shown in Table I.

The column labeled MED relates to the total measured exposure dose and MDH is the actual dose measured on the ventricles of the heart. The measured exposure dose was found to be 19% less than the routinely used extrapolated exposure dose. The maximum dose received by the right ventricle when the right lateral chest wall was exposed was 59.5% of the measured exposure dose (MED). Only 48% of the extrapolated exposure dose (EED) was measured on the right ventricle. The maximum dose received by the left ventricle using the same port of entry was 50.7% of the measured exposure dose (MED) and 41% of the extrapolated exposure dose. Note there is very little difference between the doses received by the right and left ventricles.

When the port of entry was the left lateral chest wall, the left ventricle received a maximum dose of 54.5% of the measured exposure dose (MED) and 44.5% of the extrapolated exposure dose (EED). The opposite ventricle received 44.5% of the measured exposure dose (MED) and 36% of the extrapolated exposure dose (EED).

In producing chronic congestive heart failure we have used an extrapolated exposure dose of 20,000r of Co^{60} to either the right or left laterally chest wall. According to the dosimetry measurements shown in Table I, the actual dose received by the right and left ventricle when the port of entry was via the right lateral chest wall is 9,600r and 8,200r respectively. When the port of entry is via the left lateral chest wall, the dose is 7,200r and 8,400r respectively to the right and left ventricle.

The silver activated glass phosphate dosimeters which were placed on other organs in the thoracic cavity received amounts of radiation too small to measure.

c. Gross pathological findings at autopsy

The same general pathological conditions were found at autopsy in these animals as previously reported by Stone, Bishop, Guyton (8) and others. The mass of tissue damaged in the right ventricle ranged from 70 - 90% of wet weight of the ventricle. The left ventricle appeared normal both from visual and microscopic observations. Free fluid was found in the thoracic and abdomen of these animals. Liver congestion was visibly present and pitting edema was observed.

d. Discussion

In previous studies we have observed massive hemorrhagic infiltration of the right ventricle by the 14th day following irradiation. Coupled with these pathological observations, the atrial pressures begin to rise about 6 days post-irradiation which indicates qualitatively that the heart is failing (8). However, the animals in this study are able to maintain a normal resting ventricular output until 4-6 days prior to death. This emphasizes the ability of the heart to compensate for a decrease in functional cardiac mass. This ability to compensate was measured during resting conditions and would probably not be sufficient to maintain a normal circulatory function during severe work stresses. Since it is obvious that these animals are in heart failure many days prior to death, the measurement of resting ventricular output does not quantitate any

reduction in functional cardiac muscle.

Although the dosimetry studies were preliminary, the doses obtained are extremely valuable. In all of our work thus far we have used the same Co^{60} therapy unit, and an extrapolated exposure dose of 20,000r. The measured exposure dose in this study was 19% of this extrapolated exposure dose, which is used routinely in the therapy center. Thus, in all of our work the actual exposure dose has been 16,200r. Using this exposure dose, the maximum dose to the right and left ventricle when the port of entry is the right lateral chest wall, is 9,600r and 8,200r respectively. When using a left lateral port of entry, the dose is 8,400r and 7m200r respectively to the left and right lateral ventricle. Note with only a small difference in dose the latent period for microscopic damage for the exposed and unexposed ventricle is quite different. In fact, the latent period for the unexposed ventricle exceed the life of the animal in this preparation. However, we have exposed the right and left ventricle to extrapolated exposure doses somewhat less than 20,000r and have seen microscopic damage. Of course the survival time of these animals was increased. The results at these exposure doses agree with those reported by Phillips (6) and Michaelson(4).

Using an extrapolated dose of 10,000r or an actual dose to the exposed ventricle of 4,800r (using the data in the table), we have seen limited myocardium fibrosis and complete atrial fibrosis.

IV. Summary

In summary, we would like to emphasize that doses of ionizing

radiation in the therapeutic range may produce damage to the myocardium. The effect is probably an indirect effect resulting from increased permeability and fragility of the capillaries (9, 3, 2). The injury to the myocardium resulting from therapeutic doses may not be detected under normal resting conditions. Secondly, the latent period, time from exposure to microscopic changes in the cardiac muscle, is sensitive to small changes in dose.

REFERENCES

1. Bishop, V. S., H. L. Stone, and A. C. Guyton. "Cardiac Function Curves in Conscious Dogs." Am. J. Physiol. 207: 677-682, 1964.
2. Caster, W. O., "Effects of X-rays on the Cardiovascular System." Proceedings of the 2nd United Nations International Conference on the Peaceful Uses of Atomic Energy, 22:229, 1958.
3. McCutcheon, M., "Problems and Effects of Radiation on Capillary Permealibility." J. Cell and Comp. Physiol. Supp. 39, 2:133, 1952.
4. Michaelson, S. M., B. Schreiner, Jr., C. L. Hansen, Jr., W. J. Quinlan, L. T. Odland, M. Ingram, and J. W. Howland. "Cardiopulmonary changes in the dog following exposure to X-rays." Univ. of Rochester Atomic Energy Project. UR-596, Rochester, N. Y., 1961, 16pp.
5. Moss, A. J., D. W. Smith, S. Michaelson, and B. F. Schreiner, Jr. "Radiation Technique for Production of Localized Myocardial Neurosis in the Intact Dog." Proc. Soc. Exp. Biol. and Med. 112: 903-905, 1963.
6. Phillips, S. J., J. A. Reid, and R. Rugh, "Electrocardiograph and Pathologic Changes after Cardiac X-irradiation in Dogs." Am. Heart J. 68:524-533, 1964.
7. Schulman, J. H., "Glass Dosimeters for Radiation Measurement." The Industrial Atom-Monograph. Tech. Information Services Report TID-8006, 1956.
8. Stone, H. L., V. S. Bishop and A. C. Guyton, "Progressive Changes

in Cardiovascular Function after Unilaterial Heart Irradiation." Am. J. Physiol. 206: 289-293, 1964.

9. Wish, L., J. Furth, C. W. Sheppard, and R. H. Storey, "Disappearance Rate of Lagged Substances from the Circulation of Roentgen Irradiated Animals." Am. J. Roentgenal., Radium Ther. and Nuclear Med., 67: 628, 1952.

TABLE I

DOSIMETRY RESULTS.

EXPOSURE PORT	EED*	MED*	MDH**	MED/EED	MDH***/EED	MDH**/MED
Right Lateral Chest Wall	5000r	4050		.81		
Right Ventricle			2400		.48	59.5
Left Ventricle			2050		.41	.507
Left Lateral Chest Wall	5000r	4050		.81		
Left Ventricle			2100		.42	.545
Right Ventricle			1800		.36	.445

* Extrapolated Exposure Dose Rate = 78 r/min.

Measured Exposure Dose Rate = 63.2 r/min.

** Measured Absorbed Dose on the Ventricular Wall

*** The Same Average Percentage was Found at EED of 1000r.

LEGEND

FIGURE (1) - Ventricular output, stroke volume and arterial pressure plotted against days before and after irradiation. The animals were irradiated on zero day.

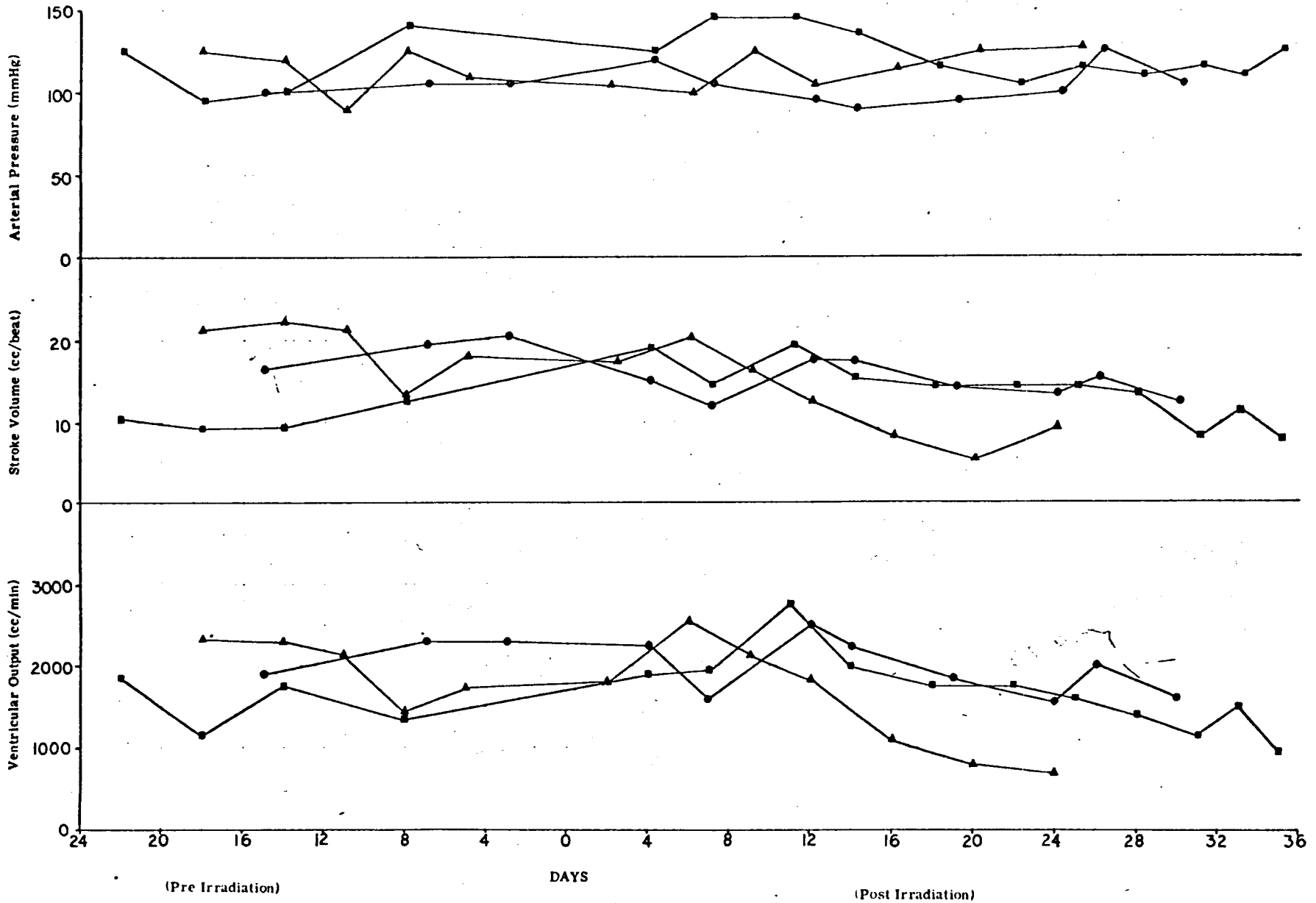
Arterial Pressure (mmHg)
150
100
50
0
Stroke Volume (cc/beat)
20
10
0
Ventricular Output (cc/min)
3000
2000
1000
0
24
20
16
12
8
4
0
4
8
12
16
20
24
28
32
36
(Pre Irradiation)
DAYS
(Post Irradiation)

SPACE TECHNOLOGY PROJECT # 13

A STUDY OF CADMIUM ABSORPTION OF RESONANCE NEUTRONS IN VARIOUS FOIL MATERIALS

A STUDY OF CADMIUM ABSORPTION OF RESONANCE NEUTRONS IN VARIOUS FOIL MATERIALS

Principal Investigators

Dr. R. G. Cochran, Professor and Head, Nuclear Engineering Department

Mr. J. E. Powell, Graduate Assistant

Mr. Robert T. Perry, Graduate Assistant

I. Status

The object of this research was to determine how the fraction of the epithermal neutrons absorbed by the cadmium covers of various resonance detectors varied with angular distribution of incident neutrons and the thickness of the detecting foil. It has been known for some time that when a metallic foil is used to detect resonance neutrons it must be covered with cadmium to eliminate the thermal neutron activation. This cadmium filter also absorbs some of the resonance neutrons and to correct for this effect a factor usually denoted as F_{cd} has been determined by a number of investigators. Each of these investigators determined F_{cd} in the isotropic neutron flux case by plotting the logarithm of the resonance activity as a function of the cadmium cover thickness and by extrapolating the resulting curve to zero cover thickness. A ratio is then taken of the activity at zero cover thickness to obtain the F_{cd}.

In a recently published paper, Powell and Walker[1] have shown that F_{cd} in the case of an isotropic flux is not a logarithmic function but instead is a third order exponential integral function.

In light of this research, a number of months has been spent carrying out preliminary theoretical calculations in order to predict the actual behavior to be expected of F_{cd} in an anisotropic neutron flux. This theoretical work has now progressed to the point where preliminary results are being obtained which are being used to compare with the experimental portion of the program. The experimental data is being obtained by activating cadmium covered 2 cm. diameter indium foils with thicknesses varying from 2 to 8 mils at eight different positions out from a plane source of fast neutrons. One inch diameter covers have been constructed for use for various thicknesses of cadmium varying from 30 to 60 mils. The source used in these experiments consists of three 2 curie plutonium beryllium neutron sources which are placed in a 60 gallon tank containing distilled water. The water is constantly recirculated through a demineralizer to maintain high purity while the water temperature is maintained to within $\pm$ 2°F. After each foil is activated, the activity is ascertained by use of the gamma ray scintillation spectrometer. Each foil is placed in a well-type sodium iodide crystal and a sufficient number of counts are recorded so that the statistical variation is within $\pm$ 1/3 of a percent. In addition, the electronic apparatus is standardized before and after each foil is counted. Statistical errors are minimized by obtaining sufficient individual activations so that the radioactivity of each foil for each cadmium covered thickness is known to within 1/2 of a percent. The experimental data is now being used in conjunction with

the preliminary theoretical calculations to evaluate these results.

In summary, due to the funds provided by this research grant, the following papers have been completed or are near completion, and will be submitted for publication to Nuclear Science and Engineering in the immediate future:

1. "Cadmium Correction Factors for Iodine, Indium, and Gold Foils," J. E. Powell and C. L. Beck.

2. "The Effects of Epithermal Neutron Flux Anisotropy on Cadmium Correction Factors for Indium Foils in Water," J. E. Powell. (Disseration now in progress). Provided as Appendix 1 to this report on Space Technology Project No. 13.

BIBLIOGRAPHY

1. Powell, J. E. and J. V. Walker, "A Determination of the Cadmium Absorption of Resonance Neutrons in Cadmium Covered Indium Foils," Nucl. Sci. Engr. 20, 476 (1964).
2. Randall, J. D. and J. V. Walker, "The Elimination of Flux Perturbation Associated with Neutron Detecting Foils," Nucl. Sci. Engr., 11, 69 (1961).
3. Randall, J. D. and J. V. Walker, "Non-Perturbing Foils - An Experimental Verification," Nucl. Sci. Engr. 15, 344 (1963).

APPENDIX I TO REPORT ON SPACE TECHNOLOGY PROJECT NO. 13

THE EFFECTS OF EPITHERMAL NEUTORN FLUX ANISTROPY ON CADMIUM CORRECTION FACTORS FOR CADMIUM COVERED INDIUM FOILS IN WATER

Objective: The object of this research is to determine how the fraction of epithermal neutrons abosrbed by the cadmium covers of resonance neutron detectors varies with the angular distribution of the incident neutrons and the thickness of the detector.

Present Status of the Question: When a foil is used to detect resonance neutrons, it is often covered with cadmium to eliminate thermal neutron activation. This cadmium filter also absorbs some of the resonance neutrons, and to correct this effect a factor usually denoted by F_{cd} has been determined by several investigators (1-9). Each of these investigators determined F_{cd} in the isotropic case by plotting the logarithm of the resonance activity as a functior of the cadmium cover thickness and by extrapolating the resulting curve to zero cover thickness. A ratio was then taken of the activity at zero cover thickness to the activity at some arbitrary cover thickness to obtain F_{cd}.

Recently, however, Powell and Walker (10) have shown that F_{cd} in the case of an isotropic flux is not a logarithmic function, but instead it is a third order exponential integral function. The resonance activity should be plotted as a function of $E_3\,\tau_c(e) - E_3\,\tau_c(e) + \tau_f(e)$ where the E_3 functions are third order exponential integrals, and the (e) are the foil and cadmium cover thicknesses

in units of absorption mean free paths. They also found that F_{cd} was a slight function of the thickness of the detector for all detector thicknesses below 90 mg/cm^2 while it reached a constant value of 1.123 above 90 mg/cm^2.

The usefulness of F_{cd} as determined by the above investigators is somewhat limited because many experiments are not carried out in isotropic fluxes. Therefore, it is important that some insight be gained into the problem of F_{cd} in the anisotropic case.

Truby, et al., (9) have been the only investigators to attempt a determination of F_{cd} in an anisotropic epithermal flux. They measured F_{cd} at various distances from a point source of resonance neutrons and found that F_{cd} was very sensitive to the angular distribution of the neutrons. However, their determination of F_{cd} by using the logarithmic fit leaves their results open to question. Since the determination of F_{cd} involves the extrapolation of a non-linear curve, it is impossible to treat the experimental data without first determining the functional dependence of the resonance activity upon the cadmium cover thickness from theoretical considerations.

So far as theoretical considerations are concerned, it should be noted that in the determination of F_{cd} all neutron energies lie above the cadmium cutoff energy so that there is essentially zero flux perturbation at the surface of the foil. Therefore, many of the problems created by an incident thermal flux do not exist.

Procedure: In order to obtain a theoretical expression for F_{cd}

in the case where the incident angular distribution of the resonance neutrons is not isotropic, it is necessary to consider the incident neutron current upon the surface of a bare and cadmium covered detector. If the detector and cadmium cover are both considered to be infinite, purely absorbing slabs it can be shown that F_{cd}^{*} is given by

$$F_{cd}^{*} = \frac{\int_{o}^{u_{cd}} e^{-u} du \int_{o}^{1} d\mu \mu \Psi(x,\mu,\mu)(1-e^{-\tau f/\mu}) + \int_{o}^{u_{cd}} e^{-u} du \int_{-1}^{o} d\mu \mu \Psi(x,\mu,u)(1-e^{+\tau f/\mu})}{\int_{o}^{u_{cd}} e^{-u} du \int_{o}^{1} d\mu \mu \Psi(x,\mu,u)(1-e^{-\tau f/\mu}) e^{-\tau cd/\mu} + \int_{o}^{u_{cd}} e^{-u} du \int_{-1}^{o} d\mu \mu \Psi(x,\mu,u)(1-e^{+\tau f/\mu}) e^{-\tau cd/}}$$

the asterisk indicating the anisotropic F_{cd} and u_{cd} being the value of the lethargy variable corresponding to the cadmium cutoff energy which may be determined from the results of Stoughton, et al., (11). The $\Psi(x,\mu,u)$ functions are solutions of the energy dependent integrodifferential Boltzmann equation (12) in slab geometry.

To obtain the $\Psi(x,\mu,u)$ functions the moments solution of the Boltzmann equation (13-15), in which the integrodifferential equation is transformed into a set of integral equations, will be used. This technique has been previously used to calculate the neutron scaler flux due to a fission source in a water medium by Aronson, et al., (17).

The assumption of an infinite slab detector in the theoretical considerations should adequately describe the 2 cm. diameter foils which will be used in the experimental investigation since it has been shown by Martinez (16) that a foil with a thickness less than .020 in. and a diameter greater than four absorber mean free paths

can be considered an infinite slab (2 cm. = 6.3 abosrber mean free paths). Although experimental verification has not been obtained directly, the same assumption for the cadmium covers should be valid since Powell, et al., (10) made this assumption in determining F_{cd} theoretically for the isotropic case and obtained substantial agreement between their experimental and theoretical results. The cadmium covers which will be used in this investigation will be equivalent to those used in reference (10).

The experimental data will be obtained by activating cadmium covered 2 cm. diameter indium foils with thicknesses varying from 2 to 8 mils at eight different positions out from a plane source of fast neutrons. One inch diameter covers will be constructed from four thicknesses of cadmium varying from 30 to 60 mils.

The source will be constructed from three 2-curie Pu-Be neutron sources which will be placed in a sixty gallon tank containing distilled water. The water will be constantly recirculated through a demineralizer to maintain a high purity, while the water temperature will be kept constant within $\pm 2^{o}F$.

The activity of each foil will be obtained by use of a gamma scintillation spectrometer. Each foil will be placed in a NaI(Tl) well type crystal, and an integral count will be taken of the indium gamma ray spectrum. The system will be standardized to within $\pm$ 1/3% before and after each count. Enough individual activations will be obtained so that the activity of each foil with each cadmium

cover thickness will be known within $\pm$ 1/2%.

The data will then be fitted according to the functional variation predicted by the theoretical considerations with F_{cd} being determined from this fit.

BIBLIOGRAPHY

1. Tittle, C. W., "Slow Neutron Detection by Foils - I," Nucleonics 8, 5(1951).

2. Tittle, C. W., "Slow Neutron Detection by Foils - II," Nucleonics 9, 60 (1951).

3. Walker, R. L., "Absolute Calibration of a Ra-Be Neutron Source," MDDC-414 (1946).

4. Dacey, J. E., R. W. Paine, Jr., and C. Goodman, Technical Report No. 23 (Massachusetts Institute of Technology, Laboratory for Nuclear Science and Engineering, Cambridge, Mass., October 20, 1949).

5. Rush, J. H., "The Range of Ra-Be Neutrons in Water," Phys. Rev. 73, 271 (1948).

6. Kunstadter, J., "A Correction to be Applied to the Activity of Neutron Activated Cadmium Covered Foils," Phys. Rev. 78, 484 (1951).

7. Martin, D. H., "Correction Factors for Cd-Covered-Foil Measurements," Nucleonics 13, 52 (1955).

8. Meister, H., "Adtivierungsstorung Von Indiumfolien in Neutronenfeld," Zeitschrift Fur Naturforschung 10a, 669 (1955).

9. Trubey, D. K., T. V. Blosser, and G. M. Estabrook, "Correction Factors for Foil - Activation Measurements of Neutron Fluxes in Water and Graphite," ORNL-2842, 204 (1959).

10. Powell, J. E., and J. V. Walker, "A Determination of the Cadmium Absorption of Resonance Neutrons in Cadmium Covered Indium Foils." Accepted for publication in Nuclear Science and Engineering, (1964).

11. Stoughton, R. W., and J. Halperin, "Effective Cutoff Energies for Boron, Cadmium, Gadolinium, and Samarium Filters," ORNL-TM-236 (1962).

12. Meghreblian, R. V., and D. K. Holmes, Reactor Analysis, McGraw-Hill Book Co., Inc., (1960).

13. Spencer, L. V., and V. Fano, "Penetration and Diffusion of X-Rays. Calculation of Spatial Distributions by Polynomial Expansion." Journal of Research of the National Bureau of Standards 46, 446 (1951).

14. Spencer, L. V., and F. Jenkins, Penetration and Diffusion of X-Rays through Thick Barriers IV. Multiply Scattered X-Rays: Angular Distribution." Phys. Rev. 76, 1885 (1949).

15. Karr, P. R., and J. C. Lamkin,"Penetration and Diffusion of Hard X-Rays through Thick Barriers III. Studies of Spectral Distributions." Phys. Rev. 76, 1842 (1949).

16. Martinez, J. S., "Neutron Self Shielding in One-Dimensional Abosrbers," UCRL-6526, TID-4500, (1961).

17. Aronson, R., J. Certaine, and H. Goldstein, "Penetration of Neutrons from Point Isotropic Monoenergetic Sources in Water." NYO-6269, (1954).

Figure 13-1

Apparatus necessary to obtain the liquid foil data including lucite foil containers, cadmium covers, four pi counting planchets, pipettes and hypodermic needles.

Figure 13-2

Counting equipment used to count the foils which includes gamma scintillation spectrometer assembly and dry box containing four pi beta detector.

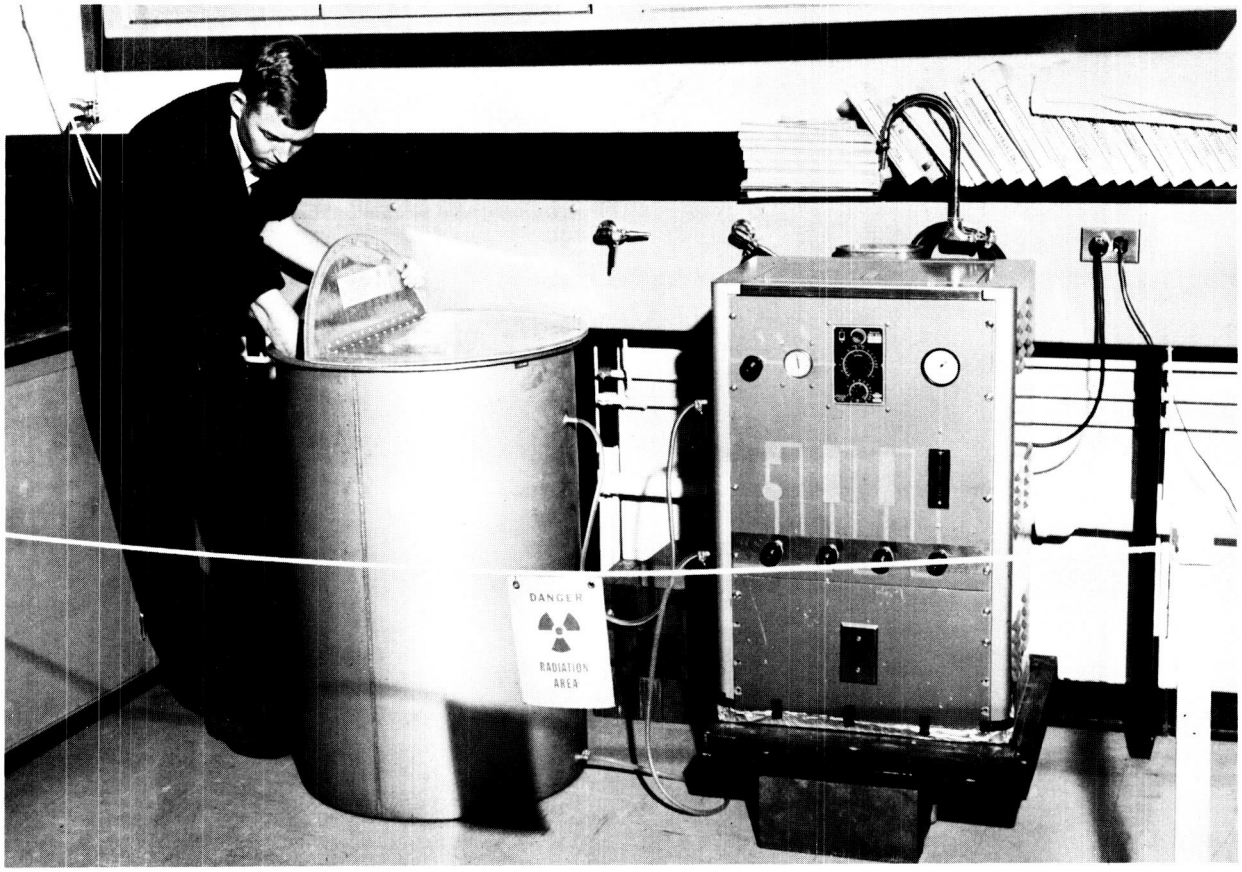

Figure 13-3

Tank and demineralizer assembly. The tank contains 60 gallons of distilled water and a 6 curie PuBe neutron source.